

AN ABSTRACT OF THE DISSERTATION OF

Youn-Hi Woo for the degree of Doctor of Philosophy in Pharmacy
presented November 21, 2002.

Title: Studies of Non-Mevalonate Isoprenoid Biosynthesis: The 1-Deoxy-D-xylulose-5-phosphate Isomeroreductase (DXR) Mediated Reaction.

Abstract approved: _____ Redacted for Privacy _____
Philip J. Proteau

This dissertation details the investigation of an alternate pathway to isoprenoids that occurs in plants and microorganisms, the non-mevalonate pathway. This exploration of the pathway focuses on the second step, the conversion of 1-deoxy-D-xylulose-5-phosphate (DXP) to 2-C-methylerythritol-4-phosphate (MEP) by the enzyme DXP isomeroreductase (DXR). These studies led to an appreciation of the stereochemical course of the enzymatic reduction step and to a better understanding of the structural requirements for inhibitors to have optimal interactions at the active site of the enzyme, DXR.

The investigation of the reduction step mediated by DXR revealed that the C1 *pro-S* hydrogen in 2-C-methylerythritol-4-phosphate derives from C3 of DXP for the DXR from *Synechocystis* sp PCC6803. The *pro-R* hydrogen originates from NADPH. The *pro-S* hydride of NADPH is transferred to the *re* face of the proposed aldehyde intermediate, which designates DXR as a class B dehydrogenase.

Based on the structural features of fosmidomycin, a known inhibitor of DXR, several analogs were synthesized and evaluated for their inhibitory activity against DXR. It was discovered that a polar head group with two ionizable groups, a suitable length of intervening carbons, and an *N*-acyl *N*-hydroxy moiety are important factors to demonstrate significant inhibition activity. These studies also provided information that is complementary to structural data obtained from recent X-ray crystal structures of DXR.

©Copyright by Youn-Hi Woo

November 21, 2002

All Rights Reserved

**Studies of Non-Mevalonate Isoprenoid Biosynthesis:
The 1-Deoxy-D-xylulose-5-phosphate Isomeroreductase (DXR) Mediated
Reaction**

**By
Youn-Hi Woo**

A DISSERTATION

Submitted to

Oregon State University

**in partial fulfillment of
the requirements for the
degree of**

Doctor of Philosophy

**Presented November 21, 2002
Commencement June 2003**

Doctor of Philosophy dissertation of Youn-Hi Woo presented on November 21, 2002.

APPROVED:

Redacted for Privacy

Major Professor, representing Pharmacy

Redacted for Privacy

Dean of the College of Pharmacy

Redacted for Privacy

Dean of the Graduate School

I understand that my dissertation will become part of the permanent collection of Oregon State University libraries. My signature below authorizes release of my dissertation to any reader upon request.

Redacted for Privacy

Youn-Hi Woo, Author

ACKNOWLEDGEMENTS

Ph. D. work cannot be done by only one person's dedication and endurance. For the past five years in Corvallis, I have learned that I am what I am because of the people around me, who believe I can do better than what I thought I can do.

First of all, I would like to express my utmost gratitude to my advisor, Dr. Phil Proteau for his support, continual inspiration, and endless patience as a mentor, in addition to being a good friend through my graduate career. I also would like to thank Dr. T. Mark Zabriskie for his encouragement, constructive criticism, and helpful conversations. Dr. William H. Gerwick is deeply appreciated for his academic guidance and great inspiration. I thank Dr. David E. Horne for his support and insightful conversations. Additionally, I would like to thank my graduate council representative Dr. Michael M. Borman for taking his time as a GCR for me.

I would like to acknowledge Brian Arbogast and Jeff Morre for their support in MS, and Rodger Kohnert for his valuable help in NMR.

I am deeply grateful to my colleagues, Xihou Yin, Shiny Phaosiri, Laura Grochowski, and Roberta Fernandes. Pharmacy staff are greatly appreciated for their friendship and technical support, which saved me hundred times for the past years.

Friendship is the most valuable thing I have earned through these challenging years, so I thank my friends in Corvallis, Dojung Kim, Heidi Zhang, Lisa Nogle, David Blanchard, Jennifer Turcot, and Andy Bauman for their love, encouragement, and patience. I send my special thanks to The Kruegers and The Lees for providing me home in Corvallis.

Finally, I would like to express my deepest gratitude and love to my wonderful family in Seoul, for their support and love, dedicating this dissertation to my greatest parents, Sangbong Woo and Heejae Gu.

CONTRIBUTION OF AUTHORS

Chapter II: Chanokporn Phaosiri performed the synthesis of the 2-C-methyl erythritol triacetate standard and explored the NMR characteristics of the bisacetonide derivative of 2-C-methyl erythritol in acetone-d₆. Dr. R. Thomas Williamson ran HSQC, HMBC, GNOESY, and 1D DPGSE NOE experiments for the bisacetonide derivative of 2-C-methyl erythritol.

Chapter III: Dr. Xihou Yin prepared the initial recombinant DXR from *Synechocystis* PCC 6803. Dojung Kim synthesized the *N*-methyl *N*-formyl derivative of fosmidomycin.

TABLE OF CONTENTS

CHAPTER I GENERAL INTRODUCTION

Isoprenoid Natural Products and the Mevalonate Pathway	1
The Non-Mevalonate Pathway	6
Elucidation of the Entire Non-Mevalonate Pathway	13
Distribution of The Non-Mevalonate Pathway	23
Deoxyxylulose Phosphate Isomeroreductase (DXR) and Fosmidomycin	25

CHAPTER II STUDY OF THE STEREOCHEMISTRY OF THE DXR REDUCTION REACTION

Introduction	32
Results and Discussion	40
Experimental	53

CHAPTER III FOSMIDOMYCIN ANALOGS: SYNTHESES AND KINETIC STUDIES

Introduction	62
Results and Discussion	74
Experimental	103

CHAPTER IV CONCLUSIONS 127

BIBLIOGRAPHY 131

LIST OF FIGURES

Figure		Page
I.1	Examples of biologically important isoprenoids.	3
I.2	An example of chain elongation and further modifications in isoprenoid biosynthesis.	4
I.3	The mevalonate pathway to IPP.	5
I.4	Incorporation of [1- ¹³ C] acetate into aminobacteriohopanetriol by <i>Rhodopseudimonas palustris</i> .	7
I.5	Labeling patterns of IPP units	8
I.6	Proposed formation of DXP from glyceraldehyde-3-phosphate and pyruvate with subsequent transformation to IPP.	10
I.7	The proposed conversion mechanism of DXP to MEP by DXR in the non-mevalonate pathway.	12
I.8	The 3 rd step of the non-mevalonate pathway; cytidylation of MEP.	13
I.9	The 4 th step of the non-mevalonate pathway; phosphorylation of CDP-ME.	14
I.10	The 5 th step of the non-mevalonate pathway; cyclization of CDP-ME ₂ P.	15
I.11	The last two steps of the non-mevalonate pathway.	18
I.12	Proposed mechanism of the IspG reaction patterned after vitamin K epoxyquinone reductase mechanism.	18
I.13	Interconversion of IPP into DMAPP catalyzed by IPP isomerase.	19
I.14	The incorporation studies by (A) Arigoni's and (B) Rohmer's group.	21
I.15	The non-mevalonate pathway for IPP biosynthesis.	22
I.16	α -Ketol rearrangement in (A) DXR (B) AHIR mediated reaction	26

LIST OF FIGURES (CONTINUED)

Figure		Page
I.17	Proposed retroaldol/aldol mechanism by (A) L-Ru5P 4-epimerase (B) by DXR.	29
I.18	α -Ketol rearrangement in DXR mediated reaction in IPP biosynthesis with its inhibitors.	30
II.1	Conversion of DXP to MEP by DXR	33
II.2	Two possible conversion mechanisms by DXR (A) α -ketol type rearrangement (B) retroaldol/aldol type mechanism.	34
II.3	Isomerization and reduction catalyzed by acetohydroxy acid isomeroreductase (AHIR) and the reaction intermediate analogs.	35
II.4	Reaction of yeast alcohol dehydrogenase (YADH) with (A) <i>pro-R</i> deuterium labeled and (B) <i>pro-S</i> deuterium labeled NADPH.	36
II.5	Proposed mechanism of conversion step by DXR.	38
II.6	2-C-methyl erythritol and the bisacetonide derivative.	40
II.7	Structural assignments for the bisacetonide derivative of ME	42
II.8	Synthesis of unlabeled and labeled DXP.	44
II.9	Treatment of enzymatic product to the bisacetonide derivative.	45
II.10	Partial ^1H NMR spectrum of 2-C-methylerythritol bisacetonide.	46
II.11	GC/EIMS spectra of triacetate derivative.	48
II.12	^1H NMR of (A) synthetic triacetate derivative	49
II.13	Stereochemical illustration of conversion of DXP to MEP by DXR.	50
III.1	Examples of natural C-P compounds with interesting biological activities.	63

LIST OF FIGURES(CONTINUED)

Figure	Page
III.2 The first committed step of peptidoglycan biosynthesis and fosfomycin.	64
III.3 Examples of phosphonic acid antibiotics synthesized as analogs of FR900098 and fosmidomycin.	65
III.4 The second step of the non-mevalonate pathway, DXR mediated conversion of DXP to MEP.	67
III.5 Fosmidomycin analogs designed and synthesized.	72
III.6 Synthesis of fosfoxacin and acetyl fosfoxacin.	74
III.7 Inhibition of DXR by fosfoxacin and acetyl fosfoxacin.	79
III.8 Synthesis of Carboxylate analog of fosmidomycin.	81
III.9 Inhibition of DXR by the carboxylate analog of fosmidomycin.	81
III.10 Synthesis of sulfamate analog of fosmidomycin.	83
III.11 Inhibition of DXR by Sulfamate analog of fosmidomycin.	83
III.12 Synthesis of <i>N</i> -methyl analogs of fosmidomycin.	85
III.13 Inhibition of DXR by <i>N</i> -methyl analogs of fosmidomycin.	86
III.14 Synthesis of hydroxamate analog of fosmidomycin.	88
III.15 Inhibition of DXR by Hydroxamate analog of fosmidomycin.	89
III.16 Kirby-Bauer disk test for fosfoxacin and acetylfosfoxacin.	92
III.17 NADPH and fosmidomycin modeled into the putative active site of DXR from its crystal structure.	97
III.18 Examples of the compounds with incomplete syntheses/kinetic studies.	98

LIST OF FIGURES(CONTINUED)

Figure	Page
III.19 Synthesis of Laurencione phosphate.	99
III.20 Synthesis of the phosphate analog of D-Glucal.	101

LIST OF ABBREVIATIONS

AHIR	Aceto Hydroxy acid Isomeroreductase
bs	broad singlet
CAT	Chloramphenicol Acetyl Transferase
CDP-ME	4-diphosphocytidyl-2-C-methylerythritol
CDP-ME2P	4-diphosphocytidyl-2C-methyl-D-erythritol-2-phosphate
CI	Chemical Ionization
CTP	Cytidine 5'-triphosphate
d	doublet
DCC	1,3-dicyclohexylcarbodiimide
DMA	<i>N,N</i> -dimethylacetamide
DMAP	4-(dimethylamino)pyridine
DMAPP	DiMethylAllyl Diphosphate
DPFGSE	Double Pulsed Field Gradient Spin Echo
DXP	1-deoxy-D-xylulose-5-phosphate
DXR	DXP isomeroreductase
EI	Electronic Ionization
FAB	Fast Atomic Bombardment
FMT	4- <i>N</i> -formyl-2-methyl-5-mercapto-1,3,4-Thiadiazole
FPP	Farnesyl Diphosphate
GC	Gas Chromatography
GNOESY	Gradient Nuclear Overhauser Effect Spectroscopy
GPP	Geranyl Diphosphate
HMBC	Heteronuclear Multiple Bond Correlation
HMB-PP	1-hydroxy-2-methyl-2-(<i>E</i>)-butenyl 4-diphosphate
HMG CoA	3-hydroxy-3-methylglutaryl-CoA
HOBt	1-Hydroxybenzotriazole hydrate
HRMS	High Resolution Mass Spectrometry

LIST OF ABBREVIATIONS (CONTINUED)

HSQC	Heteronuclear Single-Quantum Correlation
IpOHA	<i>N</i> -hydroxy- <i>N</i> -isopropylloxamate
IPP	Isopentenyl Diphosphate
IR	Infra Red
LAH	Lithium Aluminum Hydride
LAD	Lithium Aluminum Deuteride
LGT	Lateral Gene Transfer
m	multiplet
ME	2-C-methylerythritol
MECDP	2C-Methyl-D-Erythritol 2,4-CycloDiphosphate
MEP	2-C-methylerythritol-4-phosphate
MIC	Minimum Inhibitory concentration
MS	Mass Spectrometry
NADPH	reduced Nicotinamide Adenine Dinucleotide Phosphate
NMO	4-Methylmorpholine <i>N</i> -oxide
NMR	Nuclear Magnetic Resonance
NOE	Nuclear Overhauser Effect
PMA	PhosphoMolybdic Acid
q	quartet
s	singlet
SAR	Structure Activity Relationship
t	triplet
TBDMSCI	<i>tert</i> -Butyldimethylsilyl chloride
TFA	Trifluoro Acetic acid
Tf ₂ O	Trifluoromethanesulfonic anhydride
TLC	Thin-Layer Chromatography
TPAP	Tetrapropylammonium perruthenate

LIST OF ABBREVIATIONS (CONTINUED)

TsOH

p-Toluenesulfonic acid

STUDIES OF NON-MEVALONATE ISOPRENOID BIOSYNTHESIS: THE 1-DEOXY-D-XYLULOSE-5-PHOSPHATE ISOMEROREDUCTASE (DXR) MEDIATED REACTION

CHAPTER I

GENERAL INTRODUCTION

Isoprenoid Natural Products and the Mevalonate Pathway

Isoprenoids are natural compounds which are derived from one or more five-carbon isoprene (2-methylbutadiene) units as a building block. The 'biogenetic isoprene rule' by Ruzicka states that isoprenoids are derived from an integral number of biological equivalents of isoprene, condensed together in a head-to-tail or tail-to tail manner, with subsequent structural modification(s).¹ The biological equivalent of isoprene was isolated and identified as isopentenyl diphosphate (IPP) in the mid 1950's¹ and has been studied since then regarding its biosynthesis, chemistry, and incorporation into more elaborate isoprenoid compounds.

Isoprenoid natural products are ubiquitous in all forms of life, and are one of the largest group of the natural product families, composed of >30,000 compounds.² Although the function of most isoprenoids is still largely unidentified, the known critical biological functions of isoprenoids include mediation of cell wall and glycoprotein biosynthesis (dolichol phosphates), electron transport and redox systems (ubiquinone, menaquinone and plastoquinone), photooxidative protection and photosynthetic light harvesting (carotenoids), participation in lipid membrane structure (cholesterol and ergosterol in eukaryotes), biological membrane stabilizers (hopanoids), modification of proteins involved in

signal transduction (prenylated proteins), modification of *t*-RNA (*N*⁶-isopentenyladenine), and intercellular signaling and developmental control (estrogens, gibberellins),³ all of which play essential roles for organisms that produce these compounds. Despite their significant roles, distribution of these isoprenoids varies with the organisms. For example, bacterial isoprenoids differ from eukaryote isoprenoids in that bacteria do not synthesize sterols except for two species.² Instead, some bacteria produce amphiphilic hopanoids, which act as membrane stabilizers such as sterols. In contrast to archaea which lack ubiquinones, eubacteria and eukaryotes biosynthesize ubiquinones to utilize as an electron carrier in the aerobic respiratory chain. In addition to the functions above, numerous isoprenoids have demonstrated medicinal value. For example, paclitaxel is used as a potent antitumor agent and ginkgolides have been shown to be major active ingredients in the traditional herbal medicine *Gingko biloba*. The structures of isoprenoids representing the functions described above are shown in Fig.I.1.

Structural diversity of these isoprenoids is obtained through the combination of different numbers of isoprene units used, linear elongation or cyclization, and subsequent modifications, all of which originate from the condensation of IPP and dimethylallyl diphosphate (DMAPP). IPP undergoes a stereospecific isomerization to provide its allylic partner, DMAPP. Linear condensation of isoprenoids is initiated by the ionization of an allylic diphosphate ester (e.g. DMAPP), followed by a nucleophilic attack from the terminal methylene of the co-substrate IPP. The first condensation between IPP and DMAPP provides geranyl diphosphate (GPP), and the addition of one more IPP affords farnesyl diphosphate (FPP) (Fig.I.2). The linear elongation product, FPP, undergoes further modifications such as cyclization, oxidation, rearrangement, hydroxylation, etc. to give the final

compounds.⁴ The biosynthesis of an aphid inhibitor, polygodial, provides an example (Fig.1.2).

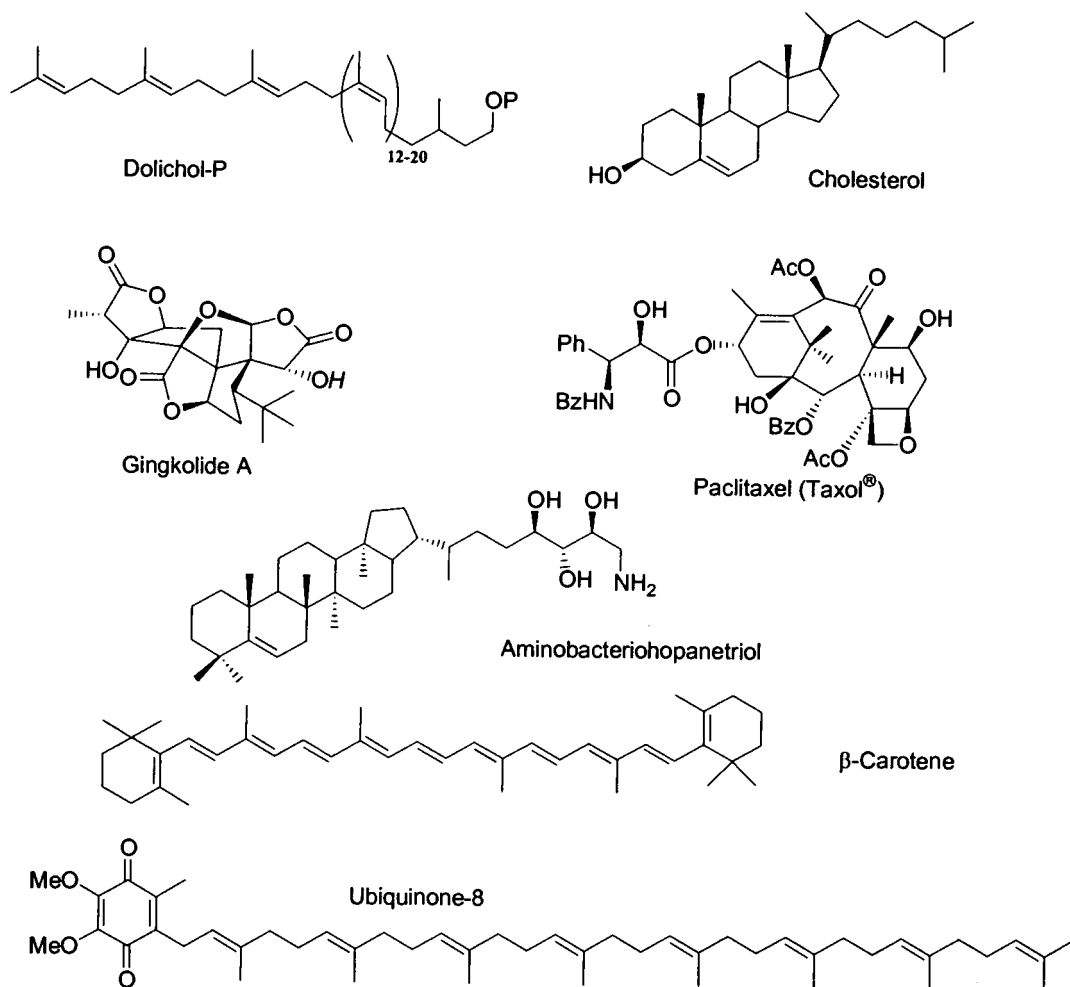


Fig.1.1 Examples of biologically important isoprenoids.

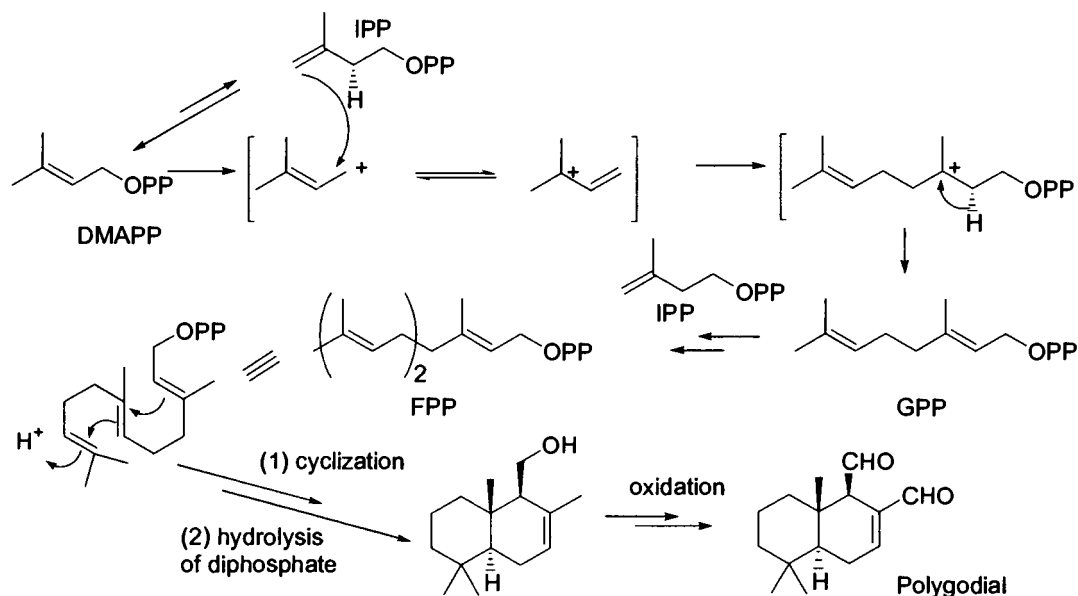


Fig.1.2. An example of chain elongation and further modifications in isoprenoid biosynthesis.

The study of isoprenoid natural products not only expands our knowledge in basic science and enzymology, but it also explores the commercial potential of isoprenoids. Besides the medical uses stated above, isoprenoids from divergent biosynthetic pathways have been studied for numerous purposes. For example, studies of sterol biosyntheses have led to the development of the sterol biosynthesis inhibitors, such as 2,3-oxidosqualene cyclase inhibitors, for agrochemical purposes as antifungal and herbicidal agents.⁴ Other sterol biosynthesis inhibitors, *i.e.* fungal sterol 14 α -demethylase and 3-hydroxy-3-methylglutaryl-CoA (HMG-CoA) reductase inhibitors, have been developed for pharmaceutical purposes such as antifungals and hypocholesterolemic agents respectively.^{1,4} In addition to the commercial value of isoprenoid biosynthesis inhibitors, studying isoprenoid biosynthesis also offers an opportunity for manipulation of isoprenoids through classical fermentation technology along with

molecular biology, genetics, and bioengineering technologies. Paclitaxel, a potent anticancer agent, is an example of an isoprenoid being studied for the purpose of improving production through a variety of those techniques.⁵

Encouraged by the interesting aspects of isoprenoid chemistry discussed above, researchers have intensively studied isoprenoid natural products. One of the early results of these studies was the discovery of the biosynthetic route to isoprenoids in the 1950's and 1960's. Early studies of the formation of isoprenoids demonstrated that IPP is derived from (3R)-3,5-dihydroxy-3-methylpentanoic acid, commonly known as mevalonic acid. Mevalonate is synthesized in three steps from acetyl CoA: (1) Condensation of two acetyl CoAs to form acetoacetyl CoA; (2) Addition of a third acetyl CoA to make 3-hydroxy-3-methylglutaryl-CoA (HMGCoA); (3) Reduction of HMGCoA by NADPH to provide mevalonic acid (Fig.1.3).⁶ Mevalonate itself undergoes three successive phosphorylations followed by a decarboxylation to form IPP. Due to the critical role of mevalonate in isoprenoid biosynthesis the pathway was named the mevalonate pathway.

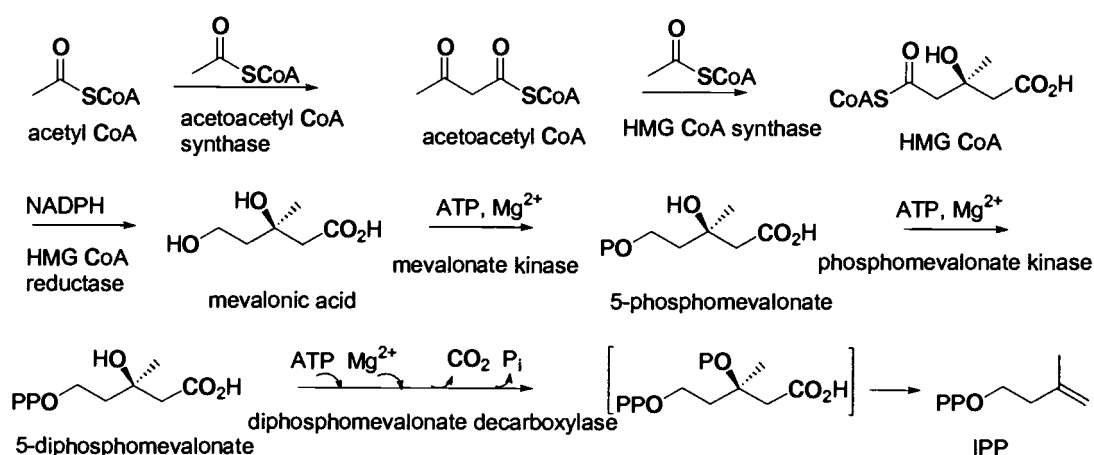


Fig.1.3 The mevalonate pathway to IPP.

As a result of extensive studies on this pathway, the enzymes involved in the early stages of the mevalonate pathway have been well characterized. HMGCoA reductase, the third enzyme in the mevalonate pathway, catalyzes the rate limiting step of this pathway and has been a target for inhibition of cholesterol biosynthesis. Investigation of this enzyme led to the development of the commercially successful inhibitors, the statins, e.g. lovastatin (Mevacor®) and simvastatin (Zocor®).

The Non-Mevalonate Pathway

Despite ambiguous and even controversial evidence found in higher plants and eubacteria,^{7,8} including *Escherichia coli*, the mevalonate pathway was believed to be the only natural method for the synthesis of IPP until the early 1990's. Although investigations on the mevalonate pathway, predominately using fungi and rat liver tissue, resulted in a thorough understanding of IPP biosynthesis, questions remained concerning isoprenoid biosynthesis in eubacteria and higher plants.⁷⁻¹¹ For example, puzzling results were obtained from the ¹⁴C- or ¹³C-labeled acetate incorporation into the prenyl side chain of ubiquinone in *E. coli*,^{9,11} [¹³C₆]glucose and [6-²H₂]glucose incorporation into pentalenolactone in *Streptomyces* UC5319,¹² and [1-¹³C]-and [2-¹³C]-acetate into hopanes from three Gram-negative bacteria, *Methylobacterium organophilum*, *Rhodopseudomonas palustris*, and *Rhodopseudomonas acidophila* (Fig.1.4). Arigoni *et al.* also observed unexpected labeling pattern from the incorporation studies into ginkgolide (Fig.1.4).¹³ Researchers tried to explain these results either by "compartmentation" of acetyl CoA metabolism or by an "as-yet-unknown sequence of fully different enzymatic reactions".¹⁴

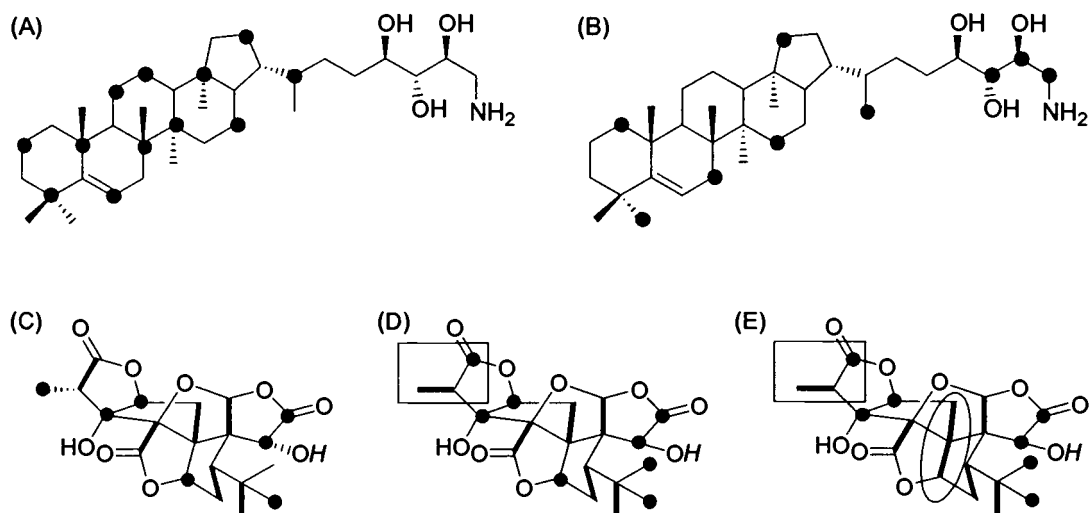


Fig.I.4 Incorporation of $[\text{1-}^{13}\text{C}]$ acetate into aminobacteriohopanetriol by *Rhodopseudomonas palustris*. (A) Expected incorporation pattern from the mevalonate pathway;(B) Observed incorporation pattern.¹⁴ Incorporation of $[\text{U-}^{13}\text{C}]$ glucose for ginkgolide. (C) Expected labeling pattern (D) Observed (40-50 %) (E) Observed (50-60 %).¹³

In 1993, however, independent studies by two different research groups clearly explained these ambiguities by the discovery of an alternate pathway to IPP.^{14,15} These reports proposed that the five-carbon framework of the IPP unit originates from the condensation of a two-carbon unit derived from pyruvate decarboxylation and a triose phosphate derivative, and that a rearrangement step is required.¹⁴ Incorporation studies utilizing ^{13}C -labeled glucose, acetate, pyruvate or erythrose allowed Rohmer and colleagues to determine the origin of the carbons of hopanoids and ubiquinones from the bacteria *Zymomonas mobilis*, *Methylobacterium fujisawaense*, *Escherichia coli*, and *Alicyclobacillus acidoterrestris*. Arigoni and Broers synthesized deuterated 1-deoxyxylulose and showed successful incorporation of it into IPP unit.¹⁵

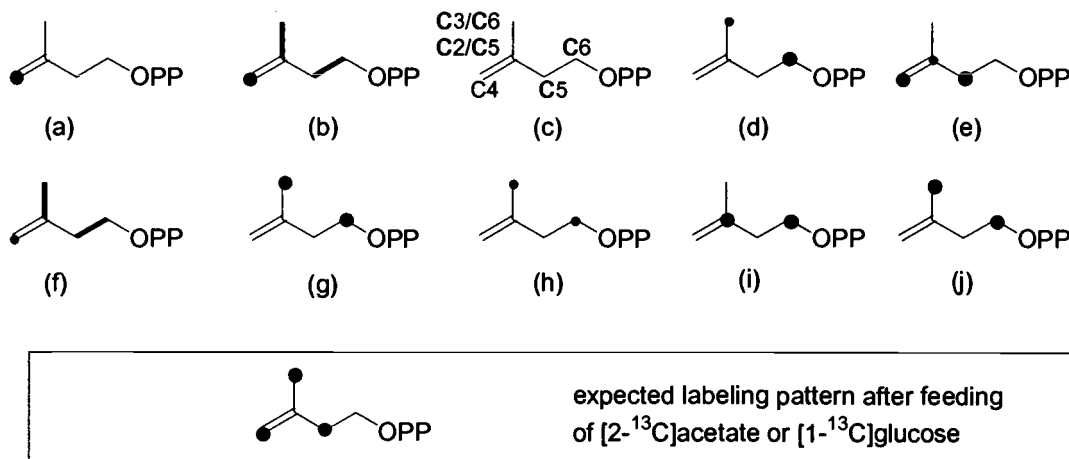


Fig.1.5 Labeling patterns of IPP units in bacteria utilizing the non-mevalonate pathway: (a) after incubation of $[1-^{13}\text{C}]$ acetate; (b) after feeding of $[1,2-^{13}\text{C}]$ acetate; (c) in *Z. mobilis* after feeding of ^{13}C -labeled glucose isotopomers; (d) in *M. fujisawaense* feeding of $[6-^{13}\text{C}]$ glucose; (e) in *M. fujisawaense* after feeding of $[4,5-^{13}\text{C}_2]$ glucose; (f) in *Z. mobilis* after feeding of $[U-^{13}\text{C}_6]$ glucose; (g) in *E. coli* and *A. acidoterrestris* after feeding of $[6-^{13}\text{C}]$ glucose; (h) in *E. coli* and *A. acidoterrestris* after feeding of $[1-^{13}\text{C}]$ glucose; (i) in *M. fulvus* after feeding of $[1-^{13}\text{C}]$ acetate; and (j) in *E. coli* and *M. fujisawaense* after feeding of $[3-^{13}\text{C}]$ pyruvate.² (labeling intensity found was represented as the size of filled dots)

Through the labeling patterns of the isoprene units in hopanoids and ubiquinone, the authors proposed: (1) C-4 and C-5 of glucose are simultaneously introduced into isoprenic units; (2) the formerly introduced C2 precursor is inserted between the C-4 and C-5 atoms; (3) a rearrangement step is required; and (4) that these observations completely rule out the classical mevalonate pathway in these bacteria. These results also ran counter to the other modified proposals for the formation of mevalonate from different sources such as leucine or acetolactate.⁹ Results

from the incubation studies with ^{13}C -labeled precursors ruled out acetyl CoA and HMGC_oA as precursors for isoprenoid biosynthesis in the bacteria investigated. Furthermore, complementary experiments with labeled HMGC_oA, mevalonate, and mevalonate-5-phosphate did not result in labeled IPP or DMAPP, supporting the absence of the mevalonate pathway and the existence of an alternate pathway to isoprenoids in, *E. coli* and *Z. mobilis*.² This alternate pathway* was referred to as the non-mevalonate pathway.¹⁴

During the search for the correct precursors, Rohmer's group performed further incorporation studies with ^{13}C -labeled glycerol or pyruvate with *E. coli* mutants lacking triose phosphate metabolism enzymes to block the interconversion between C₃ units. In addition to *E. coli*, the authors investigated incorporation patterns into hopanoids from *Z. mobilis* utilizing [U- $^{13}\text{C}_6$] glucose.¹⁶ Whereas *E. coli* utilizes a variety of carbon sources and also has a complete tricarboxylic acid (TCA) cycle, *Z. mobilis* has a very narrow substrate range and does not convert phosphoenol pyruvate and thus is unable to synthesize glyceraldehyde 3-phosphate from pyruvate. Therefore, utilizing *Z. mobilis* for incubation with glucose isotopomers allowed the authors to determine the origins of the carbons.⁷ Based on these results, Rohmer and colleagues elucidated the first step of this novel pathway to IPP (Fig. I.6), proposing: (1) pyruvate and glyceraldehyde-3-phosphate as the starting compounds; (2) a rearrangement as seen in valine and leucine biosynthesis to obtain the C₅

* Several alternatives for the name of this new pathway have been suggested: the non-mevalonate pathway, the mevalonate independent pathway, GAP/pyruvate pathway, DXP pathway, DOXP pathway, and MEP pathway. The MEP pathway was recommended as the general name for this pathway at the 4th European Symposium on Plant Isoprenoids, Barcelona, Spain, 1999. However, no consensus has been reached in the literature and the non-mevalonate pathway has the most common use. Therefore, the non-mevalonate pathway will be used for the remainder of the text.

framework of IPP; and (3) 1-deoxy-D-xylulose-5-phosphate (DXP) as the condensation product.

DXP had been proposed as an intermediate in IPP biosynthesis by Arigoni's group independently of Rohmer's work.¹⁵ Successful incorporation studies using synthetic [1-²H₁]deoxy-D-xylulose into the prenyl sidechain of ubiquinone in *E. coli* supported this pentulose as a precursor for isoprene units, most likely after phosphorylation at C-5. An enzymatic acyloin-type condensation between pyruvate and D-glyceraldehyde had been reported to provide 1-deoxy-*threo*-pentulose (*i.e.* 1-deoxy-D-xylulose), which was also known as a precursor of the C₅ unit of the thiazole ring of thiamine.^{17,18} This biochemical precedence led to the discovery of *dxs*, the gene that encodes DXP synthase. Recombinant DXP synthase was shown to efficiently produce DXP *in vitro*.¹⁹⁻²¹

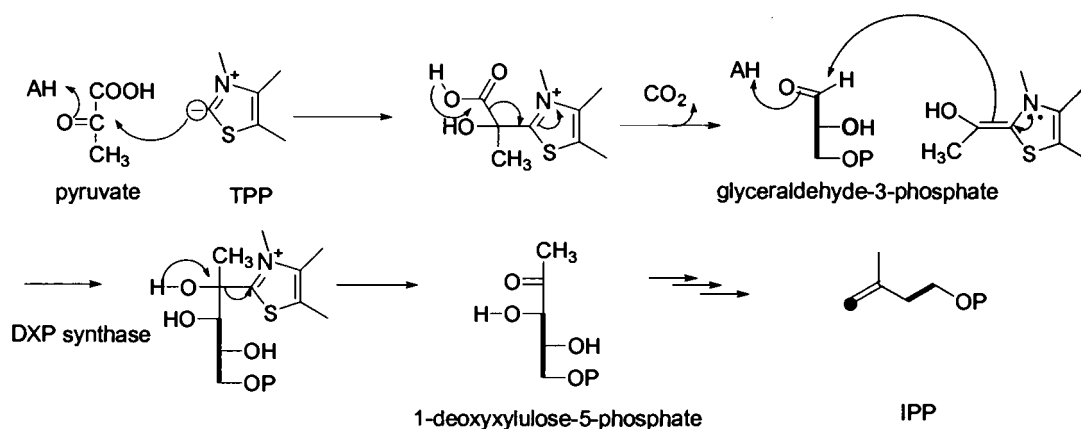


Fig.I.6 Proposed formation of DXP from glyceraldehyde-3-phosphate (labeled with ¹³C; shown by the bold line) and pyruvate with subsequent transformation to IPP.¹⁶

If DXP is a precursor to IPP, then a rearrangement step is required to provide the branched C₅ skeleton. A proposed acid catalyzed α -ketol rearrangement implicated the compound 2-C-methyl-D-erythrose or its 4-

phosphate as a possible candidate for the second step of the non-mevalonate pathway.¹⁶ The reduction product of this erythrose, 2-C-methylerythritol (ME), and its derivatives were known as natural products prior to the discovery of the non-mevalonate pathway. The 2,4-cyclodiphosphate of ME is found under normal growth conditions in *Desulfovibrio desulficans*.²² The cyclodiphosphate also accumulates under oxidative stress conditions in several bacteria,²³ including *Corynebacterium ammoniagenes*. The presence of ME or 2-C-methyl-D-erythronolactone had been reported from higher plants.²⁴ Elucidation of the second step of the non-mevalonate pathway resulted from the investigation of whether ME or its 4-phosphate analog (MEP) was an intermediate of the non-mevalonate pathway.

The biosyntheses of 2-C-methylerythritol and isoprenoids in *Corynebacterium ammoniagenes*, a bacterium which produces the 2,4-cyclodiphosphate of ME were examined using labeled glucose precursors. The labeling patterns observed were identical when [1-¹³C]-, [6-¹³C]-, or [U-¹³C₆] glucose were incorporated into the isoprenic units of dihydromenaquinones and into 2-C-methyl erythritol (ME).²⁵ This suggested that ME could be a precursor to IPP in this bacterium. Furthermore, the deuterated analog of ME, 2-C- [1,1-²H₂] methyl-D-erythritol, was incorporated in low yield into the prenyl sidechain of ubiquinone from *E. coli* while the L-isomer was not incorporated. The authors proposed that the low yield was due to the lack of a specific kinase which converts ME to MEP. This experiment, even with a low level of incorporation, strongly suggested that MEP is involved in the early steps of IPP biosynthesis, most likely from the conversion of DXP to 2-C-methylerythrose-4-phosphate and subsequent reduction to 2-C-methylerythritol-4-phosphate (MEP).

Despite the promising results from the incorporation studies, the enzyme(s) involved in this step(s) remained in question. However, in 1998,

Seto and co-workers reported a gene associated with the conversion of DXP to MEP from *E. coli*, *yaeM* (initially renamed *dxr*, currently designated as *ispC*). *IspC* was successfully overexpressed, and the recombinant protein was able to convert DXP to MEP *in vitro*.^{26,27} In this report, the authors demonstrated that the gene product, DXP isomeroreductase* (DXR),^{26,28,29} catalyzes a two step reaction, isomerization of DXP and a NADPH-dependent reduction. In addition to NADPH, a divalent metal ion(s), Mn^{2+} , Co^{2+} , or Mg^{2+} is required as a cofactor (Fig.I.7).²⁶ After the first report on DXR, there have been further reports on the orthologs of the *E. coli* DXR from *Mentha piperita*, *Arabidopsis thaliana*, *Synechocystis* sp. PCC6803, *Zymomonas mobilis*, *Streptomyces* sp. CL 190, *Pseudomonas aeruginosa*, *Synechococcus leopoliensis*, and *Plasmodium falciparum*.³⁰⁻³⁴ DXP is a biosynthetic intermediate not only for IPP but also for thiamine and pyridoxol. Therefore, DXR mediates the first committed step of the non-mevalonate pathway providing the first committed intermediate, MEP.

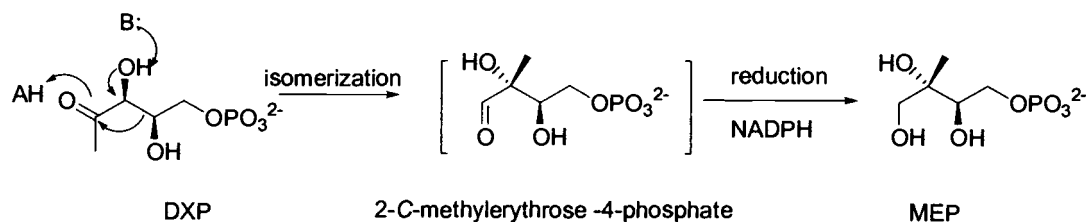


Fig.I.7 The proposed conversion mechanism of DXP to MEP by DXR in the non-mevalonate pathway.

* The initial name proposed for the *dxr* (*ispC*) gene product was deoxyxylulose 5-phosphate reductoisomerase.²⁵ Two other names have also been proposed, DXP isomeroreductase²⁷ and MEP synthase.²⁸ The name MEP synthase, while consistent with the naming of most isoprenoid enzymes as synthases, provides no descriptive information about the reaction catalyzed. Because the generally accepted mechanism requires isomerization prior to reduction, we prefer isomeroreductase as an appropriate name for this enzyme and will use it throughout the text.

Elucidation of the Entire Non-Mevalonate Pathway

Extensive studies on the non-mevalonate pathway for the past several years have elucidated all seven steps.³⁵⁻⁴² In the search for downstream intermediates after MEP in this pathway, Bacher *et al.* showed that an enzyme isolated from cell extracts of *E. coli* converts MEP to 4-diphosphocytidyl-2-C-methylerythritol (CDP-ME) by reaction with CTP (Fig.1.8). The responsible gene (*ygbP*, later designated as *ispD*) was identified and overexpressed in *E. coli*, showing that IspD (YgbP) prepares 4-diphosphocytidyl-[2-¹⁴C]2-C-methylerythritol from [2-¹⁴C]2-C-methylerythritol-4-phosphate. The resulting radiolabeled CDP-ME was successfully incorporated into carotenoids by isolated chromoplasts of *Capsicum annuum*, illustrating that CDP-ME was a viable intermediate in the pathway.³⁵ Seto *et al.* investigated the same step utilizing *E. coli* mutants and confirmed that CDP-ME is the next intermediate of the non-mevalonate pathway after MEP.³⁷ Studies of the biochemical characteristics of CDP-ME synthetase (IspD) determined that it requires CTP and divalent ion(s) (preferably Mg²⁺ but it is also active with Mn²⁺, Co²⁺) for its activity. A crystal structure of the apo form of this enzyme has been refined with a high resolution (1.55 Å), as well as the complexed form with both CTP-Mg²⁺ (1.5 Å) and CDP-ME-Mg²⁺ (1.8 Å).⁴³

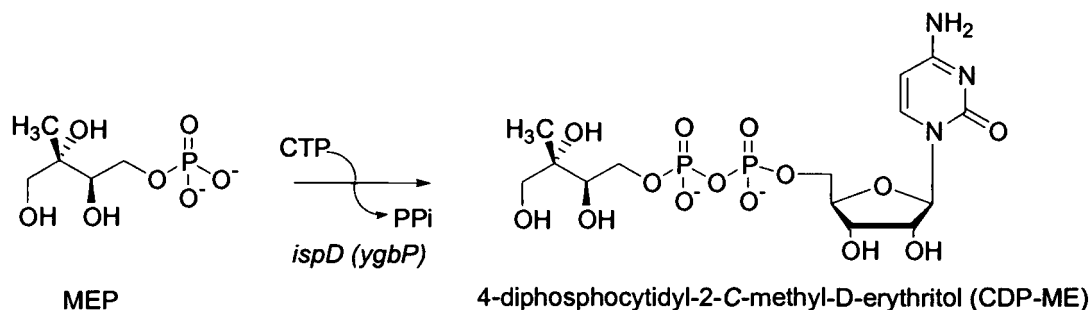


Fig.1.8 The 3rd step of the non-mevalonate pathway; cytidylation of MEP.

A search for orthologous genes with similar genomic distribution patterns to genes from the non-mevalonate pathway (*i.e.* *dxs*, *ispC* and *ispD*) suggested that the unannotated genes, *ychB* (*ispE*) and *ygbB* (*ispF*), in *E. coli* could potentially be involved in the non-mevalonate pathway. Overexpression of *ispE* and subsequent biochemical characterization of the gene product demonstrated that the next step after CDP-ME was a phosphorylation reaction at the C2 position of 4-diphosphocytidyl-2-C-methylerythritol, producing 4-diphosphocytidyl-2C-methyl-D-erythritol-2-phosphate (CDP-ME2P).³⁸ This reaction is ATP dependent, and the structure of the product was determined by ¹H, ¹³C, and ³¹P NMR. Seto's group later confirmed these results (Fig.1.9).³⁹ This enzyme is now called CDP-ME kinase.³⁸

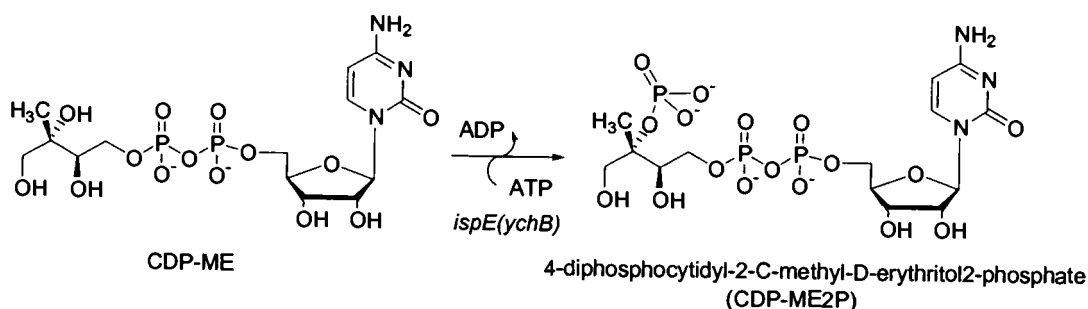


Fig.1.9 The 4th step of the non-mevalonate pathway; phosphorylation of CDP-ME.

The overexpressed *ispF* (*ygbB*) was shown to be involved in the non-mevalonate pathway.⁴⁰ The products from *IspF* action on CDP-ME2P were determined to be the structurally intriguing 2C-methyl-D-erythritol 2,4-cyclodiphosphate (MECDP) and CMP. Interestingly, MECDP had been found previously in certain microorganisms under stress conditions (Fig.1.10).^{24,40,44} A recent crystal structure of this enzyme (now named as

MECDP synthase) suggests that the mechanism of the reaction involves a Mn^{2+} -catalyzed formation of the cyclic phosphodiester bond.⁴⁵

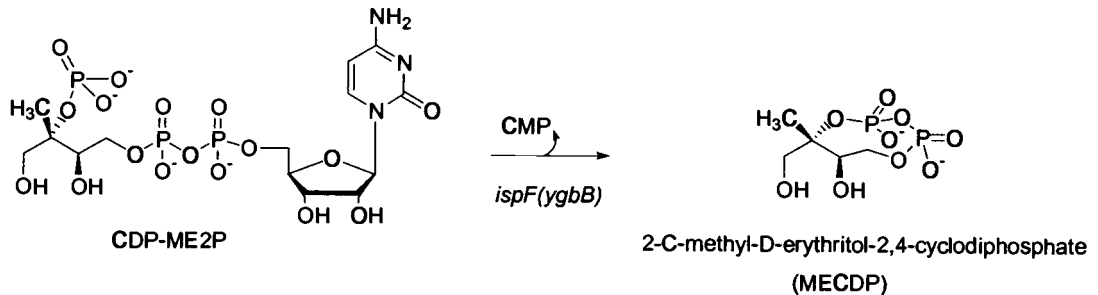


Fig.I.10 The 5th step of the non-mevalonate pathway; cyclization of CDP-ME2P.

The genes involved in the last two steps of the non-mevalonate pathway, *gcpE* (*ispG*) and *lytB* (*ispH*), were identified as potential candidates through a search for unknown genes that have the same distribution with the non-mevalonate pathway specific genes. The occurrence of the *gcpE* gene in fully sequenced bacterial genomes is well correlated with the occurrence of the *dxr* gene; 19 out of 29 genomes searched have both *gcpE* and *dxr*. The association of *gcpE* with the non-mevalonate pathway was originally accomplished through genetics studies.⁴⁶ A mutant strain of *E. coli* was designed to contain a synthetic operon encoding yeast mevalonate kinase, human 5-phosphomevalonate kinase, and yeast 5-diphosphomevalonate decarboxylase with its IPP isomerase integrated. The *gcpE* gene of this mutant *E. coli* was disrupted with a chloramphenicol acetyl transferase (CAT) cassette, which demonstrated that this mutant required mevalonate for its survival.

Later, the role of GcpE (IspG) was determined to be the formation of 1-hydroxy-2-methyl-2-(*E*)-butenyl 4-diphosphate (HMB-PP) from MECDP (Fig. I.11).⁴¹ In this report, the authors engineered recombinant *E. coli* cells expressing *xyIB* (encodes deoxyxylulose 5-kinase), *ispC*, *ispD*, *ispE*, and *ispF* to find high level of MECDP. The additional expression of the *gcpE* gene provided HMB-PP as an intermediate of the non-mevalonate pathway. Jomaa *et al.* also confirmed this result through extensive NMR experiments.⁴⁷ In their study using *lytB*-deficient mutants, a highly immunogenic compound accumulated while it was absent in *gcpE*-deficient mutants of *E. coli*. The possibility that an intermediate of the non-mevalonate pathway is responsible for the production of the immunogenic compound by activating human $\gamma\delta$ T cells has been suggested before Jomaa's report.⁴⁸ Jomaa *et al.* purified HMB-PP from *E. coli* Δ *lytB* mutants and they also showed that HMB-PP is 10^4 times more potent in activating human V γ 9/V δ 2 T cells than IPP. This result indicated that *lytB* is involved in the pathway after the point where *gcpE* plays its role, and the intermediate before *lytB*'s contribution activates human $\gamma\delta$ T cells.

Similar to the *gcpE* studies, it was predicted that the *lytB* (*ipsH*) gene is involved in the latter stages of the pathway. Gantt *et al.* provided the earliest evidence for *lytB*'s role.⁴⁹ They proposed that the *lytB* encodes an enzyme catalyzing the branching step or prior to the point where the pathway branches to form IPP and DMAPP. Their proposal was based on the observation that insertions in the coding region of *lytB* were lethal in a mutant of *Synechocystis* PCC6803 and that the supplementation with IPP and DMAPP was required for their survival.⁴⁹ This was soon supported by Jomaa *et al.* who reported that a mutant *E. coli* strain deleted for the *lytB* gene and engineered with the mevalonate pathway genes were viable only with a mevalonate supplement.⁵⁰

The metabolic role of LytB (IspH) was clarified by Rohdich and Eisenreich's work showing that exogenous [U-¹³C₅] 1-deoxy-D-xylulose (DX) was transformed into a 5:1 mixture of [U-¹³C₅] IPP and [U-¹³C₅] DMAPP in *E. coli*.⁴² The *E. coli* strain used in this study was engineered to express *lytB* (*ispH*) as well as *xylB* and the *ispC*, *D*, *E*, *F*, and *G* genes. The *xylB* gene was added to enable *E. coli* to convert exogenous [U-¹³C₅] DX to [U-¹³C₅] DXP, and the rest of known genes involved in the non-mevalonate pathway, *ispCDEFG* genes, were expressed to enable high level production of the putative LytB substrate. The metabolic products of the recombinant IspH (LytB) protein were purified and identified as DMAPP and IPP through ¹³C NMR. The authors of this paper concluded "...that LytB (IspH) is capable of generating both IPP and DMAPP...starting with 1-hydroxy-2-methyl-2-(*E*)-butenyl 4-diphosphate as a single precursor..." but mechanistic issues were unanswered.⁴² Very recently, however, Rohdich *et al.* successfully demonstrated that a cell extract of the *E. coli* strain manipulated for over-expression of the *lytB* (*ispH*) gene catalyzes the conversion of 1-hydroxy-2-methyl-2-(*E*)-butenyl 4-diphosphate into IPP and DMAPP.⁴² They also reported that the reaction requires NADH, FAD, divalent metal ion(s) (Co²⁺, preferably), and one or more unidentified proteins.⁵¹ The fact that LytB (IspH) provides both IPP and DMAPP is of particular interest when contrasted with the mevalonate pathway which strictly requires an IPP:DMAPP isomerase. Despite some unresolved questions, such as the mechanistic details of each step, the studies on the IspH (LytB) protein regarding its role in the pathway complete the elucidation of the individual steps of the non-mevalonate pathway (Fig.I.11).

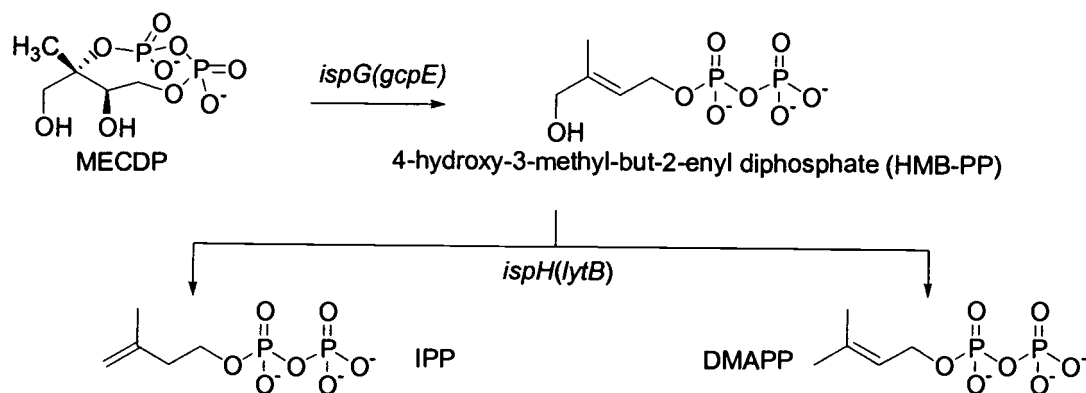


Fig.I.11 The last two steps of the non-mevalonate pathway.

Extensive studies are underway to identify the mechanistic aspects of the individual steps of the non-mevalonate pathway. For example, Bacher *et al.* suggested two possible mechanisms as to the ring opening mechanism from MECDP to HMB-PP.⁴¹ These two hypothetical mechanisms (one patterned after the mechanism of vitamin K epoxyquinone reductase and the other patterned after ribonucleotide reductase) involve the participation of well-conserved Cys residues in IspG.

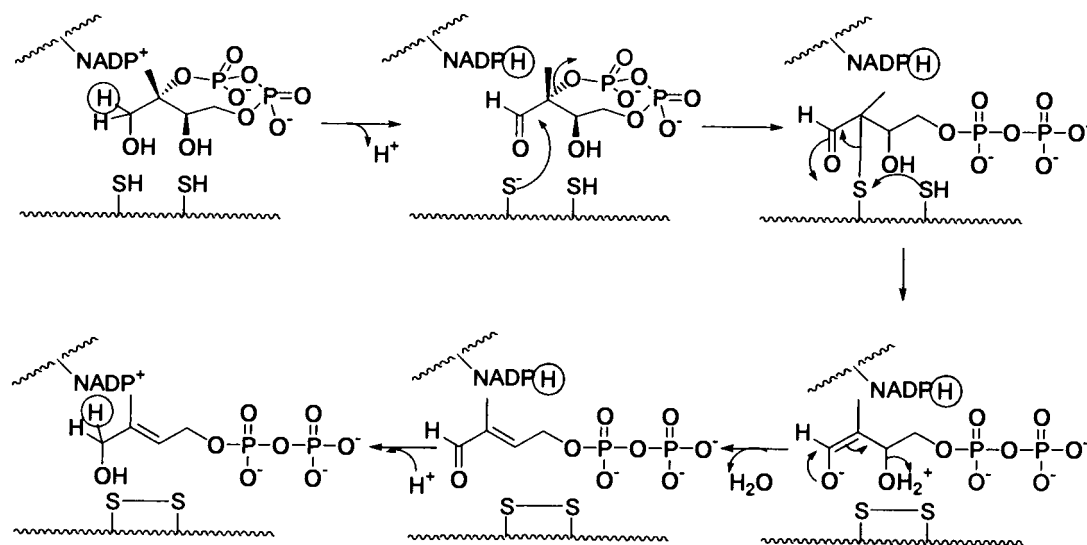


Fig.I.12 Proposed mechanism of the IspG reaction patterned after vitamin K epoxyquinone reductase mechanism.⁴¹

The later steps of the non-mevalonate pathway have been the focus of debate regarding the absence of a type I IPP isomerase in the microorganisms utilizing this alternate pathway.⁵²⁻⁵⁴ In the mevalonate pathway, IPP and DMAPP are interconverted by an isomerase, isopentenyl diphosphate isomerase (IPP:DMAPP isomerase; EC 5.3.3.2). IPP:DMAPP isomerase catalyzes the isomerization of the carbon-carbon double bond of IPP to create the electrophilic dimethylallyl unit, DMAPP. Studies on IPP:DMAPP isomerase showed that it catalyzes the interconversion of IPP and DMAPP by a stereoselective antarafacial transposition of hydrogen: the *pro-R* hydrogen at C-2 of IPP is removed and a hydrogen is added to the *re* face of C-4 in IPP (Fig.1.13).⁵⁵

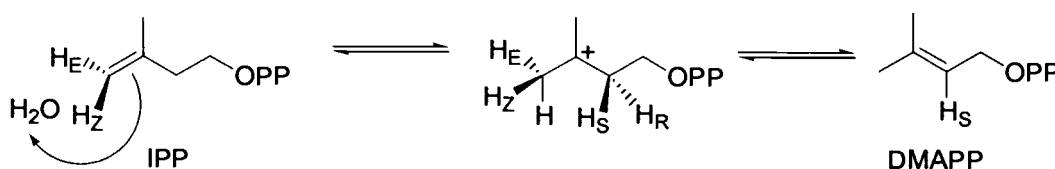


Fig.1.13 Interconversion of IPP into DMAPP catalyzed by IPP isomerase.

Because of the absence of an isomerase gene (*idi*) in the genomes of many bacteria utilizing the non-mevalonate pathway, the interconversion of IPP and DMAPP in the non-mevalonate pathway has been of interest. Rather puzzling results were obtained from incorporation studies of 1-deoxy [3-²H] xylulose and 1-deoxy [4-²H] xylulose into the *E. coli* ubiquinone side chain. In this report, 1-deoxy [3-²H] xylulose labeled the *E*-methyl group in the terminal unit and all other positions derived from the terminal methylene group of IPP, while the deuterium from 1-deoxy [4-²H] xylulose is retained exclusively in the double bond corresponding to the dimethylallyl diphosphate starter unit. The authors suggested from these results that there might be a branching point in between IPP and DMAPP or that

different hydrogens are lost from IPP in the isomerization and in the elongation process in the non-mevalonate pathway.⁵³

Studies by Poulter's group^{56,57} using stereospecifically labeled IPP and DMAPP supported the idea that *E. coli* may either have a different type of IPP isomerase or may have developed a different route to provide DMAPP and IPP separately. Poulter *et al.* first assured that the interconversion of IPP and DMAPP catalyzed by the *E. coli* is a type I isomerase, which accomplishes the isomerization by losing the *pro-R* proton at C2 of IPP analogous to the rat liver enzyme.⁵⁷ In a separate paper,⁵⁶ the authors also showed that FPP synthase from *E. coli* catalyzes the condensation of IPP and GPP with a stereoselective removal of the *pro-R* hydrogen at C2 of IPP, again the same stereochemistry observed for the yeast and pig liver enzymes. Therefore, the authors ruled out the possibility of IPP being a direct precursor of DMAPP to explain Arigoni group's results with [3-²H]- and [4-²H] DXP. Furthermore, another set of incorporation studies by Rohmer *et al.* added supporting evidence that there might be a branching point in the final step of the non-mevalonate pathway.⁵⁸ In this study, [1,1-²H₂] ME and [3,5,5,5-²H₄] ME were used to follow the hydrogens corresponding to the hydrogens of interest in IPP and DMAPP. The results from this study were: (1) the two deuterium atoms at the C1 of ME were found without loss in the prenyl chains of menaquinone and ubiquinone at the carbons derived from C4 of IPP and the *E*-methyl group of DMAPP; (2) no deuterium scrambling was observed between hydrogens attached at C4 and C5 of IPP and DMAPP; (3) deuterium at the C3 position of ME remained only in the DMAPP starter unit without a trace in all of the units derived from IPP. These observations further suggested a branching point toward IPP and DMAPP in the non-mevalonate pathway. The incorporation results from a variety of labeled ME are summarized in Fig.I.14.

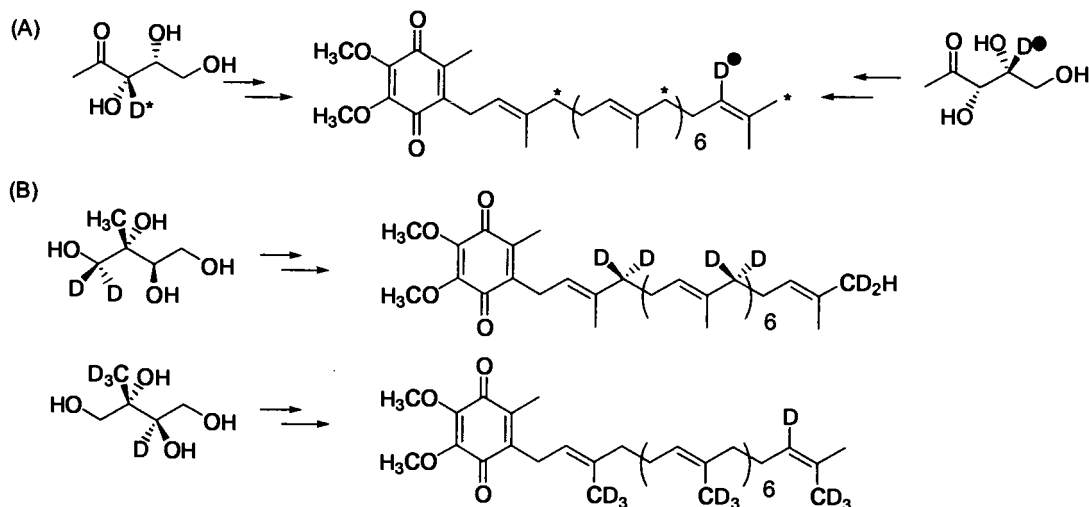


Fig.I.14 The incorporation studies by (A) Arigoni's and (B) Rohmer's groups.

The incorporation studies were also supported by an experiment explored with a genetically engineered *E. coli* strain.⁵⁹ Disruption of *idi* gene, encoding IPP isomerase, in wild type *E. coli* showed that this gene is not essential for its growth or survival.⁵⁷ This result agrees with a similar study with *Synechocystis* sp. strain PCC6803 which showed that it lacked type I IPP isomerase.⁵² All these results lead to the conclusion that there is branching of the endogenous pathway which result in the separate synthesis of IPP and DMAPP.

In summary, the entire seven steps of the non-mevalonate pathway are shown below (Fig.I.15). Because the individual steps of the non-mevalonate pathway are now uncovered, the detailed mechanistic studies of the individual enzymes remain for future investigation.

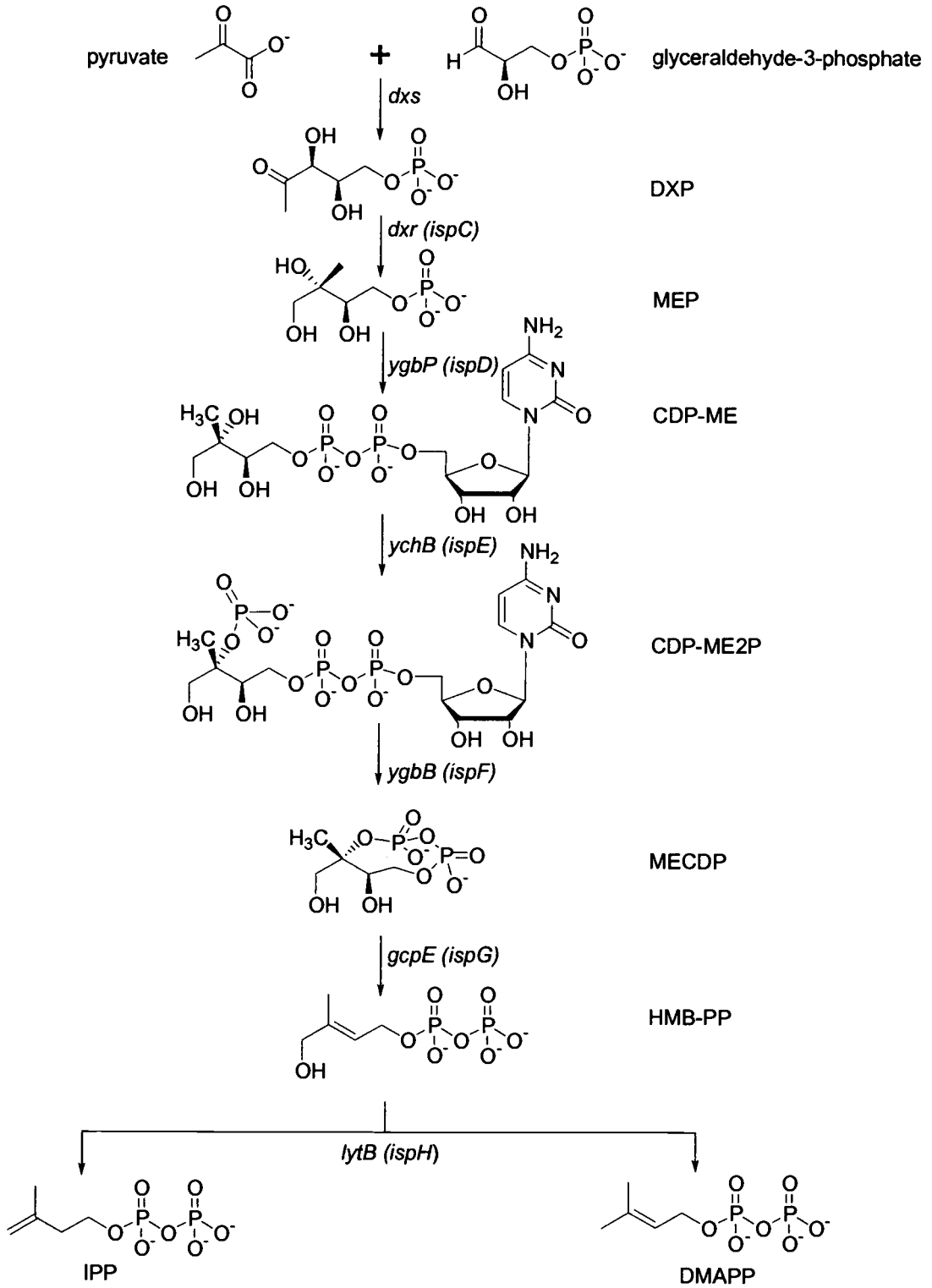


Fig.I.15 The non-mevalonate pathway for IPP biosynthesis.

Distribution of The Non-Mevalonate pathway

Although isoprenoids are one of the oldest and diverse classes of natural products, very little was known about isoprenoid biosynthesis in prokaryotes until the discovery of the non-mevalonate pathway. The presence of the classical mevalonate pathway had been reported for only a few bacteria, such as *Caldariella acidophila*, *Halobacterium cutirubrum*, *Staphylococcus sp.*, *Streptococcus mutans*, and *Halobacterium halobium* etc. based on incorporation studies using labeled acetate, mevalonate and glucose.² The discovery of the non-mevalonate pathway, however, encouraged investigations concerning the distribution of this pathway in Gram-positive and -negative bacteria, green and red algae, and higher plants.⁶⁰ This novel pathway is widely distributed amongst pathogenic prokaryotes and phototrophic eukaryotes without any representation in fungi or animals, including humans (Table.I.1).^{2,24,30,31,61} These distribution studies provided further evidence that this pathway could be a useful target for new antibiotics. The absence of the non-mevalonate pathway in humans, along with its key role in certain pathogens, makes it a viable target for drug development.

Table I.1 Distribution of the non-mevalonate pathway.²

<u>The Mevalonate Pathway only</u>
Animals
Fungi
Archaea
<i>Staphylococcus</i> sp.
<u>Both Pathways</u>
Plants
Red Algae
Some <i>Streptomyces</i> sp.
<u>The non-mevalonate Pathway only</u>
Gram-negative eubacteria
<i>Escherichia coli</i>
<i>Synechocystis</i> sp.PCC6714, PCC6803
<i>Zymomonas mobilis</i>
<i>Pseudomonas aeruginosa</i>
<i>Salmonella typhimurium</i>
<i>Helicobacter pylori</i>
Gram-positive eubacteria
<i>Corynebacterium ammoniagenes</i>
<i>Alicyclobacillus acidoterrestris</i>
<i>Bacillus subtilis</i>
Green Algae
<i>Scenedesmus obliquus</i>
<i>Chlorella fusca</i>
<i>Plasmodium falciparum</i>

One of the remaining questions regarding the non-mevalonate pathway is, "Why are there two distinct pathways to IPP and how did these two pathways distribute to evolutionarily distinct domains?" It has been shown that most eukaryotes and archaea use the mevalonate pathway while most eubacteria utilize the non-mevalonate pathway. At the same time there are some examples, e.g. plants and red algae, which possess both pathways. For example, it has been proven that both pathways are operating in *Streptomyces aeriovifer* from a study utilizing [1,2-¹³C₂]

acetate and [U-¹³C₆] glucose.⁶² In this study, the non-mevalonate pathway was the major route at the early stage of fermentation providing the primary metabolites such as menaquinone, while the mevalonate pathway replaces it at the latter stage of growth to produce the secondary metabolites such as naphterpin. This report was the first example showing the alternating operation of the mevalonate and the non-mevalonate pathway depending on the growth stage of the organism rather than depending on organelles, as in plants. This result suggests a possible Lateral Gene Transfer (LGT) of the IPP biosynthesis genes. The non-mevalonate route preceded the mevalonate pathway in eubacteria, thus primary metabolites were formed by the non-mevalonate pathway, while the mevalonate pathway was used for the secondary metabolites. The mevalonate pathway genes might be transferred laterally. The possibility of horizontal gene transfer was investigated by Croteau *et al.* through a phylogenetic distribution analysis suggesting that lateral gene transfer between eubacteria subsequent to the origin of plastids has played a major role in the evolution of this pathway.⁶³

DXR and Fosmidomycin

Deoxyxylulose-5-phosphate isomeroeductase (DXR) is the enzyme involved in the second step of the non-mevalonate pathway as discussed above. DXR (EC. 1.1.1.267) functions as a dehydrogenase using NADPH as a cofactor as well as an isomerase that catalyzes an isomerization of DXP to a corresponding intermediate. Since the first report of the recombinant *E. coli* enzyme,²⁶ its orthologs from different organisms such as, the cyanobacterium *Synechocystis* sp PCC6803, the plants *Arabidopsis thaliana* and *Mentha piperita*, and the malaria protozoan *Plasmodium falsiparum* have been reported.⁶¹

Preliminary characterization of the *E. coli* DXR in the initial report included the determination of a specific activity as $11.8 \mu\text{mol min}^{-1} \text{mg}^{-1}$ with MnCl_2 at a pH of 7.5. Recently Poulter *et al.* investigated further on this matter with Mg^{2+} and reported: $k_{\text{cat}} = 116 \pm 8 \text{ s}^{-1}$, $K_{\text{M}}^{\text{DXP}} = 115 \pm 25 \mu\text{M}$, and $K_{\text{M}}^{\text{NADPH}} = 0.5 \pm 0.2 \mu\text{M}$ and that the isomerization/reduction is reversible.²⁹ The DXR from *E. coli* was reported to have a molecular weight of 140 kDa (for the dimer), to require divalent metal ions, Mn^{2+} , Co^{2+} or Mg^{2+} for its activity, and to use NADPH as a cofactor, showing a severe decrease in its activity when NADPH was substituted with NADH (1 % of the original rate with NADPH).²⁶ A sequence alignment study with other DXR homologs revealed that there is a conserved motif (LGXTGSIG) in their N-terminal regions, which is believed to be a NADPH binding site.

Only one other known enzyme in Nature is functionally similar to DXR, acetohydroxy acid isomeroreductase (AHIR, or ketol reductoisomerase, EC1.1.1.86). AHIR, which is involved in branched-chain amino acid biosynthesis (*i.e.* valine, isoleucine, and leucine), isomerizes 2-acetolactate to an intermediate ketone, which is reduced by NADPH to 2,3-dihydroxyisovalerate (Fig.I.16).⁶⁴

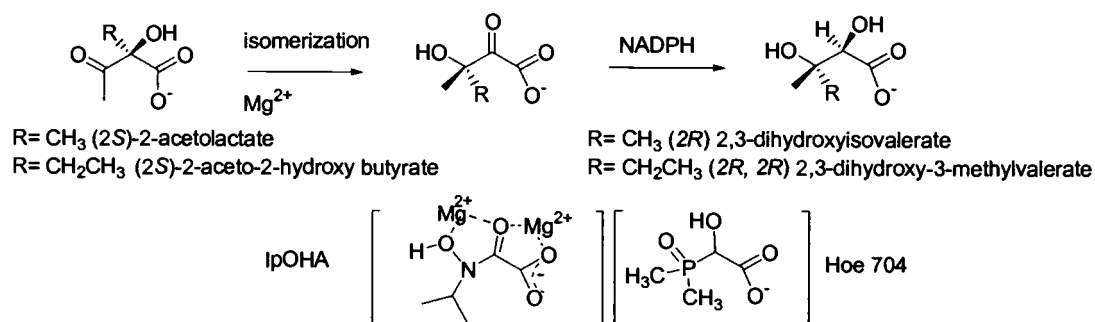


Fig.I.16 α -Ketol rearrangement in AHIR mediated reaction in branched amino acid biosynthesis with its inhibitors.

The distribution of AHIR is limited to bacteria and plants, and this enzyme is absent in animals, including humans. Developing AHIR inhibitors thus has an advantage of targeting bacteria and plants selectively. Due to its restricted distribution and thus to the possibility of being a useful target for new herbicidal agents, AHIR has been of great interest. Extensive studies on this enzyme led to the development of new herbicide candidates targeting this specific enzyme (Fig.1.16).⁶⁵

AHIR shows an absolute requirement for Mg^{2+} ions with no other divalent ions being effective for the *E. coli* enzyme.⁶⁶ It has been shown that the *pro-S* hydrogen atom of NADPH is transferred to the intermediate, which determines AHIR as a class B dehydrogenase.⁶⁴ The enzyme is inhibited by the divalent metal ion Mn^{2+} and also by the reaction intermediate analogs such as 2-dimethylphosphinoyl-2-hydroxyacetate (Hoe 704) and *N*-hydroxy-*N*-isopropylloxamate (IpOHA).⁶⁷ These inhibitors have shown nearly irreversible, competitive inhibition, and a time dependent increase in their potency.⁶⁵

As discussed above, the conversion of DXP to MEP mediated by DXR is the first committed step of the non-mevalonate pathway. Investigation of this step is particularly important because of the strong possibility that increased understanding of this step will provide insight into targeting this pathway for new antibiotics. Understanding the active site of the enzyme thus should be a focus of research on DXR. A site-directed mutagenesis study of the recombinant *E. coli* DXR by Seto *et al.* showed that the purified mutant enzyme E231K had wild type K_m values for DXP and NADPH, but it had less than 0.24 % of the wild type k_{cat} value. On the other hand, K_m values of H153Q, H209Q and H257Q for DXP increased to 3.5-, 7.6- and 19-fold of the wild type's, respectively. Based on these results, the authors suggested that Glu231 is involved in catalysis, and that His153, His209, and His257 might be involved in the binding of DXP.⁶⁸

The conversion mechanism of 2-acetolactate to 2,3-dihydroxyisovalerate by AHIR has been considered to be an α -ketol rearrangement. A similar mechanism can be envisioned for the DXR catalyzed step in the non-mevalonate pathway. The requirements for the rearrangement have been suggested since the early stage of the research on the non-mevalonate pathway, and the precedence of AHIR offers reasonable support for the α -ketol rearrangement mechanism. However, an alternative retroaldol/aldol mechanism must be taken into consideration before making a conclusion on the mechanism of DXR.

The bacterial enzyme L-ribulose 5-phosphate 4-epimerase catalyzes the interconversion of L-ribulose 5-phosphate (L-Ru5P) and D-xylulose 5-phosphate (D-Xu5P) using a divalent ion (Zn^{2+}). This enzyme epimerizes the stereogenic center which lacks an acidic proton through a retroaldol/aldol mechanism (Fig.1.17).⁶⁹ DXP has a similar structural feature to L-Ru5P the α,β -dihydroxy keto-functionality, which can support a retroaldol/aldol-type conversion. The retroaldol/aldol mechanism leads to the same putative intermediate 2-C-methylerythrose-4-phosphate which can be reduced by NADPH. However, these two distinct mechanisms can provide significantly different insights into the active site of DXR. For instance, inhibitors for DXR could be designed differently depending on which mechanism the conversion follows.

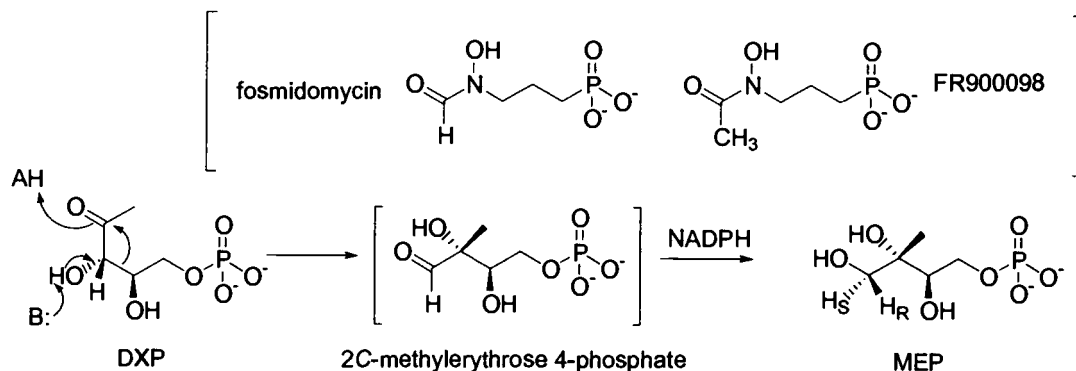


Fig.I.18 α -Ketol rearrangement in DXR mediated reaction in IPP biosynthesis with its inhibitors.

Fosmidomycin, which was initially reported to have antibacterial activity, was shown to inhibit *E. coli* DXR with a K_i value of 38 nM.⁷⁰ Later, it was reported that fosmidomycin inhibits not only bacterial DXR but it also inhibits isoprenoid biosynthesis in plant chloroplasts by blocking the DXR mediated reaction.^{71,72} Furthermore, it has been shown to cure malaria infected mice, providing a new class of low toxicity antimalarial agents.^{32,73,74} Therefore, the inhibition of DXR, and thus isoprenoid biosynthesis, of the target organisms is promising to be very selective and less toxic than commonly known methods. These results, in addition to the limited distribution of the pathway, have stimulated intense studies to understand the pathway as well as to develop this pathway as a target for new antibiotics.

Besides its medical significance, DXR is important in that it is one of only two known isomeroreductases. It is interesting that these two enzymes do not show significant sequence identity (15 % identity for *E. coli* AHIR and DXR) despite their related functions. However, they do share the conserved NADPH binding motif and similar amino acid composition at their active site, such as glutamates and aspartates.^{64,68}

Taken together, the significance of further investigation of DXR is as follows: (1) DXR is a promising target for new antibiotic, herbicidal, and antimalarial agents; (2) Studies of the unique reaction mechanism that DXR might share with the known enzyme, AHIR, will provide further understanding of these enzymatic reactions; and (3) A better understanding of DXR will expand our knowledge of isoprenoid biosynthesis in Nature. Therefore, in the following chapters DXR is investigated for its stereoselective reaction mechanism and for the structural constraints of inhibitors utilizing synthetic analogs of a known inhibitor, fosmidomycin.

The investigation of the stereochemical course of the DXR catalyzed reduction step using NADPH is described in Chapter II. This information will offer an improved understanding of the orientation of DXP and NADPH at the active site which can be applied to developing better inhibitors of DXR.

Potential inhibitors were designed and synthesized based on the structure of fosmidomycin and evaluated for the ability to inhibit DXR. These synthetic analogs of fosmidomycin were expected to give better insight into the structural requirements of the inhibitors for optimal interactions with the active site residues. The synthetic procedures, technical problems encountered, and DXR inhibition activity for each compound, and the implications of these results are discussed in Chapter III.

CHAPTER II

STUDY OF THE STEREOCHEMISTRY OF THE DXR REDUCTION REACTION

Introduction

Isoprenoids are ubiquitous and play numerous crucial biological functions in all living organisms. The biological significance of this group of compounds has stimulated extensive studies and tremendous progress has been made, especially in isoprenoid biosynthesis, chemistry, and molecular genetics. Understanding the early steps in isoprenoid biosynthesis, *i.e.* the formation of isopentenyl diphosphate (IPP) through the mevalonate pathway, is an area of successful research. Since its initial report in the mid-1950's until the disclosure of the non-mevalonate pathway, the mevalonate pathway was believed to be the universal method for isoprenoid biosynthesis in nature. In 1993,¹⁴ however, Rohmer's report on the existence of the non-mevalonate pathway as an alternate route to IPP in some bacteria forever changed the landscape of our understanding of isoprenoid biosynthesis.

Due to the importance of understanding isoprenoid biosynthesis and the significance of being the first reported alternate route to IPP, the non-mevalonate pathway has been studied intensively over the last several years. Organisms utilizing the non-mevalonate pathway² include certain bacteria, (*i.e.* *Escherichia coli*, *Synechocystis* sp. PCC6714, *Streptomyces argenteolus*, etc), phototrophic eukaryotes, (*i.e.* green algae, red algae, and higher plants), and the malaria protozoan, *Plasmodium falciparum*. One of the implications of studying this pathway is that it is a promising target for a new class of antibiotics because most eukaryotes, including humans and animals, do not utilize the non-mevalonate pathway for the biosynthesis of

isoprenoids. Therefore, the non-mevalonate pathway can provide an effective target to manipulate parasitic systems without affecting the host.

As a result of a decade's worth of studies, all seven steps of this pathway have been elucidated.^{16,26,35,36,40,42} The non-mevalonate pathway to IPP starts from the condensation of glyceraldehyde-3-phosphate (GAP) and pyruvate,¹⁶ which provides 1-deoxy-D-xylulose 5-phosphate (DXP, **1**). The second step of this pathway is the conversion of DXP to 2-C-methyl-D-erythritol 4-phosphate (MEP, **2**), which is catalyzed by one enzyme, DXP isomeroeductase (DXR) (Fig.II.1).²⁶

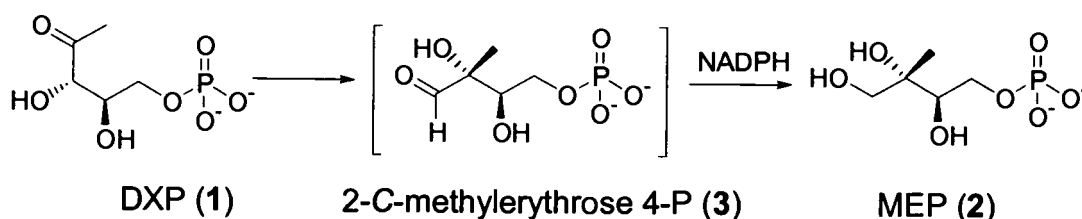


Fig.II.1 Conversion of DXP to MEP by DXR (2-C-methylerythrose-4-P (**3**) has been proposed as the product of the isomerization step).

According to the proposed α -ketol rearrangement model, DXR catalyzes the isomerization of DXP (**1**) to the putative intermediate 2-C-methyl erythrose-4-phosphate (**3**) then reduces it to MEP (**2**) with the assistance of NADPH.⁷⁵ The other possible mechanism for the conversion of DXP to MEP is a retroaldol/aldol mechanism, which involves a retroaldol fragmentation then an aldol condensation.⁶⁹ General schemes for these two possible mechanisms of conversion are illustrated in Fig.II.2.

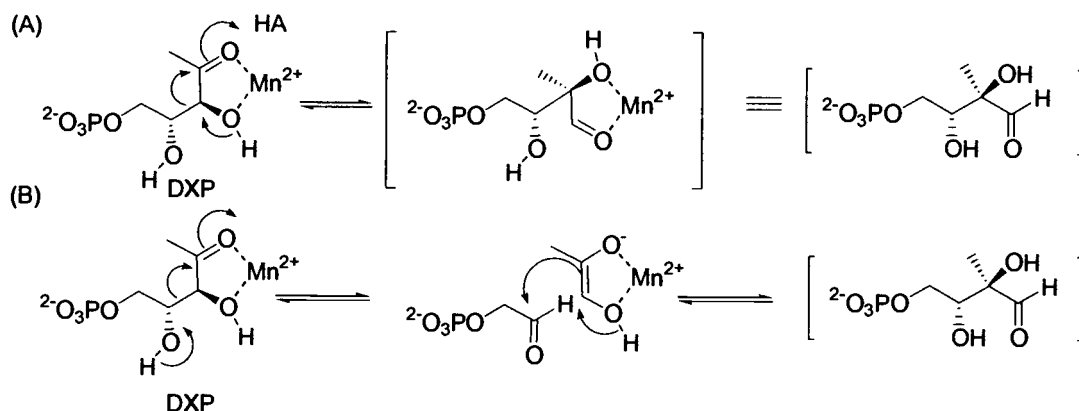


Fig.II.2 Two possible DXR mechanisms (A) α -ketol rearrangement (B) retroaldol/aldol mechanism.

MEP (**2**) is the first committed intermediate of the non-mevalonate pathway whereas DXP (**1**) can be used in other biosynthetic pathways, *i.e.* thiamine and pyridoxol biosynthesis.²⁰ Blocking the biosynthesis of DXP (**1**) for the purpose of inhibiting isoprenoid biosynthesis will thus affect the several other metabolic pathways, while blocking the MEP (**2**) synthesis will selectively affect isoprenoid biosynthesis. Therefore, blocking the synthesis of MEP (**2**) will provide more selective inhibition of isoprenoid biosynthesis. A known natural compound, fosmidomycin, has shown potent antibacterial,⁷⁰ antimalarial,^{32,70} and herbicidal activity⁷¹ by inhibiting DXR. Therefore, a better understanding of the second step of the non-mevalonate pathway catalyzed by DXR could be a key step in developing a new class of antibiotics.

The proposed α -ketol rearrangement and subsequent reduction classifies DXR as an example of an isomeroreductase, which catalyzes an isomerization reaction followed by a reduction with a NADPH cofactor. The other example of this α -ketol rearrangement can be found in the reaction

catalyzed by acetohydroxy acid isomeroreductase (AHIR, EC 1.1.1.86) in the biosynthesis of valine and isoleucine.⁷⁶

Microorganisms and plants can synthesize essential amino acids while animals are deficient in these biosynthetic pathways. Therefore, understanding AHIR offers the promising opportunities of developing antibacterial and herbicidal agents selectively targeting these organisms.⁶⁵ These efforts have led to the emergence of the reaction intermediate analogs such as *N*-hydroxy-*N*-isopropylloxamate (IpOHA, 4) and 2-dimethylphosphinoyl-2-hydroxy acetate (Hoe 704, 5), potent inhibitors of AHIR. AHIR requires a divalent ion, Mg^{2+} and NADPH as co-substrates,⁶⁶ while DXR requires Mn^{2+} , Mg^{2+} , or Co^{2+} and NADPH.²⁹ The crystal structure⁷⁷ of AHIR was obtained with an inhibitor (IpOHA) bound, where a Mg^{2+} ion was shown to be coordinated by the carbonyl and *N*-hydroxyl group of the inhibitor.

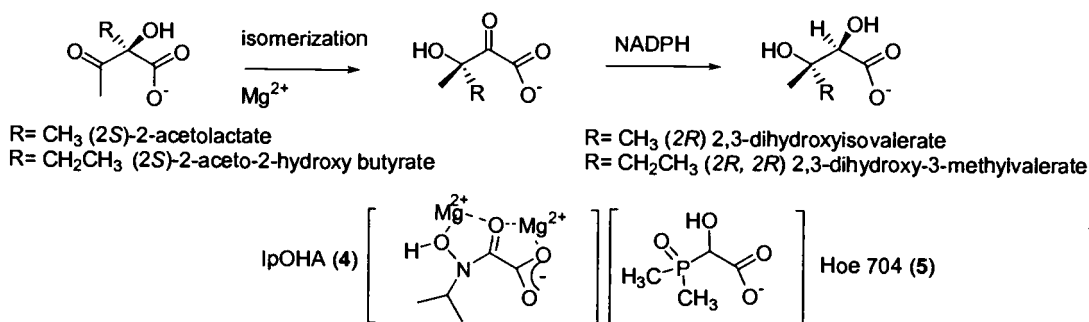


Fig.II.3 Isomerization and reduction catalyzed by acetohydroxyacid isomeroreductase (AHIR) and the reaction intermediate analogs, IpOHA (4) with two Mg^{2+} ions and Hoe 704 (5).

The positions of these Mg^{2+} ions in the crystal structure suggest that they might facilitate the migration of the adjacent alkyl group in the acetolactate substrate (Fig.II.3). After the isomerization step, both DXR and

acetohydroxy acid isomeroreductase (AHIR) catalyze a reduction step using NADPH, which provides MEP (2) and the desired branched amino acid precursors respectively.

Besides being only the second known isomeroreductase to date, DXR is also a dehydrogenase. Because all of the pyridine-nucleotide dependent dehydrogenases undergo a stereospecific reaction, DXR should also catalyze a stereoselective reaction. In other words, NADPH should deliver its hydride to the substrate, putatively 2-C-methyl erythrose-4-phosphate (3), in a stereospecific manner. Depending on which hydride is transferred, the dehydrogenases are classified as Class A dehydrogenases (*pro-R* hydride transfer) or Class B dehydrogenases (*pro-S* hydride transfer). An example of this stereospecific hydride transfer is represented by the reaction of yeast alcohol dehydrogenase (YADH).⁷⁸ As shown in Fig.II.4 an example of Class A dehydrogenase, YADH, transfers only the *pro-R* hydride from stereoselectively deuterium-labeled NADPH.

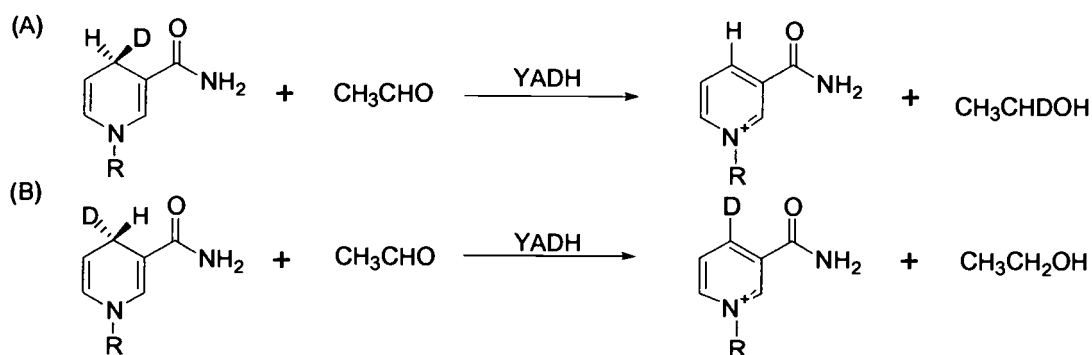


Fig.II.4 Reaction of yeast alcohol dehydrogenase (YADH) with (A) *pro-R* deuterium labeled and (B) *pro-S* deuterium labeled NADPH.

When DXR was first reported in 1998,²⁶ it had not yet been classified into either of these subcategories. Therefore, determining which hydride

DXR transfers will classify DXR either as a class A or class B dehydrogenase.

Determining the dehydrogenase class of DXR will also provide a better understanding of the stereochemical interactions between DXR, NADPH, and DXP (1). To be more specific, dehydrogenases are proposed to undergo conformational changes after cofactor and substrate binding,⁷⁹ NADPH is a flexible molecule that can exist in many different conformations,⁸⁰ and DXP can have numerous potential binding modes. In a dehydrogenase-catalyzed reaction, the nucleotide part of a cofactor plays a crucial role in binding to the enzyme, whereas the nicotinamide participates in hydride delivery. These two distinct groups of NADPH are responsible for determining the conformation of NADPH. The class A dehydrogenases (*pro-R* hydride transfer) bind the cofactor with the nicotinamide ring of the cofactor in an *anti* conformation to the ribose at the transition state whereas class B dehydrogenases (*pro-S* hydride transfer) bind a *syn* conformation.⁷⁵ Therefore, by determining the dehydrogenase class, the conformation of NADPH (either *anti* or *syn*) at its transition state of the DXR mediated conversion can be predicted. Moreover, understanding the stereochemical course of this step will provide knowledge of the following items: (1) how NADPH binds to DXR; (2) how the proposed substrate, 2-C-methyl erythrose-4-phosphate, gets access to the cofactor, *i.e.* which side of the aldehyde (*re* or *si*) will face NADPH; and (3) how these two small molecules, NADPH and 2-C-methyl erythrose-4-phosphate, interact to transfer a hydride from one to the other.

Because many enzyme inhibitors mimic the natural substrate, a better understanding of the interaction between DXR and DXP will offer researchers more accurate insights into developing inhibitors of DXR. These goals will be more tangible if we can understand the active site of DXR in detail. Based on the desire to understand the DXR-mediated

conversion step in the non-mevalonate pathway and encouraged by the interest in targeting this step for a new class of antibiotics, the stereochemistry of the reduction step was investigated in depth. Based on an α -ketol rearrangement model, the mechanism of the conversion of DXP to MEP is illustrated in Fig.II.5.

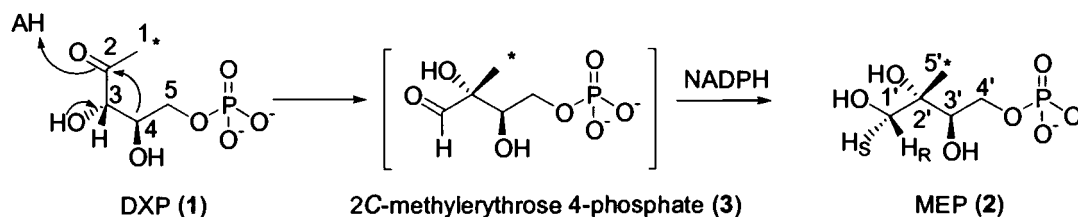


Fig.II.5 Proposed mechanism of conversion step by DXR (the fate of the C1 methyl group of DXP is indicated by an *).

During this conversion, the hydrogen at the C3 position of DXP becomes one of the hydrogens at C1 of MEP (1' in Fig.II.5), the C1 methyl group from DXP repositions to the C2 of MEP (2' in Fig.II.5), and NADPH transfers a hydride to the C1 position of the putative intermediate 2-C-methylerythrose 4-phosphate (3). As a result, one of the hydrogens at the C1 of MEP originates from the C3 of DXP while the other derives from NADPH, one of which is *pro-S* and the other is *pro-R*. But the question remains as to which one derives from DXP and which one originates from NADPH. Furthermore, it is still necessary to address the facial selectivity of hydride delivery to the carbonyl of 3, and to address which hydride of NADPH, *pro-S* or *pro-R*, is delivered to the substrate.

To address these questions, it was necessary: (1) to distinguish the diastereotopic hydrogens at the C1 position of MEP; (2) to follow the hydrogen from C3 of DXP to C1 of MEP; (3) to obtain DXR to

convert DXP to MEP *in vitro*; and (4) to stereospecifically label NADPH with deuterium.

DXP was synthesized in unlabeled form and with the C3 hydrogen replaced with deuterium. The labeled DXP was incubated with recombinant DXR and the enzymatic product from the incubation experiments was transformed to the bisacetonide derivative. The ^1H NMR spectrum of the bisacetonide from the enzymatic experiment was compared with the ^1H NMR spectrum obtained from the synthetic standard to identify the origin of hydrogen at the C1 position of ME.

The hydrogens at the 4-position of the nicotineamide ring of NADPH were labeled stereospecifically to afford [4S- ^2H]- and [4R- ^2H]-NADPH, which were incubated with unlabeled DXP and recombinant DXR in two separate experiments. The enzymatic products from the two incubation experiments were converted to triacetate derivatives of 2-C-methylerythritol and also compared with synthetic standard using MS and ^1H NMR.

Results and Discussion

It was necessary to distinguish the *pro-R* from the *pro-S* hydrogens at C1 of MEP as the first step for addressing these stereochemical questions. As a model compound to assign these two hydrogens, the bisacetonide derivative of 2-C-methyl erythritol was synthesized.⁸¹ In an early study on branched chain carbohydrates, the synthesis and structure determination of a bisacetonide derivative of 2-C-methyl erythritol (ME) was reported.⁸² In this report, the authors were able to distinguish the methyl group at C2 from the four acetonide methyl groups using ¹³C NMR. The bisacetonide derivative tethers the four hydroxyls of 2-C-methyl erythritol (ME, **6**) into a pair of acetonides rigidly positioning one of the hydrogens at C1 on the same side with the methyl group at the C2 of **6** (Fig.II.6). In the first part of the study, therefore, a bisacetonide derivative of ME was synthesized as a model compound in which the diastereotopic hydrogens at the C1 position of ME become distinguishable due to restricted rotation about the C1-C2 bond. The hydrogen on the same side as the methyl group at C2 will show a stronger Nuclear Overhauser Enhancement (NOE) effect. The bisacetonide derivative of 2-C-methylerythritol was thus chosen to tether the four hydroxyls into five-membered rings so that the free rotations among the C1-C2 and C3-C4 bonds were prevented.

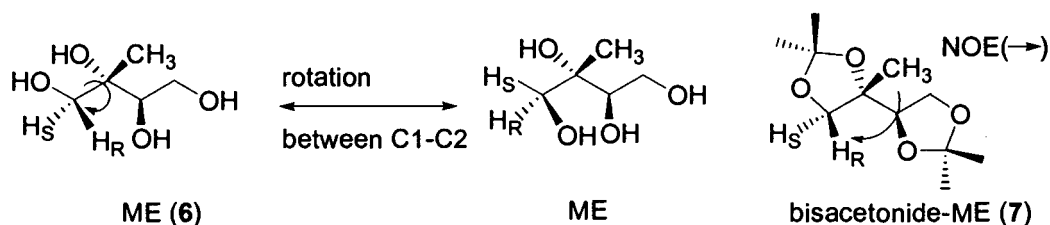
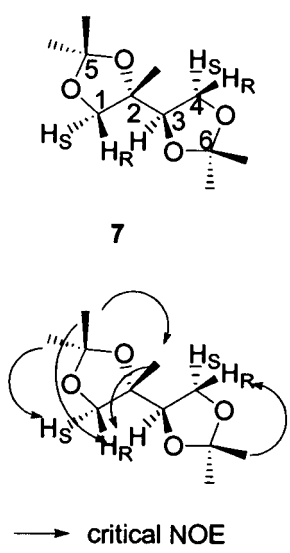


Fig.II.6 2-C-methyl erythritol (ME, **6**) and the bisacetonide derivative (**7**).

The synthesis of 2-C-methyl erythritol (ME) was accomplished by a reported method⁸³ and this tetrol was converted to the bisacetonide with 2,2-dimethoxy propane and TsOH to afford a white solid.

The bisacetonide of ME (**7**) was used as a model compound to distinguish the *pro-R* and *pro-S* hydrogens at C1 of ME. Initially the NMR spectrum of this compound was obtained in CDCl₃, but the resolution of the five protons was not as clear as that of the spectrum acquired in acetone-d₆. Once a clear resolution of these five protons had been acquired, acetone-d₆ was used as a solvent for further studies. The 2-C methyl group of ME was distinguished from the four acetonide methyl groups of bisacetonide using a Heteronuclear Multiple Bond Correlation (HMBC) experiment. Further extensive NMR experiments on this compound, *i.e.* Heteronuclear Single Quantum Coherence (HSQC), Gradient NOESY (GNOESY), and 1D Double Pulsed Field Gradient Spin-Echo (DPFGSE) NOE, allowed the assignment of all five protons of **7**. The NMR data of **7** showed that the four acetonide methyl groups to be four singlets at 1.35, 1.310, 1.306, and 1.27 ppm and the methyl group at C2 to be a singlet at 1.21 ppm in the ¹H NMR. The corresponding carbons for the four methyls were also determined from these experiments to resonate at 26.60, 27.58, 27.02, and 24.04 ppm respectively. The five backbone carbons were assigned to be 73.49 (C1), 81.83 (C2), 79.44 (C3), 66.00 (C4), and 19.80 ppm for 2-C-methyl group. The carbon at 19.80 ppm showed strong correlations with a doublet of doublets at 4.09 ppm, a doublet at 3.95 ppm, and another doublet at 3.71 ppm. The HSQC-COSY experiment further confirmed that a doublet at 3.95 ppm and a doublet at 3.71 ppm are strongly correlated to the C1 carbon. This experiment also showed a correlation between a doublet of doublets at 4.09 ppm and the C3 carbon and two doublets of doublets at 4.00 and 3.84 ppm to the C4 carbon. Once ¹H and ¹³C chemical shifts were assigned, the stereochemical relations

were determined through GNOESY and 1D DPGSE NOE experiments. Irradiation of the methyl proton signal at 1.21 ppm revealed a strong NOE effect with one of the C1 hydrogens, a doublet at 3.71 ppm, which leads to the conclusion that this hydrogen is on the same side with the 2-C methyl group. This assigned the doublet at 3.71 ppm as the *pro-R* hydrogen at the C1 of ME and the doublet at 3.95 ppm as the *pro-S* hydrogen at C1 of ME. One acetonide methyl signal (1.27 ppm) also showed a strong NOE effect with both the 2-C-methyl and the *pro-R* hydrogen at C1, which indicates this methyl is also on the same side with the 2-C-methyl group and the *pro-R* hydrogen at C1. Taken together, the carbons and protons of **7** were fully assigned (Fig.II.7)



position	$^1\text{H } \delta$ (mult, J in Hz)	$^{13}\text{C } \delta$
1	H1R 3.71 (d, 8.7)	73.49
	H1S 3.95 (d, 8.7)	
2		81.83
3	4.09 (dd, 7.0, 5.8)	79.44
4	H4R 3.84 (dd, 8.7, 5.8)	66.00
	H4S 4.00 (dd, 8.7, 7.0)	
5	C5-CH ₃ R 1.306 (s)	110.11 (C5)
	C5-CH ₃ S 1.310 (s)	27.02 (R), 27.58 (S)
6	C6-CH ₃ R 1.35 (s)	110.11 (C6)
	C6-CH ₃ S 1.27 (s)	26.60 (R), 25.04 (S)
2-C-methyl	1.21 (s)	19.80

→ critical NOE

Fig.II.7 Structural assignments for **7** through HMBC, HSQC, GNOESY, and 1D DPGSE NOE experiments. ^1H NMR (600 MHz, acetone- d_6) and ^{13}C 150 MHz, acetone- d_6).

In order to follow the hydrogen at C3 of DXP, a synthetic scheme was required that could stereospecifically replace this hydrogen with deuterium. Therefore, a known procedure⁸⁴ for the synthesis of [3-²H]1-deoxy-D-xylulose was modified to add a phosphate at the C5 position. Unlabeled DXP was prepared as a model compound, while the C3 deuterium labeled DXP was synthesized for stereochemical studies (Fig.II.8). Benzyl protected prop-2-yn-1-ol (**8**) was deprotonated with BuLi and condensed with an acetaldehyde. A hydride/deuteride was transferred regioselectively to the alkyne intermediate **9** using LAH/LAD. Attempts at this reaction following the brief published details failed to produce the desired product. However, lowering the reaction temperature (0 °C) and decreasing the reaction time from 12 h to 3-4 h finally provided the desired intermediate (**10**) with a reasonable yield (70 %). After the oxidation of the resulting secondary alcohol to the α,β -unsaturated ketone (**11**), the two hydroxyl groups were introduced in a stereospecific manner by a Sharpless asymmetric dihydroxylation reaction using AD mix- β .⁸⁵ Because the starting material for the stereospecific dihydroxylation is a tri-substituted olefin, methane sulfonamide⁸⁶ was added for a better yield. After protecting the diol (**12**, **12-a**) as an acetonide (**13**, **13-a**), the terminal hydroxyl was phosphorylated. The phosphate group was introduced as a dibenzylphosphite initially, and the phosphite was oxidized further to the phosphate ester **15** using *t*-BuOOH (Fig.II.8). The phosphate and hydroxyl protecting groups were removed by using H₂, Pd/C and Dowex 50 (H⁺ form), respectively. The final unlabeled and labeled DXP samples were purified by cellulose chromatography eluting with water/methanol mixtures.

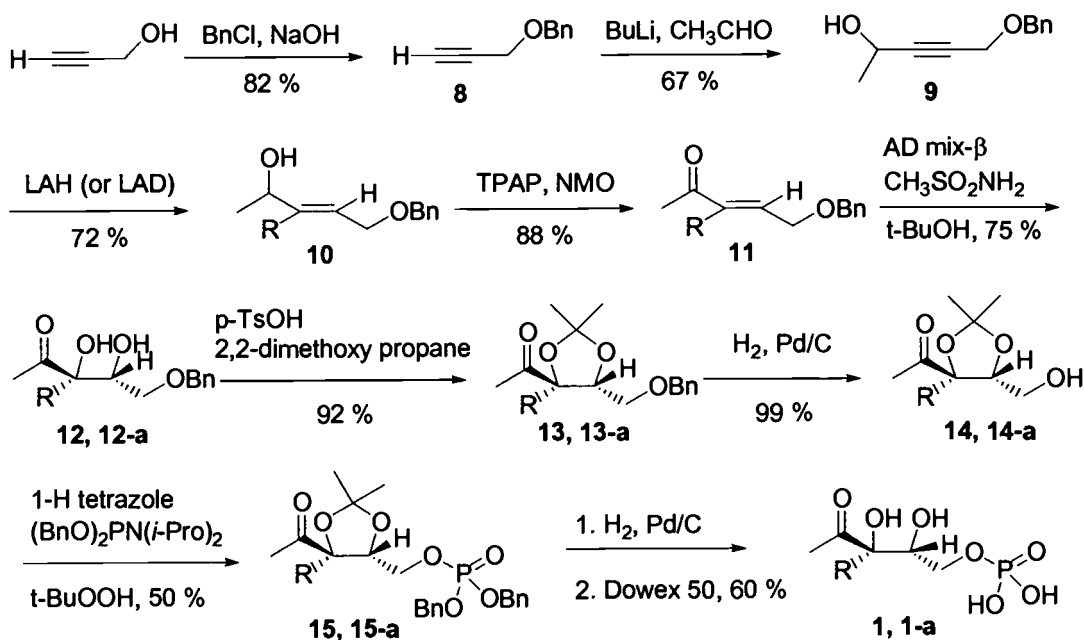


Fig.II.8 Synthesis of unlabeled and labeled DXP(R=H or D).

The next step after the assignment of the diastereotopic protons and the synthesis of DXP was the enzymatic synthesis of 2-C-methyl erythritol (ME, **6**), which required DXR. Therefore, recombinant *Synechocystis* sp. PCC6803 DXR was prepared as a 6xHis tagged form.²⁸ DXP prepared above was incubated with recombinant DXR as reported earlier.²⁶ The crude product of the enzyme reaction was dephosphorylated with bacterial alkaline phosphatase, which converted MEP (**2**) to 2-C-methyl erythritol (ME, **6**). The crude dephosphorylated product was transformed into a triacetate derivative (**16**) with acetic anhydride and pyridine. The triacetate derivative was easily purified by organic solvent extraction from the rest of the aqueous enzymatic reaction residue before purification by flash chromatography. The triacetate was then deacetylated with Amberlite IRA400 (OH⁻) and the resulting ME was converted to the bisacetonide derivative (**7**, Fig. II.9). The final bisacetonide product was purified with

flash chromatography to afford a white solid. It was not realized until this point that the bisacetonide derivative of ME (**7**), which is a white solid, readily sublimes. When it was first synthesized chemically, the small loss of the compound to sublimation was hidden by the overall amount of product remaining (50-100 mg scale reaction; 70-80 % yield). The loss, however, was more significant when dealing with the small scale (2-3 mg) of the product resulting from the enzymatic reaction. Thus, the final bisacetonide product was handled with caution in this specific aspect. Instead of using an EtOAc/hexanes mixture for chromatography, an ether/pentane solvent mixture was used. The bisacetonide solution was concentrated using a rotary evaporator at low temperature (20 °C) to remove the solvent and then blown dry with a very gentle flow of nitrogen gas until the white solid formed.

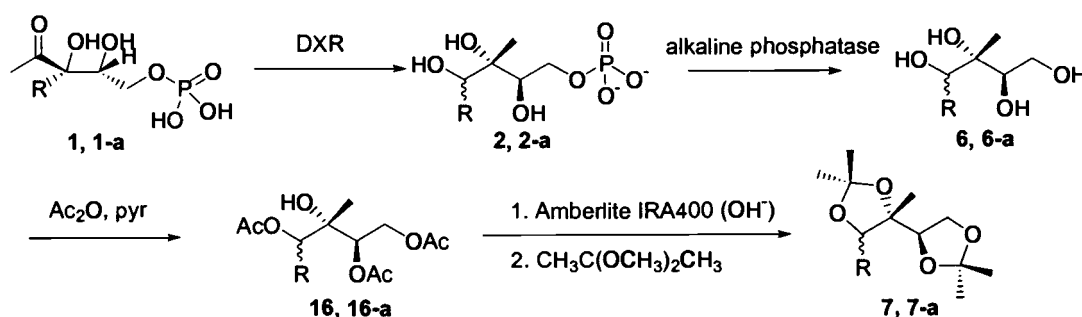


Fig.II.9 Treatment of enzymatic product, MEP (**2**), to the bisacetonide derivative (**7**, R=H or D).

The bisacetonide of the enzymatic product from the experiment above was analyzed by ¹H NMR under the same conditions as with the synthetic model compound. The ¹H NMR spectrum of the enzymatic products acquired from the incubation experiments with [3-²H] DXP were compared with the ¹H NMR spectrum from the synthetic standard. The

partial ^1H NMR from this product is shown below (Fig.II.10). The ^1H NMR spectrum of the bisacetonide from the enzymatic reaction with labeled DXP revealed a broad singlet at 3.69 ppm (H1_R) and the absence of a doublet at 3.95 ppm (H1_S). This result indicates that the hydrogen from C3 of DXP becomes the *pro-S* hydrogen at C1 of MEP and the *pro-R* hydrogen at C1 of MEP derives from NADPH. A broad singlet at 3.69 ppm, which is slightly up field from the unlabeled shift (3.71 ppm), can be explained by a deuterium isotope shift. In addition to the determination of the origins of these two hydrogens, it can also be demonstrated that NADPH delivers its hydride to the *re* face of the putative erythrose intermediate.

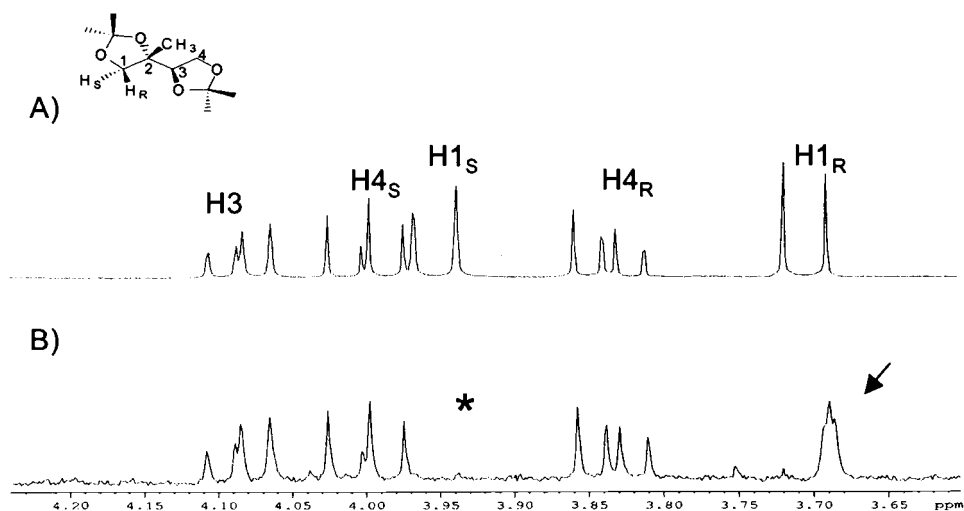


Fig.II.10 Partial ^1H NMR spectrum of 2-C-methylerythritol bisacetonide. (A) Unlabeled synthetic standard. (B) Mono-deuterated product from DXR enzymatic reaction.

Stereospecifically deuterated $[4S\text{-}^2\text{H}] \text{NADPH}^{87}$ and $[4R\text{-}^2\text{H}] \text{NADPH}^{88}$ were prepared as reported in the literature to probe the question of which hydride is delivered from NADPH to the aldehyde intermediate. The $[4S\text{-}^2\text{H}] \text{NADPH}$ was prepared using glucose dehydrogenase (NADP^+

dependent, from *Cryptococcus uniguttulatus*) and [1-²H]glucose, and [4*R*-²H] NADPH was prepared from [²H₈]-2-propanol and alcohol dehydrogenase (NADP⁺ dependent, from *Thermoanaerobium Brockii*). NADPH samples thus prepared were purified by reversed phase HPLC with 0.1 M NaCl at pH 8.5.³⁰ In the case where the deuteride is transferred, the H-1_R signal will be missing from the ¹H NMR spectrum. If a hydride is transferred, a ¹H NMR spectrum identical to the standard will be expected. Based on this rationale, these stereospecifically labeled NADPH samples were incubated separately with unlabeled DXP and recombinant DXR. Instead of converting the enzymatically prepared MEP to the bisacetonide, the crude enzymatic product was transformed and purified as the triacetate derivative of 2-*C*-methylerythritol. As discussed earlier, the bisacetonide derivative of 2-*C*-methylerythritol (**7**) is a volatile white solid, which demands careful handling when it is present in small amounts. In addition, formation of the bisacetonide requires two additional steps, deacetylation and acetonide formation. Because it was already determined that H-1_S of MEP is from the C3 of DXP, the C1 stereochemical assignments of the triacetate derivative of 2-*C*-methylerythritol were rather straightforward. The ¹H NMR spectrum in CDCl₃ of this triacetate derivative of ME (**16-a**) from [3-²H]DXP lacked the doublet at 4.16 ppm and had a broadened singlet slightly upfield of 3.90 ppm. This result established the H-1_S hydrogen at C1 of the triacetate to resonate at 4.16 ppm while the doublet at 3.90 ppm corresponds to the H-1_R hydrogen.

The crude enzymatic products from the stereospecifically labeled NADPH experiments were treated with alkaline phosphatase and followed by acetylation with acetic anhydride and pyridine. The fragmentation patterns of the triacetate derivative of 2-*C*-methylerythritol (**16**) from these separate enzymatic reactions were investigated by GC/EIMS analysis. The unlabeled triacetate derivative showed major fragment ions at *m/z* 159, 129,

117. The crude product from the [4S-²H] NADPH experiment had ions at *m/z* 160, 129, 118, while the product from the [4R-²H] NADPH showed the same mass spectrum as the unlabeled standard (Fig.II.11). This result clearly indicates that the H_R hydrogen at C1 of MEP originates from the 4S hydride of NADPH. It also classifies DXR as a Class B dehydrogenase.

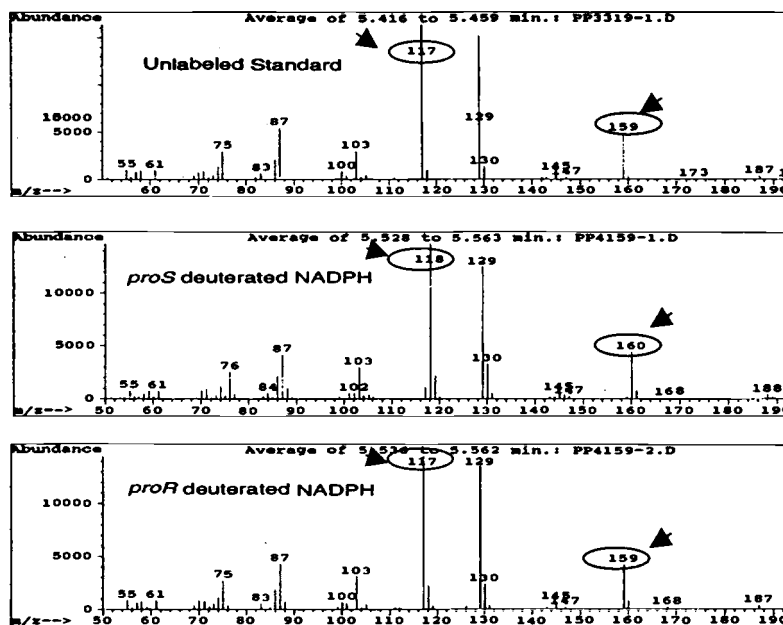


Fig.II.11 GC/EIMS spectra of triacetate derivative from (top) the synthetic unlabeled standard, (middle) the incubation product from [4S-²H]NADPH, (bottom) the incubation product from [4R-²H]NADPH

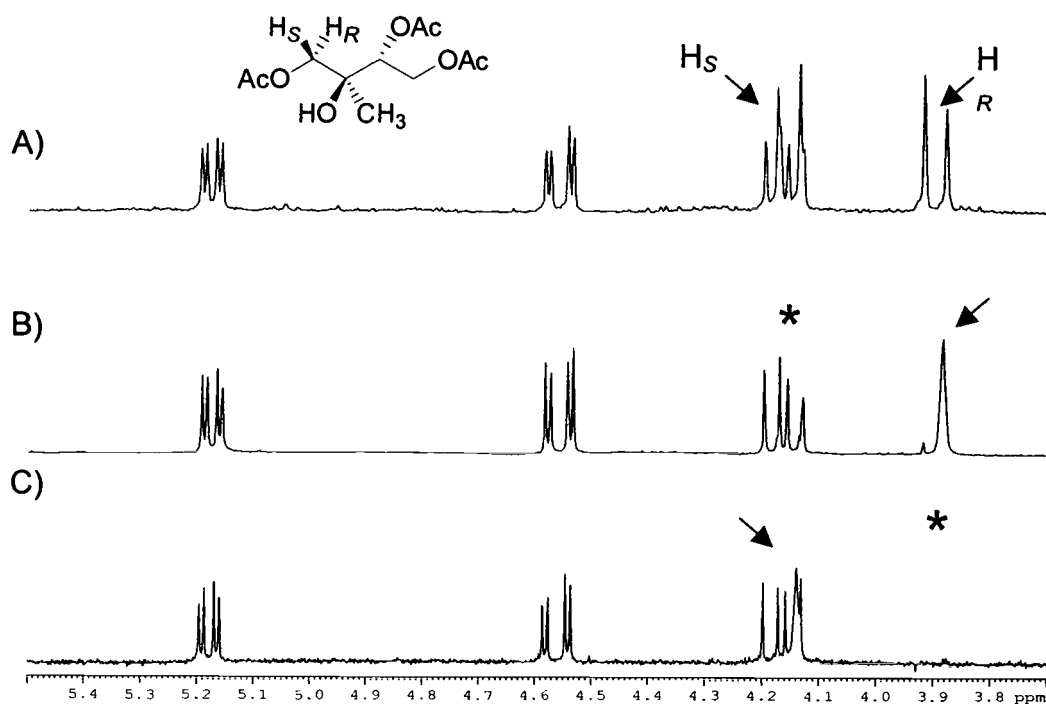


Fig.II.12 ^1H NMR of (A) synthetic triacetate derivative standard, (B) triacetate derivative product from $[3\text{-}^2\text{H}]$ DXP, (C) triacetate derivative product from $[4S\text{-}^2\text{H}]$ NADPH.

This result was further confirmed when the ^1H NMR of the monodeuterated **16-a** from $[4S\text{-}^2\text{H}]$ NADPH experiment was compared with the synthetic triacetate standard⁸⁹ and also with the enzymatically prepared triacetate derivative of 2-C-methylerythritol from $[3\text{-}^2\text{H}]$ DXP. As shown in Fig.II.12, the *pro-R* and *pro-S* hydrogens at C1 of the triacetate derivative of ME appeared as two doublets (panel A) in the standard molecule. However, the H_S signal is absent from the enzymatic product with $[3\text{-}^2\text{H}]$ DXP and the H_R hydrogen signal was slightly broadened (panel B). Furthermore, this H_R peak disappeared when the triacetate was prepared from MEP formed from $[4S\text{-}^2\text{H}]$ NADPH as shown in panel C, which reveals

that H_R is derived from the 4S hydrogen of NADPH thus classifying DXR as a class B dehydrogenase. In conclusion, the *pro-S* hydrogen at the C1 of MEP derives from the C3 of DXP, the *pro-R* hydrogen originates from the 4S hydrogen of NADPH, and the delivery of the hydride occurs on the *re* face of the intermediate.

As discussed above, it is known that NADPH binds to the enzyme in a *syn* conformation when it delivers the *pro-S* hydride.⁷⁶ Based on these results from our experiments, the whole stereochemical course for the isomerization/reduction step by DXR is illustrated as below (Fig.II.13).

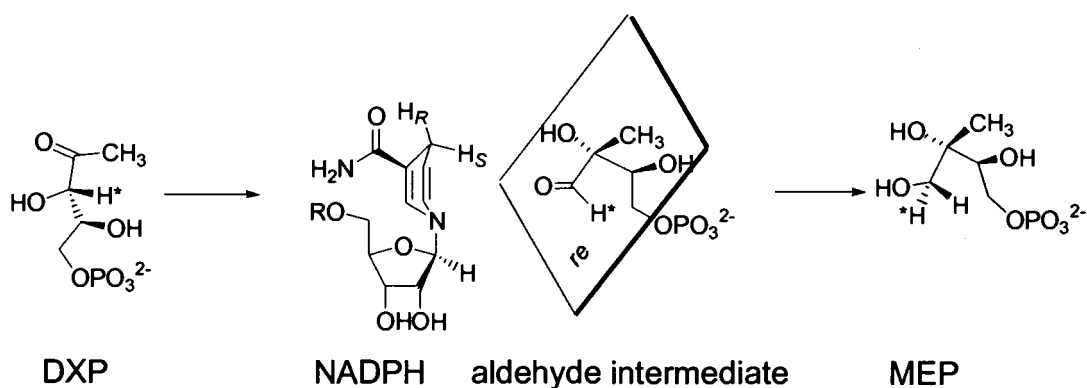


Fig.II.13 Stereochemical illustration of conversion of DXP to MEP by DXR.

Better insight into the stereochemical course of the conversion of DXP to MEP by DXR provides more information to understand the active site of DXR as well as to develop new inhibitors. There have been a couple of hypotheses to explain the stereospecificity of dehydrogenases, but none of them seem to account for all cases.^{76,91}

Among them, the one proposed by Benner and colleagues⁹¹ is that thermodynamically unstable carbonyls are reduced by a *pro-R* hydride of NADPH, while thermodynamically stable carbonyls are reduced by a *pro-S* hydride. To predict the stereochemical preference of the enzyme, Benner *et al.* suggested three criteria that the reaction of interest should meet: (1)

the enzyme must catalyze the interconversion of “simple” unconjugated carbonyls with the corresponding alcohol; (2) the “natural” substrate must be well defined; and (3) the equilibrium constant for the overall reaction must lie at least one log unit away from the position of the “break” in the values of $-\log K_{\text{eq}}$ between the reactions catalyzed by the *pro-R* and *pro-S* specific enzymes. Their proposal is interesting because it explains the stereochemical preference of the dehydrogenases based on their natural substrates. In the DXR mediated conversion, however, the exact intermediate (*i.e.* the exact substrate for the reduction) has not yet been confirmed probably because the putative aldehyde intermediate has not been synthesized or isolated.

Regarding the identification of the intermediate, Poulter *et al.*²⁹ reported their attempts to be unsuccessful presumably because of the short lifetime of the intermediate. Our group also has tried both synthesis and isolation of this putative intermediate but it has not been successful. First, a reduced analog of NADPH, 5,6-dihydro-NADPH (NADPH₃), was prepared by a known method.⁹² The structures of NADPH₃ and NADPH are similar enough that the isomerization may be able to occur, but NADPH₃ cannot transfer a hydride. Therefore, using NADPH₃ instead of NADPH may allow formation of the aldehyde, but prevent reduction to MEP. A ¹H NMR experiment using NADPH₃, however, did not identify the intermediate. In this experiment, the DXR reaction with NADPH₃ was monitored by ¹H NMR. However, the ¹H NMR spectrum of the starting material (DXP) remained the same without any significant new signals.

Next, [3,4,5-¹³C₃]DXP was prepared to follow C3 of DXP more efficiently using ¹³C NMR during the DXR mediated reaction.⁹³ This experiment also failed to demonstrate the possible structure of the reaction intermediate. Therefore, under the circumstance that the exact natural substrate has not been elucidated yet, Benner’s rule could not be applied to

DXR catalyzed conversion. However, if the proposed intermediate 2-C-methylerythrose-4-phosphate is the substrate of the reduction step an investigation if this reaction follows Benner's rule should be carried out once it is shown that.

Another proposed hypothesis to predict the stereochemical preference of dehydrogenases, the simplest and most accepted one,⁹³ is that primordial dehydrogenases only carried out a reaction with either *pro-S* or *pro-R* stereospecificity, and then all enzymes that evolved from these primordial enzymes retained this original stereospecificity. The only known example of an isomeroreductase other than DXR is acetohydroxy acid isomeroreductase, which is a class B dehydrogenase.⁹⁴ Furthermore, the active sites of these two enzymes have similar composition of amino acids even though they do not show high sequence identity.^{77,95,96} The latter theory⁹³ would therefore predict that DXR would be a Class B dehydrogenase, and thus, this hypothesis seems to work for the DXR-mediated reduction reaction.

This study on the stereochemistry of the reduction step provides valuable information on how NADPH and DXP (or the intermediate) interact with each other at the active site. NADPH binds the enzyme in the *syn* conformation. NADPH delivers its *pro-S* hydride to the substrate, which designates DXR as a class B dehydrogenase, and the isomerization product (the putative intermediate aldehyde) faces its *re* plane toward NADPH when the reduction occurs. This knowledge will aid future studies on designing inhibitors for DXR based on the knowledge of the stereochemical interaction between NADPH and the natural substrate.

Experimental

General experimental procedures

Infrared (IR) spectra were obtained using a Nicolet 510 Fourier transform IR (FTIR) spectrophotometer. Nuclear magnetic resonance (NMR) spectra were recorded on Bruker AM 400, AC 300 or DRX 600 instruments, where noted. ^1H and ^{13}C NMR chemical shifts were reported as δ using the residual solvent signal as an internal standard (CHCl_3 at 7.26 ppm for ^1H NMR and 77.00 ppm for the center line of the triplet for ^{13}C NMR samples in CDCl_3 , H_2O at 4.80 ppm for ^1H NMR samples in D_2O). Either *tert*-butanol (31.21 ppm for the CH_3) or MeOH-d_4 (49.15 ppm for the center line of the quintet) was added as an internal standard for the samples in D_2O for their ^{13}C NMR. Phosphoric acid (85 % in water) was used as an external standard for ^{31}P NMR spectra (0.00 ppm). Low and high-resolution chemical ionization and fast atom bombardment mass spectra (CIMS and FABMS) were obtained on a Kratos MS50TC spectrometer. Ion Spray mass spectra were obtained on a PerkinElmer SCIEX API3 spectrometer. Silica gel (Merck, grade 60, 220-400 mesh) was used for flash column chromatography.⁹⁷ Merck glass-backed TLC plates (Si gel 60 F₂₅₄) were used for thin-layer chromatography (TLC). The solvents used for most of the synthetic procedures were dried before use as commonly recommended.⁹⁸ The water used in the experiments was double-deionized water. (Milli Q Millipore). Commercial grade reagents and starting materials were purchased from Sigma-Aldrich and used without further purification. Unless stated otherwise, synthetic reactions were performed in oven-dried glassware under a positive pressure of argon. Bacteria alkaline phosphatase was purchased from Sigma.

*Synthesis of DXP (1-deoxy-D-xylulose-5-phosphate, 1) and [3-²H]DXP (1-a)
5-benzlyoxypent-3-yn-2-ol (9)*

To a solution of prop-2-yn-1-ol (5.6 g, 100 mmol) in benzene (150 ml) was added NaOH (4 g, 100 mmol) and benzyl chloride (12.65 g, 100 mmol) at room temperature. The reaction flask was equipped with a Dean-Stark apparatus and the mixture was stirred at reflux for 5 h. The resulting dark brown mixture was cooled, filtered, and washed with diethylether (30 ml). The filtrate was dried over Na₂SO₄, filtered, concentrated to a yellow brown oil, and purified by distillation using a short path to give a colorless oil (12 g, bp 77 °C at 45 mmHg, 82 %). The ¹H NMR of the oil acquired from the distillation matched with the previously reported one.⁹⁹

To a solution of **8** (130 mg, 890 μmol) in dry THF (30 ml) was added *n*-BuLi (1.6 M solution in hexanes, 610 μl, 980 μmol) dropwise at -78 °C. The resulting solution was stirred for 1 h at the same temperature before slowly adding acetaldehyde (120 mg, 2.67 mmol). The reaction was quenched with water 1 h later. The solvent was removed under reduced pressure and the residual oil was diluted with EtOAc. The organic layer was washed with a saturated sodium bicarbonate solution, water and brine, dried over MgSO₄, filtered and concentrated before purification by flash column chromatography (EtOAc/hexanes, 1:3) to give a pale yellow oil (113 mg, 67 %). IR (neat) cm⁻¹ 3400, 2250, 1738, 1683, 1452, 1358, 1238, 1088; ¹H-NMR (300 MHz, CDCl₃) δ (ppm) 7.39-7.28 (m, 5H), 4.59 (s, 2H), 4.57 (qt, *J* = 6.5, 1.8 Hz, 1H), 4.19 (d, *J* = 1.8 Hz, 2H), 1.46 (d, *J* = 6.5 Hz, 3H); ¹³C NMR (75 MHz, CDCl₃) δ (ppm) 137.17, 128.36, 128.02, 127.83, 88.51, 79.66, 71.58, 58.16, 57.27, 24.10; LRMS (CI) *m/z* 190.1[M⁺] HRMS Calcd for C₁₂H₁₄O₂ 190.09938 Found 190.09977.

5-Benzlyoxypent-3-en-2-ol (10)

To a solution of **9** (100 mg, 0.53 mmol) in dry THF (20 ml) was added LAH (20 mg, 0.53 mmol) at 0 °C and stirred for 4 h at the same temperature.

The reaction was quenched by the slow addition of water at 0 °C after the mixture was diluted with ethyl ether (20 ml). The resulting mixture containing a white precipitate was filtered through Celite® and concentrated before purification by flash column chromatography (EtOAc/hexanes, 1:3) to yield a colorless oil (75 mg, 72 %). IR (neat) cm^{-1} 3393, 2974, 2860, 1363, 1117, 1063, 973; $^1\text{H-NMR}$ (300 MHz, CDCl_3) δ (ppm) 7.33-7.29 (m, 5H), 5.75-5.72 (m, 2H), 4.47 (s, 2H), 4.27-4.25 (m, 1H), 3.96 (d, $J = 4.5$ Hz, 2H), 1.22 (d, $J = 6.4$ Hz, 3H); $^{13}\text{C NMR}$ (75 MHz, CDCl_3) δ (ppm) 137.20, 128.27, 127.65, 127.52, 138.05, 125.87, 72.12, 69.99, 67.92, 23.06; LRMS (CI) m/z 192.1 [M⁺] HRMS Calcd for $\text{C}_{12}\text{H}_{16}\text{O}_2$ 192.11503 Found 192.11523

5-Benzlyoxypent-[3- ^2H] 3(E)-en-2-ol (10-a)

To a solution of 5-benzlyoxy-pent-3-yn-2-ol (**9**, 100 mg, 0.53 mmol) in dry THF (20 ml) was added LAD (22 mg, 0.53 mmol) at 0 °C and stirred for 4 h at the same temperature. The reaction was quenched with the slow addition of water at 0 °C after the mixture was diluted with ethylether. The resulting mixture with white precipitate was filtered through Celite® and concentrated before purified with flash column chromatography (EtOAc/hexanes, 1:3) to give a colorless oil (77 mg, 72 %). $^1\text{H-NMR}$ (300 MHz, CDCl_3) δ (ppm) 7.36-7.28 (m, 5H), 5.78 (bs, 1H), 4.52 (s, 2H), 4.33 (bs, 1H), 4.02 (d, $J = 5.9$ Hz, 2H), 1.29 (d, $J = 6.4$ Hz, 3H)

5-Benzlyoxypent-3(E)-en-2-one (11)

To a solution of 5-Benzlyoxy-pent-3-en-2-ol (**10**, 70 mg, 0.36 mmol) in dry CH_2Cl_2 (15 ml) were added activated 4 Å molecular sieves, NMO (55 mg, 0.49 mmol), and a catalytic amount of TPAP at room temperature. The resulting heterogeneous reaction mixture was stirred at the same temperature for 12 h. The mixture was filtered through Celite® and Florisil® and the filtrate was concentrated before purification by flash column

chromatography (EtOAc/hexanes, 1:4) to yield a colorless oil (61 mg, 88 %). IR (neat) cm^{-1} 3033, 2662, 1682, 1638, 1360, 1119, 979; $^1\text{H-NMR}$ (300 MHz, CDCl_3) δ (ppm) 7.37-7.30 (m, 5H), 6.80 (dt, $J = 16.1, 4.4$ Hz, 1H), 6.35 (dt, $J = 16.1, 1.9$ Hz, 1H), 4.57 (s, 2H), 4.19 (dd, $J = 4.4, 1.9$ Hz, 2H), 2.27 (s, 3H); $^{13}\text{C NMR}$ (75 MHz, CDCl_3) δ (ppm) 198.13, 142.96, 137.53, 130.35, 128.51, 127.91, 127.71, 72.94, 68.77, 27.28; LRMS (CI) m/z 190.1 $[\text{M}^+]$ HRMS Calcd for $\text{C}_{12}\text{H}_{14}\text{O}_2$ 190.09938 Found 190.09970

5-Benzyloxy-pent-[3, ^2H] 3(*E*)-en-2-one (11-a)

$^1\text{H-NMR}$ (300 MHz, CDCl_3) δ (ppm) 7.35-7.31 (m, 5H), 6.79 (bs, 1H), 6.35 (dt, $J = 16.1, 1.9$ Hz, 1H), 4.57 (s, 2H), 4.21 (d, $J = 4.4$ Hz, 2H), 2.27 (s, 3H); $^{13}\text{C NMR}$ (75 MHz, CDCl_3) δ (ppm) 198.24, 142.96, 137.59, 130.26, 128.51, 127.91, 127.71, 72.94, 68.77, 27.28

(3*S*, 4*R*)-5-Benzyloxy-3,4-dihydroxy-pentan-2-one (12)

To a room temperature mixture of AD mix- β (6 g) and methane sulfonamide (420 mg, 4.4 mmol) in *t*-BuOH and H_2O (1:1 v/v, 12 ml) was added 5-benzyloxypent-3-en-2-one (11, 420 mg, 2.2 mmol) with vigorous stirring. Sodium sulfite (6g) was added to the reaction flask above after 1 h and the resulting mixture was stirred for 1 h. The reaction mixture was diluted with EtOAc (40 ml) and the organic layer was washed with water and brine, dried over MgSO_4 , filtered and concentrated before purification by flash column chromatography (EtOAc/hexanes, 1:2) to afford a colorless oil (370 mg, 75 %). IR (neat) cm^{-1} 3464, 2927, 2060, 1715, 1550, 1362, 1118, 1006; $^1\text{H-NMR}$ (300 MHz, CDCl_3) δ (ppm) 7.36-7.31 (m, 5H), 4.57 (s, 2H), 4.23 (d, $J = 2.0$ Hz, 1H), 4.21 (dt, $J = 2.0, 6.0$ Hz, 1H), 3.62 (d, $J = 6.0$ Hz, 2H), 2.27 (s, 3H); $^{13}\text{C NMR}$ (75 MHz, CDCl_3) δ (ppm) 208.34, 137.55, 128.46, 127.90, 127.82, 77.13, 73.59, 70.96, 70.40, 25.52; LRMS (CI) m/z 225.1 $[\text{M}+1]$ HRMS Calcd for $\text{C}_{12}\text{H}_{17}\text{O}_4$ 225.11268 Found 225.11349

1-((3S, 4R) 5-Benzoyloxymethyl-2,2-dimethyl-[1,3]dioxolan-4yl)-ethanone (13)

A solution of **12** (360 mg, 1.6 mmol), *p*-TsOH·H₂O (50 mg, 0.2 mmol), and 2,2-dimethoxy propane (3 ml, 3.4 mmol) in dry THF (50 ml) was stirred for 12 h at room temperature. The solvent was removed *in vacuo*, the residue was diluted with EtOAc (30 ml) and the resulting solution was washed with saturated sodium bicarbonate solution, water and brine. The organic layer was dried over MgSO₄, filtered and concentrated before purification (Silica, EtOAc/hexanes, 1:4) to give a colorless oil (390 mg, 92 %). IR (neat) cm⁻¹ 2990, 1720, 1549, 1376, 1242, 1095; ¹H-NMR (300 MHz, CDCl₃) δ (ppm) 7.35-7.29 (m, 5H), 4.61 (s, 2H), 4.21-4.19 (m, 2H), 3.76-3.72 (m, 1H), 3.65-3.60 (m, 1H), 2.27 (s, 3H), 1.48 (s, 3H), 1.44 (s, 3H); ¹³C NMR (75 MHz, CDCl₃) δ (ppm) 208.34, 137.84, 128.37, 127.68, 111.06, 81.93, 77.29, 73.58, 70.21, 26.89, 26.44, 26.25; LRMS (CI) *m/z* 264.1 [M⁺] HRMS Calcd for C₁₅H₂₀O₄ 264.13630 Found 264.13616

1-((3S, 4R) 5-Hydroxymethyl-2,2-dimethyl-[1,3]dioxolan-4yl)-ethanone (14)

To a solution of **13** (380 mg, 1.4 mmol) in methanol (40 ml) was added a catalytic amount of 10 % Pd/C. The resulting mixture was stirred for 12 h with a positive pressure (1 atm) of H₂ gas at room temperature. The reaction mixture was filtered and concentrated to give a colorless oil (250 mg, 99 %), which was used without further purification. ¹H-NMR (300 MHz, CDCl₃) δ (ppm) 4.26 (d, *J* = 7.8 Hz, 1H), 4.12-4.07 (m, 1H), 3.91 (dd, *J* = 12, 3.5 Hz, 1H), 3.74 (dd, *J* = 11.9, 3.9 Hz, 1H), 2.31 (s, 3H), 1.48 (s, 3H), 1.43 (s, 3H); ¹³C NMR (75 MHz, CDCl₃) δ (ppm) 209.19, 110.72, 81.65, 77.96, 62.27, 26.77, 26.65, 26.10

1-[(3S, 4R) 5-Hydroxymethyl-2,2-dimethyl-[1,3]dioxolan-4-yl]-ethanone (14-a)

$^1\text{H-NMR}$ (300 MHz, CDCl_3) δ (ppm) 4.09 (t, $J = 3.5$ Hz, 1H), 3.91 (dt, $J = 12, 3.5$ Hz, 1H), 3.76-3.71 (m, 1H), 2.31 (s, 3H), 1.48 (s, 3H), 1.43 (s, 3H); ^{13}C NMR (75 MHz, CDCl_3) δ (ppm) 209.45, 110.97, 78.14, 62.48, 27.04, 26.91, 26.36

Phosphoric acid [(4S, 5S) 5-acetyl-2,2-dimethyl-[1,3]dioxolan-4-yl]methyl ester dibenzyl ester (15)

To a solution of **14** (250 mg, 1.4 mmol) in dry CH_2Cl_2 (40 ml) was added 1-*H*-tetrazole (201 mg, 2.87 mmol) and dibenzyl diisopropyl phosphoramidite (991 mg, 2.87 mmol) at room temperature. This mixture was stirred for 4 h at the same temperature before adding 70 % *t*-BuOOH (2 ml, 19 mmol) at 0 °C. After stirring the reaction mixture for 12 h at room temperature, the aqueous layer was extracted with CH_2Cl_2 (5 ml x 3). The combined organic layers were washed with saturated aqueous sodium bicarbonate solution, water and brine, dried over MgSO_4 , filtered, and concentrated before purification by flash column chromatography (EtOAc/hexanes, 1:2) to afford a colorless oil (300 mg, 50 %). IR (neat) cm^{-1} 2350, 1719, 1251, 1222, 1016; $^1\text{H-NMR}$ (300 MHz, CDCl_3) δ (ppm) 7.35-7.32 (m, 10H), 5.07-5.04 (m, 4H), 4.26-4.04 (m, 4H), 2.24 (s, 3H), 1.41 (s, 3H), 1.37 (s, 3H); ^{13}C NMR (75 MHz, CDCl_3) δ (ppm) 207, 135.69, 135.60, 128.50, 127.91, 127.78, 111.20, 81.11, 76.09 (d, $^3J_{\text{CP}} = 8.0$ Hz), 69.34 (d, $^2J_{\text{CP}} = 5.2$ Hz), 66.68, 26.66, 26.45, 26.17; ^{31}P NMR (121 MHz, CDCl_3) -1.14; LRMS (CI) m/z 434.1 [M⁺] HRMS Calcd for $\text{C}_{22}\text{H}_{27}\text{O}_7\text{P}$ 434.14944 Found 434.15073

Phosphoric acid [(4S, 5S) 5-acetyl-2,2-dimethyl-[1,3]dioxolan-4-yl]methyl ester dibenzyl ester (15-a)

$^1\text{H-NMR}$ (300 MHz, CDCl_3) δ (ppm) 7.55-7.26 (m, 10H), 5.06 (dd, $^2J_{HP} = 8.3$ Hz, $^2J_{HH} = 1.2$ Hz, 4H), 4.27-4.18 (m, 2H), 4.12-4.08 (m, 1H), 2.25 (s, 3H), 1.42 (s, 3H), 1.38 (s, 3H); $^{13}\text{C NMR}$ (75 MHz, CDCl_3) δ (ppm) 207.87, 135.69 (d, $^3J_{CP} = 5.1$ Hz), 128.56, 128.37, 127.97, 111.00, 76.09 (d, $^3J_{CP} = 8.0$ Hz), 69.40 (d, $^2J_{CP} = 5.7$ Hz), 66.72 (d, $^3J_{CP} = 5.7$ Hz), 26.74, 26.52, 26.24; $^{31}\text{P NMR}$ (121 MHz, CDCl_3) -1.17

1-Deoxy-D-xylulose-5-phosphate (DXP, 1)

To a solution of **15** (130 mg, 300 μmol) in methanol (15 ml) was added a catalytic amount of 10 % Pd/C. The resulting mixture was stirred for 12 h with a positive pressure of H_2 (1 atm) at room temperature. The reaction mixture was filtered and the filtrate was concentrated to a colorless film, which was purified by Varian Bond Elute[®] C18 SepPack eluting with gradient methanol (0 to 50 % methanol/water). The PMA stain active fractions were pooled and concentrated to colorless film (60 mg, 80 %). $^1\text{H-NMR}$ (300 MHz, MeOH-d_4) δ (ppm) 4.52 (d, $J = 7.3$ Hz, 1H), 4.38-4.28 (m, 1H), 4.20-3.93 (m, 2H) 2.25 (s, 3H), 1.43 (s, 3H), 1.35 (s, 3H); $^{13}\text{C NMR}$ (75 MHz, MeOH-d_4) δ (ppm) 210.83, 106.05, 77.05, 70.75 (d, $^3J_{CP} = 8.0$ Hz), 66.52 (d, $^2J_{CP} = 5.31$ Hz), 25.57, 23.20; $^{31}\text{P NMR}$ (121 MHz, MeOH-d_4) 0.02.

To a solution of benzyl deprotected **15** (50 mg, 0.2 mmol) in methanol (15 ml) was added Dowex50 X8 (H^+ form, ca 1 g) and stirred for 5 h at room temperature. The resulting mixture was filtered and concentrated *in vacuo* to afford a colorless film (35 mg, 83 %). $[\alpha]_D^{20} +5.6^\circ$ (c 0.77, H_2O); $^1\text{H NMR}$ (300 MHz, MeOH-d_4) δ (ppm); 4.39 (s, 1H), 3.86 (t, $J = 7.6$ Hz, 1H), 3.68 (t, $J = 7.6$ Hz, 2H), 2.29 (s, 3H); $^{13}\text{C NMR}$ (100 MHz, MeOH-d_4) δ (ppm) 214.01, 78.31, 77.23, 63.34, 26.83; $^{31}\text{P NMR}$ (121 MHz, MeOH-d_4) 2.1.

[3-²H]1-Deoxy-D-xylulose-5-phosphate ([3-²H]DXP, 1-a)

¹H NMR (300 MHz, MeOH-d₄) δ (ppm); 4.30 (t, *J* = 6.4 Hz, 1H), 4.00-3.90 (m, 2H), 2.23 (s, 3H); ¹³C NMR (100 MHz, MeOH-d₄) δ (ppm) 207.5, 72.06 (d, ³*J*_{CP} = 8.0 Hz), 68.07, 28.04; ³¹P NMR (121 MHz, MeOH-d₄) 0.25

Preparation and conversion of MEP to ME bisacetone and ME triacetate

The synthetic DXP and [3-²H] DXP were incubated separately with recombinant DXR from *Synechocystis* sp. PCC6803 under the same conditions as reported earlier.²⁶ The crude enzymatic reaction mixture was adjusted to pH 9-10 with 1 M glycine buffer and treated with bacteria alkaline phosphatase (25 μg of 30 unit/mg protein for each of 2 ml of the DXR reaction) in (pH 10.3) at 37 °C for 5 h. The reaction mixture was removed from the incubator before cold absolute ethyl alcohol (equal volume to the reaction mixture) was added to precipitate proteins. The crude mixture was kept at -20 °C for 1 h to maximize precipitation, then centrifuged using Beckman J2-HS. The supernatant was transferred to another container and concentrated *in vacuo* to a yellow brown residue. The equal amounts of Ac₂O and pyridine were added to this residue (total 10 ml for ca 500 mg of the crude residue) before stirring for 5 h at room temperature. The residual Ac₂O and pyridine were removed *in vacuo* and the crude triacetate was purified by flash column chromatography (SiO₂, EtOAc/hexanes 4:6). The triacetate was analyzed by GC/MS, which found the major fragment ions at *m/z* 159 (94 %), 129 (31 %), and 117 (100 %) from the reaction with the unlabeled DXP. Triacetate derivative of 2-C-methylerythritol (**16**): ¹H-NMR (600 MHz, CDCl₃) δ (ppm) 5.18 (dd, *J* = 8.0, 2.8 Hz, H3), 4.56 (dd, *J* = 11.8, 2.8 Hz, H4a), 4.163 (dd, *J* = 11.8, 8.0 Hz, H4b), 4.156 (d, *J* = 11.7 Hz, H1S), 3.90 (d, *J* = 11.7 Hz, H1R), 2.11 (s, 3H), 2.09 (s, 3H), 2.05 (s, 3H), 1.24 (s, C2-CH₃). Purified **16** was deacetylated with Amberlite IRA400 (OH⁻), in methanol (5 ml for 50 mg of the crude

reaction mixture) at room temperature before filtered and concentrated. The crude residue (30 mg) was transformed to the bisacetonide derivative (**7**) with TsOH and 2,2-dimethoxy propane (0.5 ml) in CH₂Cl₂ (5 ml). The crude **7** thus prepared was purified by flash chromatography (EtOAc/hexanes, 2:3) to give a white solid. Synthetic standard bisacetonide derivative of 2-C-methylerythritol (**7**): ¹H-NMR (600 MHz, acetone-*d*₆) δ (ppm) 4.09 (dd, *J* = 7.0, 5.8 Hz, H3), 4.00 (dd, *J* = 8.7, 7.0 Hz, H4S), 3.95 (d, *J* = 8.7 Hz, H1S), 3.84 (dd, *J* = 8.7, 5.8 Hz, H4R), 3.71 (d, *J* = 8.7, H1R), 1.35 (s, C6-CH₃R), 1.310 (s, C5-CH₃S), 1.306 (s, C5-CH₃R), 1.27 (s, C6-CH₃S), 1.21 (s, C2-CH₃); ¹³C NMR (150 MHz, acetone-*d*₆) δ (ppm) 110.11 (C5), 110.00 (C6), 81.83 (C2), 79.44 (C3), 73.49 (C1), 66.00 (C4), 27.58 (C5-CH₃S), 27.02 (C5-CH₃R), 26.60 (C6-CH₃R), 25.04 (C6-CH₃S), 19.80 (C2-CH₃).

CHAPTER III

FOSMIDOMYCIN ANALOGS:SYNTHESES AND KINETIC STUDIES

Introduction

Phosphonic acid containing natural products (natural compounds containing a direct carbon-phosphorous (C-P) bond) have attracted considerable interest since the first report on the discovery of 2-aminoethyl phosphonic acid (1).¹⁰⁰ The first appearance of 1 was a surprise to the researchers who were investigating the amino acid composition of a rumen protozoan, *Tetrahymena pyriformis* because of its unusual C-P bond.¹⁰¹ This new compound has attracted additional interest since then because of its anti-bacterial and fungicidal effects along with the occurrence of other C-P bonds in many lipids, polysaccharides, or proteins.^{102,103} Even though the distribution of phosphonic acid containing natural compounds is quite limited, many have shown significant biological activities, such as antibacterial and herbicidal effects. Studies on this type of compound have thus attracted considerable attention, particularly in terms of understanding their biosyntheses, chemistry, and how to develop analogs with better biological activity. For example, fosfomycin (2) and bialaphos (3) have been studied and commercially used as an antibiotic and an herbicide, respectively.¹⁰⁰ Examples of known C-P compounds with interesting biological activities in this class are shown in Fig.III.1.

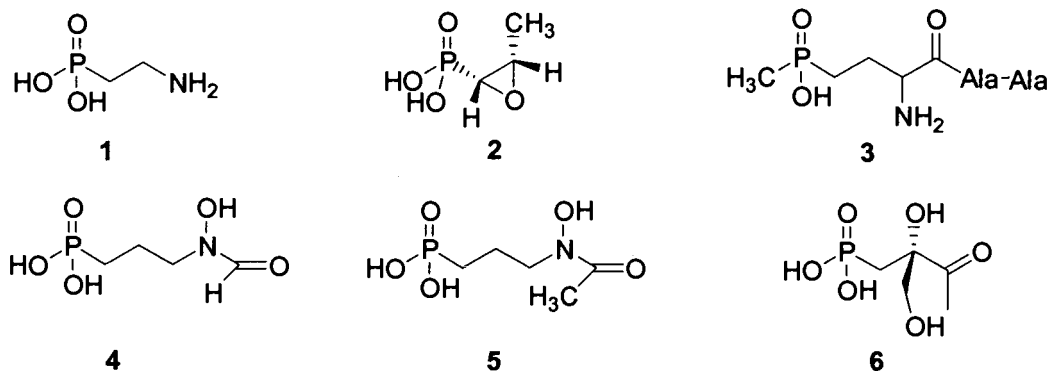


Fig.III.1 Examples of natural C-P compounds with interesting biological activities (1: 2-aminoethylphosphonic acid, 2: fosfomicin, 3: bialaphos, 4: fosmidomycin, 5: FR900098, 6: phosphonothrixin)

Among those shown in Fig.III.1, fosfomicin (2) has been studied more extensively than others due to its broad antibacterial spectrum and low toxicity in humans. While its structure is quite simple, fosfomicin has unique characteristics such as an epoxide and a carbon-phosphorous (C-P) bond that contribute to its bioactivity. Its antibacterial activity derives from a structural similarity with phosphoenol pyruvate, which allows it to inhibit phosphoenol pyruvate UDP-*N*-acetylglucosamine-3-O-enolpyruvyltransferase, an enzyme in peptidoglycan biosynthesis,¹⁰⁰ thus inhibiting bacterial cell wall biosynthesis (Fig.III.2). Despite the development of resistance in some *E. coli* strains, fosfomicin remains a clinically useful antibacterial agent.^{104,105}

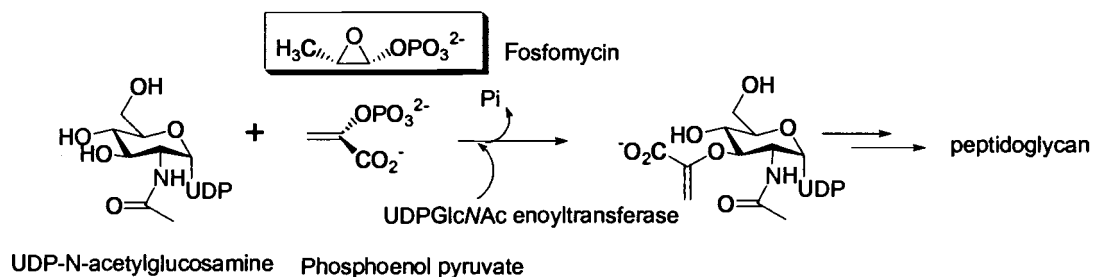


Fig.III.2 The first committed step of peptidoglycan biosynthesis and fosfomycin (2).

In addition to fosfomycin (2), another natural C-P compound, fosmidomycin (4), has attracted attention since the individual steps of the non-mevalonate pathway were elucidated.¹⁴ Originally, fosmidomycin (4) was synthesized as an analog of FR900098 (5), which was reported as a phosphonic acid antibiotic from *Streptomyces rubellomurinus* in 1980.¹⁰⁶ Later, fosmidomycin (also called FR31564) was found to be a natural phosphonic acid antibiotic from isolates of *Streptomyces lavendulae*.¹⁰⁷ Two other phosphonic acid antibiotics, FR-33289 (7, isolated from *Streptomyces rubellomurinus*) and FR32863 (8, isolated from *Streptomyces lavendulae*) were reported with fosmidomycin (4).¹⁰⁷ These phosphonate-containing antibiotics have attracted significant interest for their antibacterial and herbicidal activity against certain species of bacteria and plants.¹⁰⁸ The appearance of this new class of antibiotics, along with the attention being given fosfomycin, has led to intensive investigations of these types of molecules in search of more effective antibacterial agents. In the early 1980's, these compounds were explored as lead compounds and several candidates were synthesized as potential phosphonic acid antibiotics (Fig.III.3).¹⁰⁹⁻¹¹²

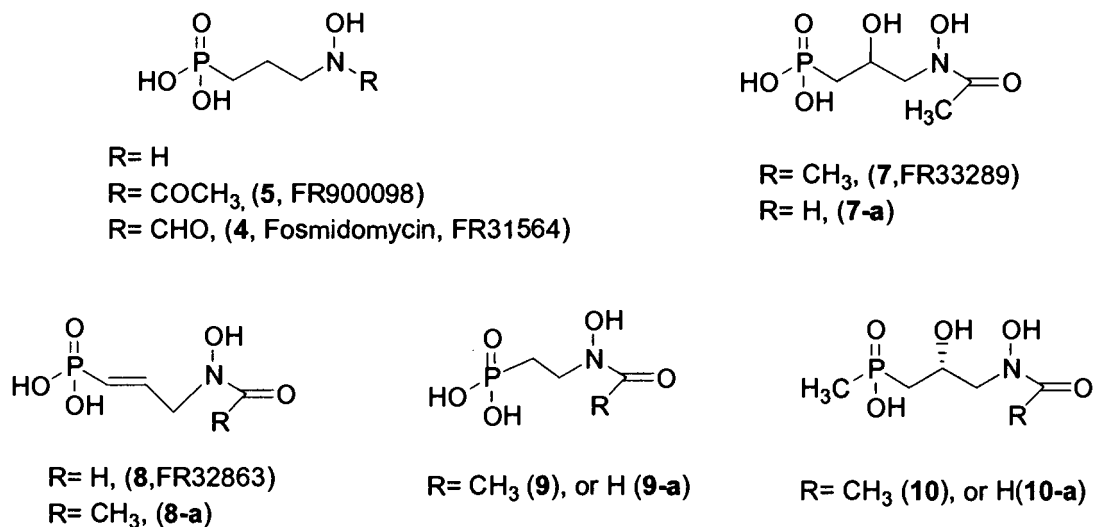


Fig.III.3 Examples of phosphonic acid antibiotics synthesized as analogs of FR900098 (5) and fosmidomycin (4).

These phosphonate-containing antibiotics showed rather unusual characteristics in that the potency of their antibiotic activity lies in the increasing order of: *Pseudomonas*, *Proteus*, *Salmonella*, and *E. coli*, but with practically no inhibitory effect against *Staphylococcus*.¹⁰⁸ A further study performed with fosmidomycin demonstrated that it was active against most Gram-negative bacteria showing greater potency than fosfomycin (2), especially against *E. coli*, *Klebsiella pneumoniae*, *Enterobacter* species, and *Pseudomonas aeruginosa*.¹¹³ Although fosmidomycin (4) was studied in human Phase I and preliminary Phase IIa clinical trials in the 1980's,^{114,115} further development of this compound was not pursued, probably because of its narrow spectrum of antibiotic effect.

Despite sharing some structural features, the basis for the difference in antibiotic action of fosfomycin (2) and fosmidomycin (4) was not understood clearly until recently. Initially, it was believed that the antibiotic effect of fosmidomycin (4) and related compounds came from inhibiting cell wall biosynthesis as does fosfomycin (2).¹⁰⁶ Later, it was proposed that

fosmidomycin (**4**) blocks terpenoid biosynthesis based on the observation that it inhibits the biosyntheses of menaquinone and carotenoids in *Micrococcus luteus*.¹¹⁶ However, no specific step of isoprenoid biosynthesis was identified as a target until Seto *et al.* investigated the inhibition of 1-deoxy-D-xylulose 5-phosphate (DXP) isomeroreductase by fosmidomycin (**4**) in 1998.⁷⁰ In this *in vitro* study, the authors showed that fosmidomycin (**4**) is a potent inhibitor of DXP isomeroreductase (DXR) with a K_i value of 38 nM.

Understanding how fosmidomycin (**4**) inhibits DXR has significant implications because DXR is a key enzyme involved in the non-mevalonate pathway for isoprenoid biosynthesis.²⁶ The non-mevalonate pathway is an alternate route to isoprenoids in certain species of bacteria, algae, and higher plants.² Considering that isoprenoids are one of the largest natural product families and include a variety of biologically important compounds, this alternate route to isoprenoids has been studied extensively.¹⁴ DXR is the enzyme that mediates the second step of this pathway, catalyzing the conversion of DXP to 2-C-methyl erythritol 4-phosphate (MEP) (Fig.III.4). Seto's report⁷⁰ on fosmidomycin inhibiting DXR has renewed interest in this compound as a potential antibiotic. It also implied that blocking DXR, and thus the non-mevalonate pathway, could provide new targets for antibiotic development. Soon after Seto's report,⁷⁰ Lichtenthaler and his colleagues reported that fosmidomycin effectively inhibits isoprenoid biosynthesis not only in some bacteria but also in plants.⁷¹ Jomaa and his coworkers also found fosmidomycin to be a potent candidate to cure malaria by blocking isoprenoid biosynthesis in the malaria protozoan, *Plasmodium falciparum*.³²

powerful ways to lower cholesterol levels in humans. Therefore, DXR is a reasonable target for developing a new class of antibiotics against pathogens that utilize the non-mevalonate pathway for isoprenoid biosynthesis.^{70,32,71,73,74}

In the early 1980's when fosmidomycin was first reported to have potent antibacterial and herbicidal effects, the structure-activity-relationship (SAR) studies on this compound were based solely on the structure of fosmidomycin. Among those analogs, there are a few important results regarding the modification of fosmidomycin. First, researchers modified its intervening carbon chain making ethylene (**9** and **9-a**), 2-(*R*)-hydroxypropyl (**10** and **10-a**), and propenyl analogs (**8-a**).¹¹¹ Of these analogs, however, only the propenyl analog (**8** and **8-a**), which was also reported as natural product (**8**), showed significant antibacterial activity (see Fig.III.2 above for structures). The polar head group of fosmidomycin was also modified to the methylphosphonic acid analogs (**10** and **10-a**), which displayed no significant antibiotic effect. In these studies, fosmidomycin had antibacterial efficacy superior to all of the synthetic analogs, specifically against Gram-negative bacteria. Now that fosmidomycin's mechanism of inhibition has been disclosed at the molecular level,⁷⁰ researchers have a better insight towards utilizing fosmidomycin as a lead compound in the search of an alternative antibiotic.

In order to find more efficient ways to inhibit DXR and thus the non-mevalonate pathway, it is necessary to understand the active site architecture of DXR. The significance of this current SAR study on fosmidomycin is that it should provide better insight into the active site of DXR by using fosmidomycin and its analogs. DXR is a Class B dehydrogenase utilizing NADPH as a cofactor as reported earlier, which provides a schematic outline of the reduction step by DXR.^{28,119} However, it is still, however, in question which part(s) of the natural substrate, DXP, or

the inhibitor, fosmidomycin, DXR specifically recognizes. With no X-ray crystallographic structure of DXR available with its inhibitor bound, searching for an improved fosmidomycin analog will provide information about the essential length, functionalities, stereochemistry, and other features necessary for inhibitors to favorably interact with the active site of DXR.

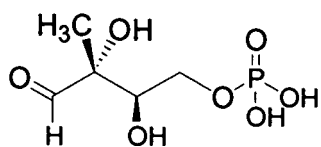
There have been some proposed ideas about the responsible moieties in fosmidomycin for its inhibitory activity based on the common features of DXP and fosmidomycin, but the details have not been suggested or proven yet. Possible clues to fosmidomycin's action may come from the known isomeroreductase, acetohydroxyacid isomeroreductase (AHIR). Isomeroreductases catalyze an alkyl migration followed by a reduction. Alkyl migrations are usually found in cobalamin-dependent enzymes, but the two isomeroreductases known to date do not use cobalamin as a cofactor. Instead, they use divalent metal ions and share a conserved NADPH binding motif. The metal ion, Mg^{2+} , is required for AHIR,⁶⁴ while Mn^{2+} , Mg^{2+} , or Co^{2+} work for DXR.²⁶

Acetohydroxyacid isomeroreductase⁶⁶ has been studied to develop inhibitors of this enzyme for use as herbicidal agents and to understand the mechanism of this unique enzyme. Studies on the active site of AHIR have employed various techniques and it will be useful to apply those methods to the investigation of the DXR active site.

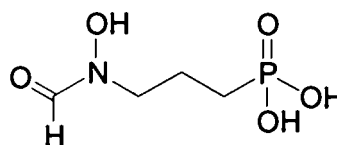
Even though these two enzymes, AHIR and DXR, do not show significant sequence identity, they are related in their functions and in their use of the same cofactor, NADPH. In a crystal structure study of the spinach AHIR,⁷⁷ the enzyme was complexed with NADPH, Mg^{2+} ions, and the competitive inhibitor *N*-hydroxy-*N*-isopropylloxamate (IpOHA). In this study, two Mg^{2+} ions were seen to interact with the inhibitor molecule, connecting the inhibitor with the carboxylate moiety of an aspartate residue

in the active site of AHIR. Inhibitors of AHIR such as IpOHA and 2-(dimethylphosphinoyl)-2-hydroxyacetic acid (Hoe 704) proved to be tight-binding, competitive inhibitors of the bacterial and plant enzymes.¹²⁰ These compounds and other inhibitors of this enzyme provided important information on the active site of acetohydroxy acid isomeroreductase¹²⁰ through kinetic studies and MS analysis. Therefore, from the idea that a similar approach can be used with DXR, analogs of fosmidomycin were designed to expand the understanding of the active site of DXR. The information provided by these SAR studies will be particularly valuable because of the absence of an X-ray structure of DXR complexed with an inhibitor.

The inhibition mechanism of fosmidomycin has been suggested to originate from its structural similarity with the putative intermediate, 2-C-methyl erythrose-4-phosphate, and/or the natural substrate, DXP. The structural features of this proposed intermediate are: (1) a 4-phosphate, originated from the 5-phosphate of DXP; (2) a 2-hydroxy acetaldehyde, which putatively can chelate a divalent metal ion. Fosmidomycin, in comparison, has phosphonate and *N*-hydroxy formamide groups.



2-C-methyl erythrose-4-phosphate



Fosmidomycin

The structural motifs of fosmidomycin that can be modified based on these features are the polar head group (phosphonate), the intervening three-carbon chain, and the *N*-hydroxy amide. In addition to conferring the general structural features of fosmidomycin, design of the fosmidomycin analogs in this study was also based on the earlier synthetic studies

discussed above.¹⁰⁹⁻¹¹² Another factor taken into consideration for designing the fosmidomycin analogs was how the inhibitor of AHIR interacts with the amino acid residues at the active site. Based on the studies of AHIR, it can be proposed that the *N*-acyl, *N*-hydroxy functionality of fosmidomycin might be responsible for chelating with metal ion(s), and that the phosphate is probably responsible for binding with the charged amino acid (e.g. Glu, Asp, His etc.) residues at the active site of DXR. As shown from the study on AHIR,¹²⁰ one of the ways to prove these assumptions is modifying putatively responsible moieties and observing the changes in their kinetic parameters. Therefore, in the current study, the analogs of fosmidomycin were synthesized, and the kinetic values as inhibitors of DXR were evaluated to understand which functionalities of fosmidomycin are most responsible for its inhibition activity.

During the latter phase of this project, two independent X-ray crystallographic reports on DXR were published by Reuter and Jomaa and by Yajima and Seto.^{95,96} Both studies confirmed the presence of the N-terminal dinucleotide binding domain. They also revealed that the strictly conserved acidic residues, Asp¹⁵⁰, Glu¹⁵², Glu³²¹, and Glu²³⁴, are clustered at the proposed active site of DXR. An interesting observation from both studies is that there is a flexible loop region spanning residues 186-216. The authors suggested that this loop region might be responsible for controlling substrate specificity and closing the catalytic site after the substrate binding. Neither of these crystal structures, however, was successful in showing DXR coordinated to an inhibitor. As a result, the exact binding mode of fosmidomycin with DXR and the exact function of this loop region are still in question. Studies on the analogs, therefore, provide complementary information to the crystal structure work and understanding of the active site of DXR.

Based on the discussion above, the following compounds were designed and synthesized (Fig.III.5). The phosphonate of fosmidomycin was modified as phosphate (11), carboxylate (12), and sulfamoyl (13) functionalities. The *N*-hydroxy-*N*-formyl moiety of fosmidomycin was substituted with *N*-methyl-*N*-formyl (14), *N*-methyl-*N*-acetyl (14-a) and hydroxamate (15) groups. While both 11 and 15 are hydroxamates, the orientation of the hydroxyl and carbonyl groups has been reversed in 15. The intervening carbon chain was not changed because the analog with a shorter chain was inactive in antibacterial assays in the preceding studies.¹⁰⁷ Syntheses of these small molecules with various functionalities were more complicated than initially anticipated. Additional syntheses were completed, but the final products were not stable enough to be carried on to enzyme assay experiments.

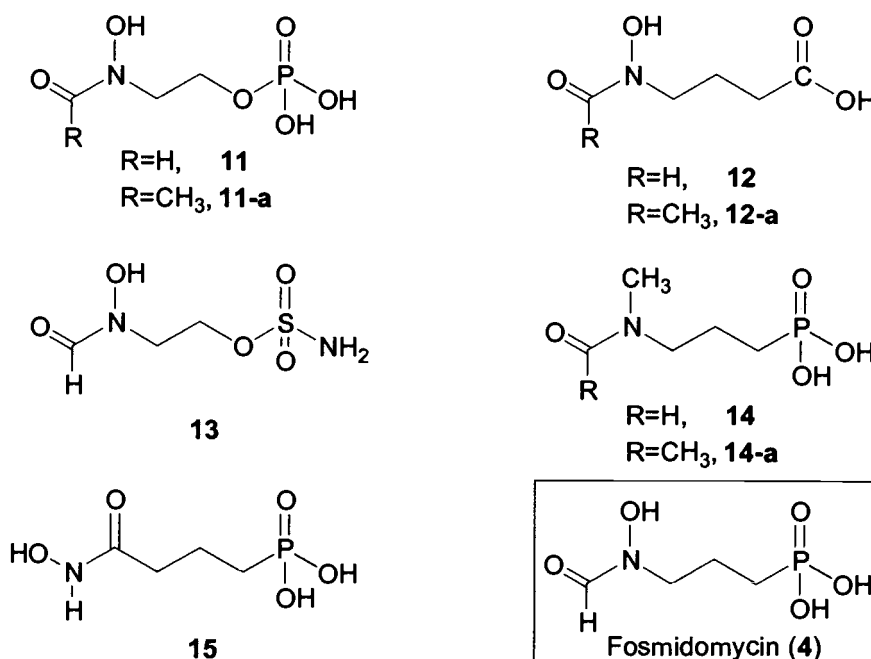


Fig III.5 Fosmidomycin analogs designed and synthesized.

The fosmidomycin analogs shown in Fig.III.5 were designed, successfully synthesized, and purified for testing against DXR. The individual synthetic schemes and kinetic data for the compounds, along with technical difficulties encountered in this project will be presented in the following section. Additionally, details of how those difficulties were overcome and how the results should be taken into account for the future studies on the non-mevalonate pathway will be discussed.

Results and Discussion

The phosphate derivative of fosmidomycin (**11**) was an early target compound because the natural substrate DXP has a phosphate instead of a phosphonate. To our surprise, a literature search for this compound revealed that it is a natural product¹²¹ named fosfoxacin (**11**). Fosfoxacin (**11**) was reported in 1990 as a new antibiotic from the culture filtrates of *Pseudomonas fluorescens* PK-52. Although the synthesis of **11** appeared to be straightforward, it held unexpected challenges (Fig.III.6).

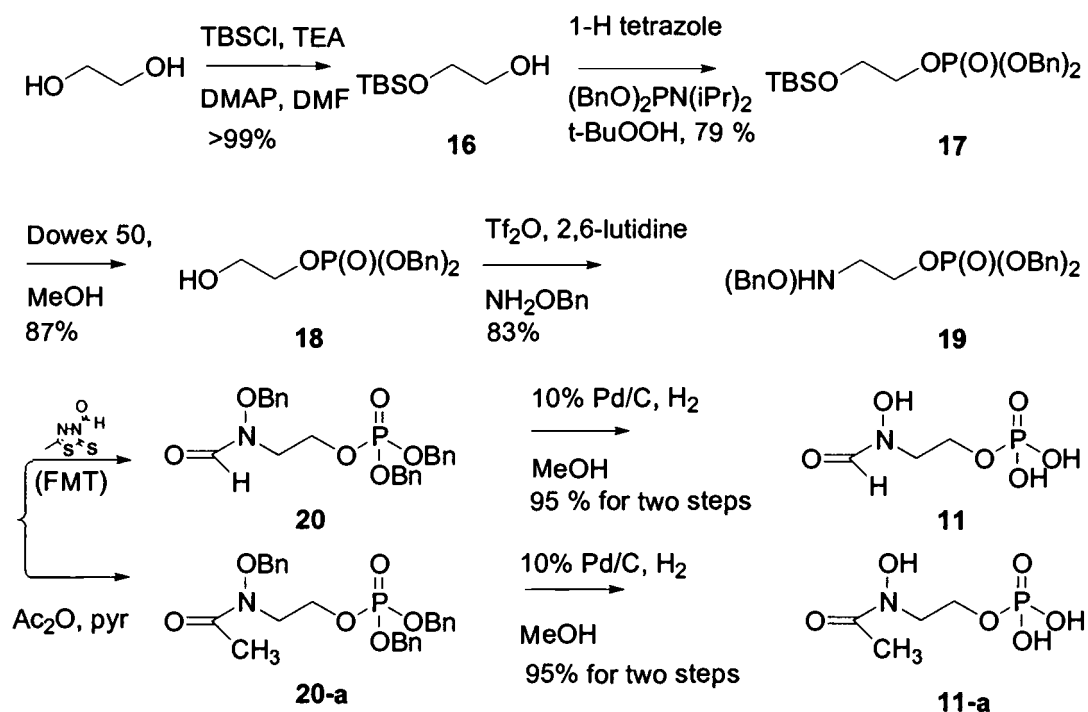


Fig. III.6 Synthesis of fosfoxacin (**11**) and acetyl fosfoxacin (**11-a**).

The phosphate was introduced to the mono-protected ethylene glycol (**16**) with *N,N*-diisopropyl dibenzylphosphoramidite to yield **17**. The next step, introduction of the *N*-hydroxy functionality, provided an unexpected challenge due to the weak nucleophilicity of the amine,

O-benzylhydroxylamine. Several commonly used leaving groups were tried (*i.e.* -OMs, -OTs or Mitsunobu type substitution) to facilitate *N*-alkylation, none of which provided the desired product, **19**. O-Benzylhydroxylamine was chosen as the nucleophile because of the technical convenience that it could be deprotected at the same time as the phosphate group.

Methoxyamine was also tried but yielded no better result. After numerous trials with different leaving groups, the triflate group was used in the presence of 2,6-lutidine to successfully introduce the benzyl-protected *N*-hydroxyl moiety into the desired position. Once the *N*-hydroxyl group was introduced, the nitrogen was acylated with either a formyl or acetyl group to give **20** and **20-a**, respectively. 4-*N*-Formyl-2-methyl-5-Mercapto-1,3,4-Thiadiazole (FMT) introduced a formyl moiety on the nitrogen of **19** under mild conditions with a high yield (90 %). These intermediates, with all the necessary functionalities at the desired positions, were deprotected with Pd/C and H₂ to provide **11** and **11-a**.

In order to obtain reliable enzyme kinetic data, high purity of the substrates or inhibitor is necessary. There is, however, no efficient and universal method for the purification of low molecular weight phosphate/phosphonate compounds. Several features of phosphates/phosphonates contribute to this drawback. First, phosphates and phosphonates can exist in multiple ionization states depending on the pH; therefore, an appropriate buffer system is required to maintain a constant charge. Another challenging aspect of the purification of these compounds is that using techniques which target the characteristics of the phosphate might not be useful because the impurities also often have a phosphate group. Lastly, a common method of purification for phosphate compounds has been re-crystallization, which is not conveniently applicable for a small scale synthesis. Therefore, development of a more readily applicable purification method for phosphate/phosphonate compounds on a

smaller scale will make this field of study more approachable. A variety of purification techniques were thus explored after the synthesis of fosfoxacin (11) and acetylfosfoxacin (11-a) in search of a better purification method for these types of compounds.

HPLC has been used to purify phosphonate compounds in the past.^{122,123} One method utilized a reversed phase C18 silica column with the ion-pairing reagent, tetrabutyl ammonium hydrogen sulfate. The ion-pairing reagent leads to a longer retention.¹²⁴ Ion-pairing reagents, however, must be removed after use.

Another obstacle in the purification of these compounds is that they typically do not have a chromophore for detection by a UV detector. In early studies, refractive index was the most commonly used detection method. Radiodetection and LC/MS have been used, but the target molecules were not radioactive and an LC/MS was not available for routine use. An Evaporative Light Scattering (ELS) detector was used in the current study with a variety of volatile buffers.

Because of the high polarity of the target compounds, a reversed-phase column was tried first with different mobile phases. Despite trying a variety of reverse phase columns (*i.e.* C18, C8, and Hamilton PRP-1) samples eluted as broad peaks with practically no retention, even with 100% aqueous mobile phase and an ion-pairing reagent. Various mobile phases (acetonitrile/water, methanol/water, ammonium acetate/water) were also tried with the different combinations of columns, but resulted in no better of a resolution.

Based on the fact that the phosphate has two ionizable groups, which can be negatively charged under physiological conditions, an ion exchange column was tried. Utilization of an anion exchange column (Partisil™ 10 SAX column) resulted in an extended retention time, but the resolution was still poor. Polysulfoethyl A was tried next for the purification

of these compounds. This hydrophilic material, poly (2-sulfoethyl aspartamide)-silica (PolySulfoethyl A), has been used for hydrophilic-interaction chromatography (HILIC).¹²⁵ In this method, elution occurs in roughly the opposite order of reversed phase chromatography and thus works better for the separation of compounds that are not retained well or elute near the void volume. Therefore, a longer retention time was expected for the polar compounds through the combination of a hydrophilic stationary phase and a hydrophobic mobile phase. It did improve the retention of the sample, but did not provide a pure product.

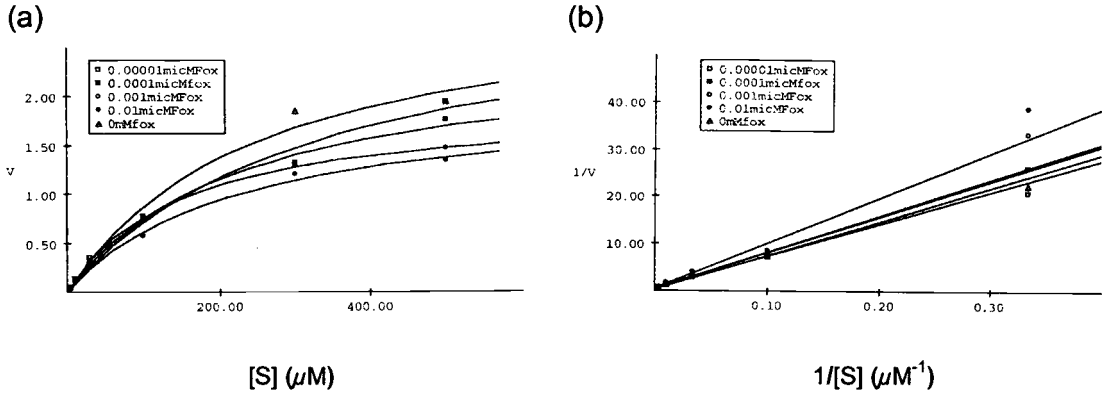
A literature survey on the purification of sugar phosphates and small diphosphate compounds revealed that cellulose column chromatography has been used for the purification of synthetic DXP¹²⁶ and also for the purification of IPP and DMAPP.¹²⁷ Synthetic DXP was purified by a cellulose column eluting with 10% of 0.1% TFA/THF in water.¹²⁶ When this elution system was first applied for the purification of fosfoxacin, however, the sample was destroyed. A small aliquot of the crude fosfoxacin sample was dissolved in 10 % of 0.1 % TFA/THF in D₂O and checked with ¹H NMR to discover that the sample had been decomposed. Later, milder gradient conditions were tried (from 0 % to 1 % of 0.1 % TFA/THF in water over 3h), and the fosfoxacin eluted around 0.1 % of 0.1 % TFA/THF in water. However, the efficiency of this elution system did not give consistent results with different samples which varied in the level of their impurities. The ¹H and ¹³C NMR spectra of the sample showed improved purity after a cellulose column while the ³¹P NMR spectrum did not show improvement. This might imply that the cellulose column is capable of clean some hydrocarbon related impurities, but it does not work with phosphorous related ones. An extensive survey of different eluent systems (*i.e.* acetonitrile/water, THF/water, methanol/water) did not improve the purification either. The cellulose column was thus found to be only useful in

the purification of a sample of phosphate/phosphonate compounds when its impurities are not phosphorous related compounds.

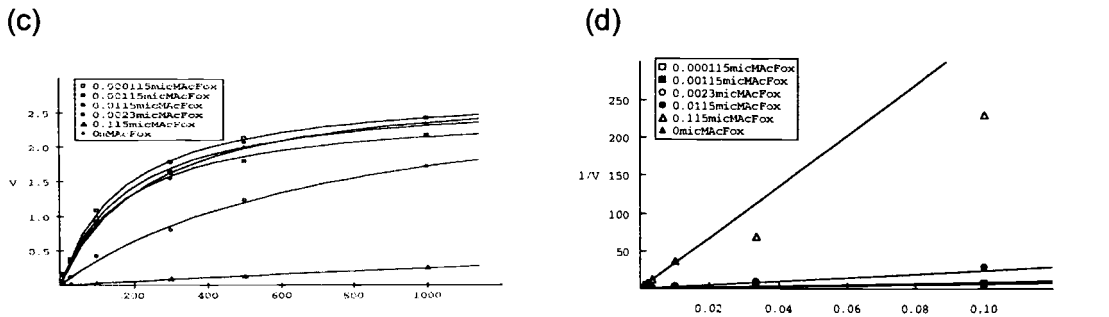
To summarize, there seems to be no universal method for the purification of low molecular weight phosphate/phosphonate compounds. A cellulose column works better than any other methods tried to date in our lab, but work still remains to be done to improve the purification of these compounds.

One final obstacle to overcome before performing the kinetic evaluation of these compounds was to quantitate the exact amount of fosfoxacin (**11**) in hand. Phosphate compounds often form hydrates with different numbers of water molecules, which are not removed even after lyophilization. Therefore, the weight does not reflect only the pure compound. The exact amount of the phosphate compounds, therefore, had to be determined by another method in addition to weighing. The concentration of purified samples of fosfoxacin (**11**) and acetyl fosfoxacin (**11-a**) was determined by phosphate analysis¹²⁸ before they were used for kinetic studies with recombinant DXR.

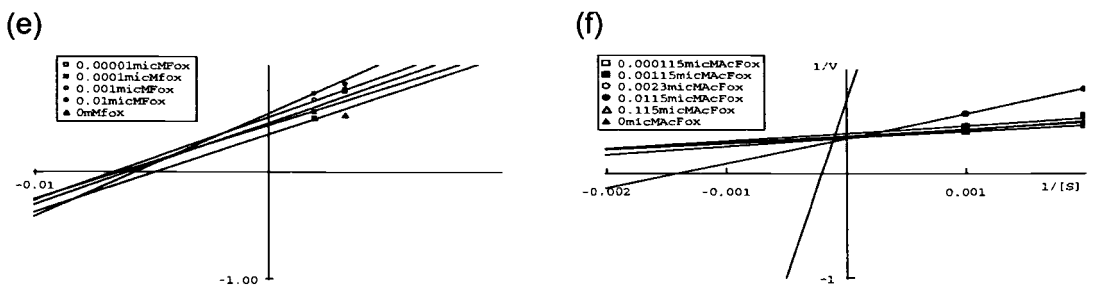
Recombinant DXR from *Synechocystis* sp. PCC6803 was expressed as an-N-terminal 6xHis tagged form in *E. coli*. Each assay was performed as Seto *et al.* reported,⁷⁰ monitoring the consumption of NADPH at 340 nm with a given concentration of DXP and the inhibitors. Each assay was run in triplicate with at least four different concentrations of each inhibitor. Before testing any of the synthetic compounds, it was necessary to reevaluate the K_i value of fosmidomycin (**4**) with *Synechocystis* DXR, because the known K_i value of 38 nM was determined with DXR from *E. coli*.⁷⁰ The K_i value of fosmidomycin (**4**) for *Synechocystis* DXR was determined to be 57 nM.



(a) Non-linear regression representation of inhibition of DXR by fosfoxacin (11) (b) Lineweaver-Burk linear representation of inhibition of DXR by fosfoxacin (11)



(c) Non-linear regression representation of inhibition of DXR by acetyl fosfoxacin (11-a) (d) Lineweaver-Burk linear representation of inhibition of DXR by acetyl fosfoxacin (11-a).



(e) A mixed inhibition by fosfoxacin (11). (f) A mixed inhibition mechanism by acetyl fosfoxacin (11-a) (zoomed-in view of (b) and (d) above).

Fig.III.7 Inhibition of DXR by fosfoxacin (11) and acetyl fosfoxacin (11-a).

The values thus acquired were averaged and analyzed using Enzyme Kinetics software package (Trinity Software). As shown in Fig.III.7 above, approximately 0.1 μ M of acetylfosfoxacin (**11-a**) or fosfoxacin (**11**) inhibited DXR activity almost completely. The K_i values of fosfoxacin (**11**) and acetylfosfoxacin (**11-a**) were calculated as 19 nM and 2 nM, respectively (b and d in Fig.III.7), from the Lineweaver-Burk method, showing that these two compounds are more potent inhibitors of DXR than fosmidomycin (**4**). In Seto's study,⁷⁰ the authors reported that fosmidomycin (**4**) showed a mixed (competitive and noncompetitive) inhibition mechanism. The Lineweaver-Burk graph of fosfoxacin (**11**) and acetyl fosfoxacin (**11-a**) indicated that these two compounds also showed competitive and non-competitive mixed inhibition mechanism (e and f in Fig.III.7).

Carboxylate analogs (**12** and **12-a**) were designed as another phosphonate alternative to fosmidomycin. The pK_a of a carboxylate is 4.8 while a phosphonate has pK_a 's of approximately 2 and 8. The advantage of the carboxylate analog is that the synthesis and purification of carboxylates have been better studied than the cases of phosphonate/phosphate compounds. Therefore, it will be more practical to develop them as new antibiotic candidates than the phosphorous containing analogs if it is proven they have comparable inhibitory activity. The synthesis of the carboxylate analog of fosmidomycin was performed as shown in Figure III.8. The *N*-hydroxyl amine was introduced as in an earlier fosmidomycin (**4**) synthesis using an activated benzyloxyamine, *N*-tosyl,*N*-benzyloxy amine.¹⁰⁹ *N*-tosyl,*N*-benzyloxy amine was deprotonated by NaH and used to displace the bromide from 4-bromo-ethyl butyrate. All three protecting groups of **21**, benzyl-, tosyl, and ethyl, were removed by acid hydrolysis under reflux conditions. The crude reaction residue of the deprotected 4-*N*-hydroxy amino butyrate (**22**) was readily purified by ion-exchange chromatography, and the pure product was acylated by acetylformic anhydride or acetic

anhydride. FMT could not be used for this scheme because **22** was insoluble in methylenechloride in which FMT should be used. The final product was purified by ion exchange chromatography with a reasonable overall recovery.

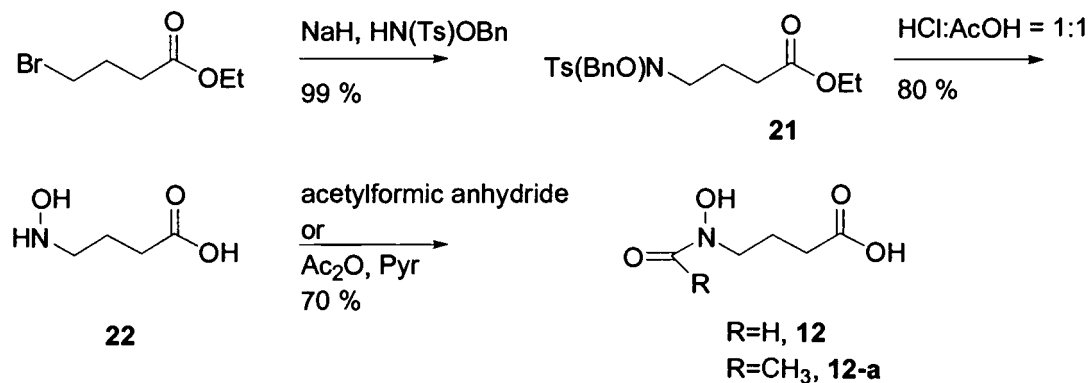
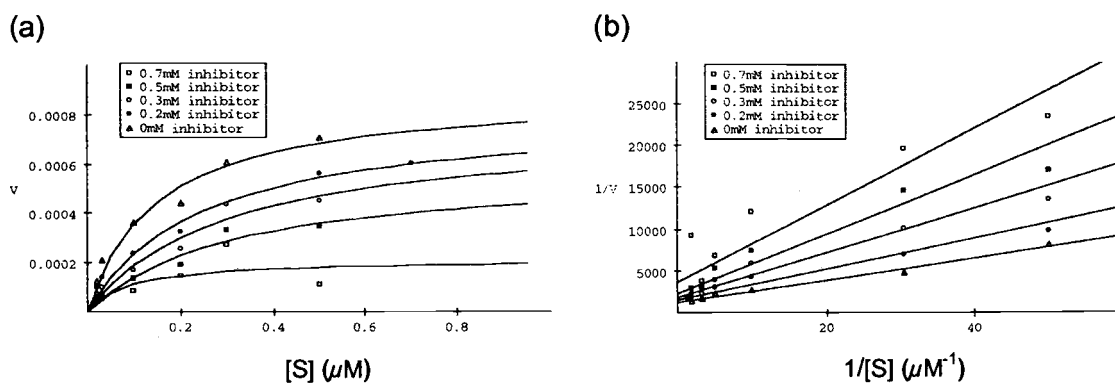


Fig.III.8 Synthesis of carboxylate analogs (**12**, **12-a**) of fosmidomycin.



(a) Non-linear regression representation of inhibition of DXR by carboxylate analog (**12**) (b) Lineweaver-Burk linear representation of inhibition of DXR by carboxylate analog (**12**).

Fig.III.9 Inhibition of DXR by the carboxylate analog of fosmidomycin (**12**).

The K_i value of the carboxylate analog (**12**) calculated from the Lineweaver-Burk method was 240 μ M, which suggests that this carboxylate analog is 6000-fold less potent than fosmidomycin (**4**). Similar to fosfoxacin (**11**)/acetyl fosfoxacin (**11-a**), the carboxylate analog also showed a mixed inhibition pattern (Fig.III.19).

In addition to phosphate and carboxylate analogs, a sulfamate (sulfamoyloxy) analog (**13**) of fosmidomycin was prepared as another modification of the polar head group of fosmidomycin. Introduction of a sulfonate group also had been attempted, but the synthesis of the sulfonate analog encountered technical challenges. The sulfamate analog of fosmidomycin (**13**) was thus chosen to substitute for the sulfonate analog. The sulfamate group has a similar structure to the phosphonate and the sulfonate, but without an ionizable group, which makes **13** a good probe to evaluate the significance of negatively charged oxygens in the phosphonate group. Besides its structural similarity with the phosphonate, the sulfamate group is present in many biologically interesting compounds, *i.e.* nucleoside antibiotics,¹²⁹ and sulfatase inhibitors in estrone sulfamate.¹³⁰ However, despite its potential importance, sulfamoylation of a hydroxyl group has typically proceeded in low yield. In a recent report,¹³¹ however, Howarth *et al.* reported that the sulfamoylation using *N,N*-dimethylacetamide (DMA) as a solvent led to a higher yield. Their modified method was applied in current study to provide the desired product. The synthetic scheme for the sulfamate analog (**13**) of fosmidomycin is shown in Fig.III.10. The sulfamoyloxy group was introduced to the mono-protected ethylene glycol (**16**) before the *N*-alkylation using the same method as in the fosfoxacin synthesis (see Fig.III.6) to give **24**. The resulting *O*-benzyl hydroxylamine was formylated with FMT, then deprotected to the sulfamate analog **13**.

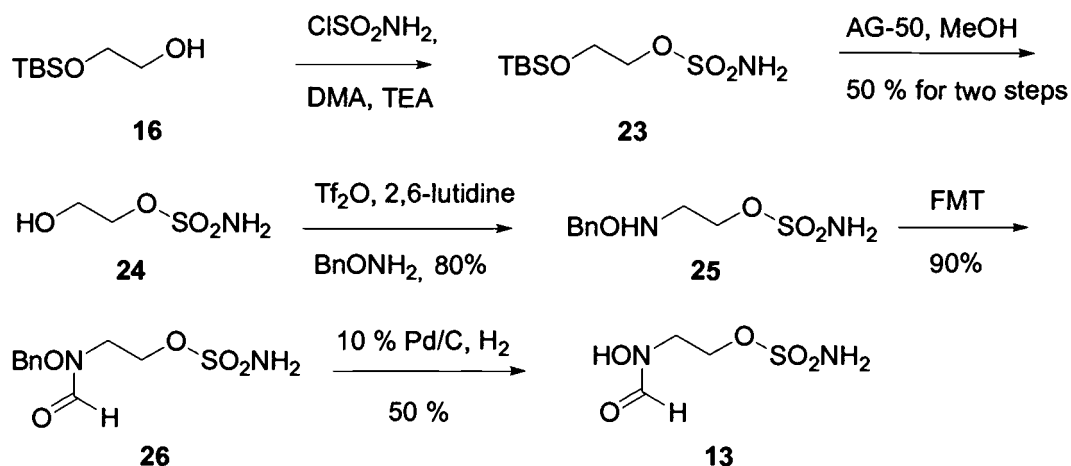
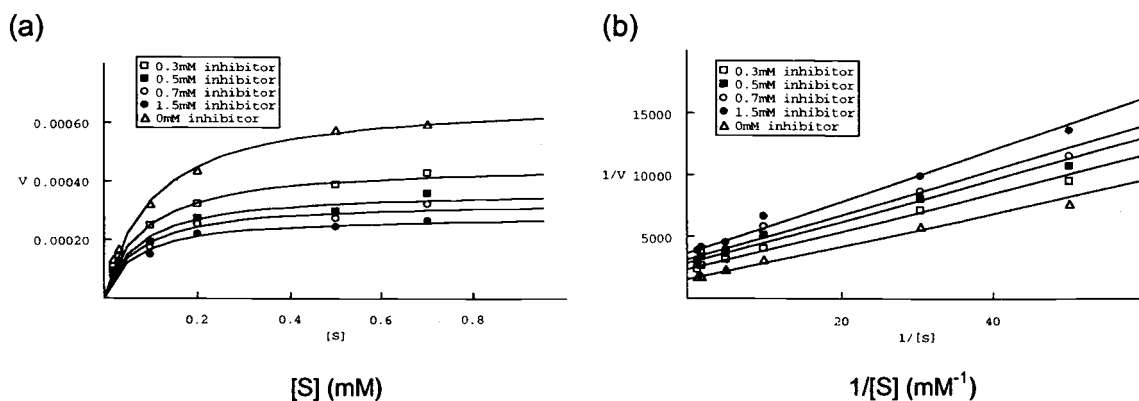


Fig.III.10 Synthesis of sulfamate analog (13) of fosmidomycin.

The K_i value for the sulfamate analog (13) was much greater than that of fosmidomycin (2.8 mM vs 57 nM). This indicates that an ionizable moiety, more specifically a negative charge, likely plays a significant role in the substrate/inhibitor recognition by DXR. This sulfamate analog (13) also inhibited DXR with a mixed mechanism (Fig.III.11).



(a) Non-linear regression representation of inhibition of DXR by sulfamate analog (13) of fosmidomycin.
 (b) Lineweaver-Burk linear representation of inhibition of DXR by sulfamate analog (13) of fosmidomycin.

Fig.III.11 Inhibition of DXR by sulfamate analog (13) of fosmidomycin.

In addition to exploring three different modifications of the polar head group of fosmidomycin, the *N*-hydroxy formamide moiety of fosmidomycin was been also altered. The *N*-hydroxyl moiety of fosmidomycin is proposed to chelate with a metal divalent ion(s) in cooperation with the adjacent carbonyl group. An *N*-methyl analog (**14**) of fosmidomycin was thus prepared to evaluate the significance of the *N*-hydroxyl group in the inhibition efficacy.

An acetyl analog of fosmidomycin (FR900098, **5**) was reported as a natural product showing antibacterial activity even before fosmidomycin (**4**) was reported.¹⁰⁹⁻¹¹¹ Early SAR studies thus investigated both formyl and acetyl derivatives of each analog. Therefore, both formyl (**14**) and acetyl analogs (**14-a**) of the *N*-methyl analog of fosmidomycin were synthesized based on a known method for fosmidomycin synthesis.¹¹⁰ Again, the activated methyl amine, *N*-tosyl, *N*-methyl amine, was deprotonated by NaH and substituted for one bromo group of 1,3-dibromopropane. The phosphonate group was introduced as a diethyl phosphonate to provide **28**. The protecting groups on both nitrogen and the phosphonate were removed by acid hydrolysis to provide a free secondary amino phosphonate, **29**, which was readily purified by a cation exchange chromatography. These two analogs were purified using a Varian BondElute[®] C18 columns and anion exchange chromatography, which afforded the products in reasonable purity (>95 %). The easier purification of **14** and **14-a**, which are phosphonates, might be explained by their different deprotection method (acidic hydrolysis) from the fosfoxacin (**11**) synthesis. This also indirectly suggests that the final deprotection step (debenzylation using Pd/C, H₂) of fosfoxacin synthesis might have a disadvantage of introducing undesirable impurities. Further identification of the undesirable impurities was not pursued in the current study, but they are believed to be different species of phosphorous compounds based on the ³¹P NMR spectrum.

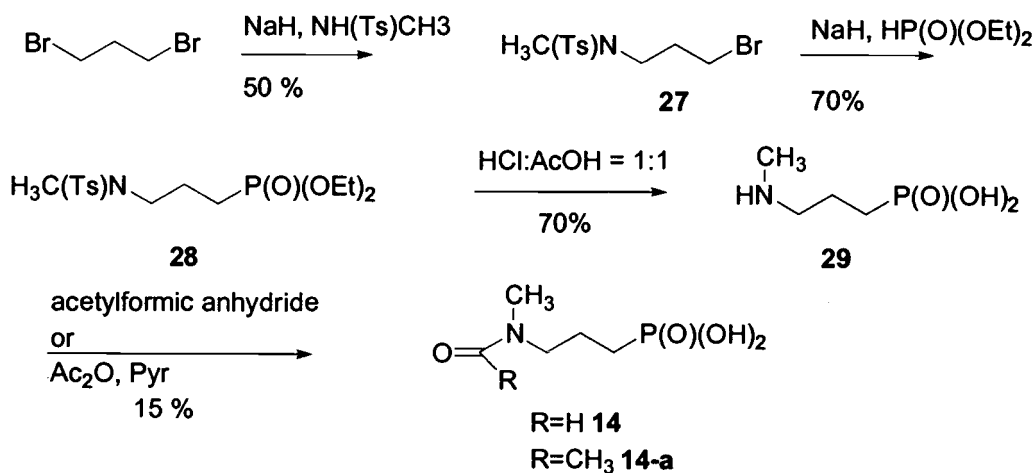
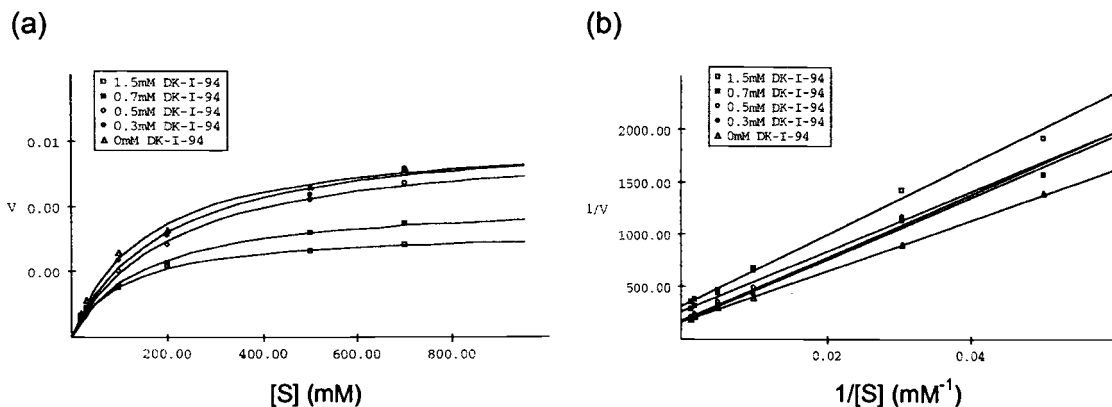
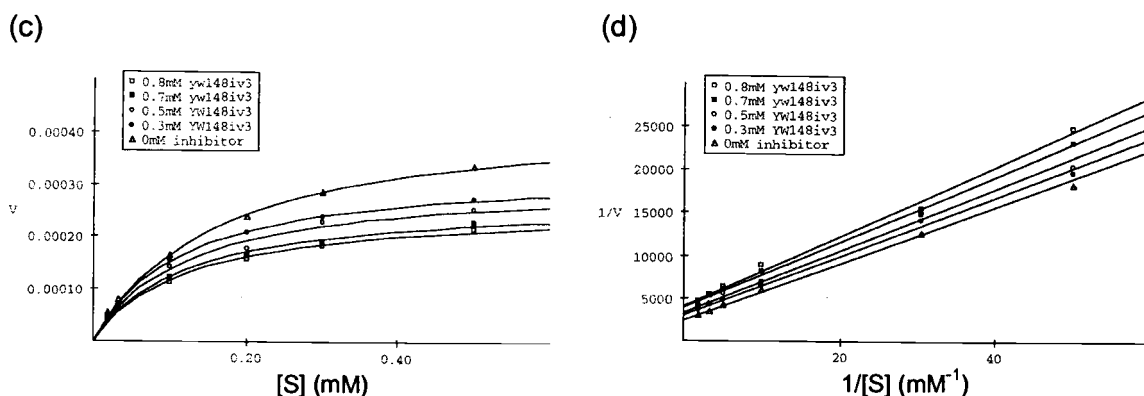


Fig.III.12 Synthesis of *N*-methyl analogs (**14**, **14-a**) of fosmidomycin.

As expected, the inhibition efficacy of these *N*-methyl analogs of fosmidomycin was very low with K_i values of 5 mM and 3.6 mM for the *N*-formyl, *N*-methyl analog of fosmidomycin (**14**) and the *N*-acetyl, *N*-methyl analog of fosmidomycin (**14-a**), respectively (Fig.III.13). As with the fosmidomycin (**4**)/FR900098 (**5**) (IC_{50} values against *P.falciparum* HB3, 350 ± 170 nM and 170 ± 100 nM, respectively³²) and fosfoxacin (**11**)/acetylfosfoxacin (**11-a**) pairs, the *N*-methyl analogs also showed that the acetyl analog (**14-a**) was a slightly better inhibitor of DXR than its formyl counterpart (**14**).



(a) Non-linear regression representation of inhibition of DXR by *N*-methyl, *N*-formyl analog of fosmidomycin (14) (b) Lineweaver-Burk linear representation of inhibition of DXR by *N*-methyl, *N*-formyl analog of fosmidomycin (14).



(c) Non-linear regression representation of inhibition of DXR by *N*-methyl, *N*-acetyl analog of fosmidomycin (14-a) (d) Lineweaver-Burk linear representation of inhibition of DXR by *N*-methyl, *N*-acetyl analog of fosmidomycin (14-a).

Fig.III.13 Inhibition of DXR by *N*-methyl analogs (14, 14-a) of fosmidomycin.

The low inhibitory activity from these compounds supports the critical role that the *N*-hydroxyl group of fosmidomycin plays in inhibition of DXR. In terms of the exact function of this hydroxyl, a few suggestions can be made. First, as shown from the plant acetohydroxy isomeroreductase (AHIR), the hydroxyl group and the adjacent carbonyl group of the

inhibitor/natural substrate can be used as a chelation site for a divalent metal ion(s). The other possibility is that this hydroxyl group can form an important hydrogen bond with an active site amino acid residue(s). In an earlier study on plant acetohydroxy acid isomeroreductase,⁷⁷ the *N*-hydroxy group of the inhibitor IpOHA was shown to form a hydrogen bond network with Glu496 as well as to provide a chelation site for Mg²⁺. Seto *et al.* reported⁶⁸ a mutation study on DXR in which they demonstrated that changing some of the residues decreased the activity of DXR significantly. Some of these changes included the acidic residues, glutamate and aspartate while some histidine residues were also suggested to be important residues in DXR activity. Therefore, it is very likely that these residues interact with some polar moieties, *i.e.* hydroxyl groups and phosphates, of natural substrate/inhibitors.

It is possible that the *N*-hydroxyl moiety of fosmidomycin might function in a similar way, not only providing a chelation site but also interacting with the active site amino acid residues. To address this question, an appropriate analog was required. If the *N*-hydroxyl and the carbonyl next to it are involved only in the chelation of the divalent metal ion, switching the position of the hydroxyl and the carbonyl should not greatly change the inhibition efficacy much. The hydroxamate analog (**15**) with the opposite positioning of the *N*-hydroxyl group and the carbonyl group from the ones of fosmidomycin was thus synthesized and tested for its inhibitory effect.

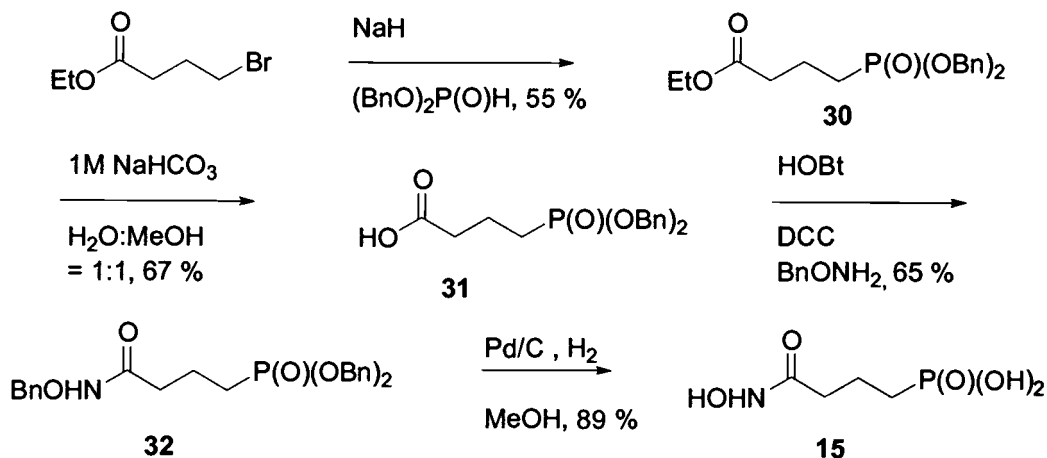
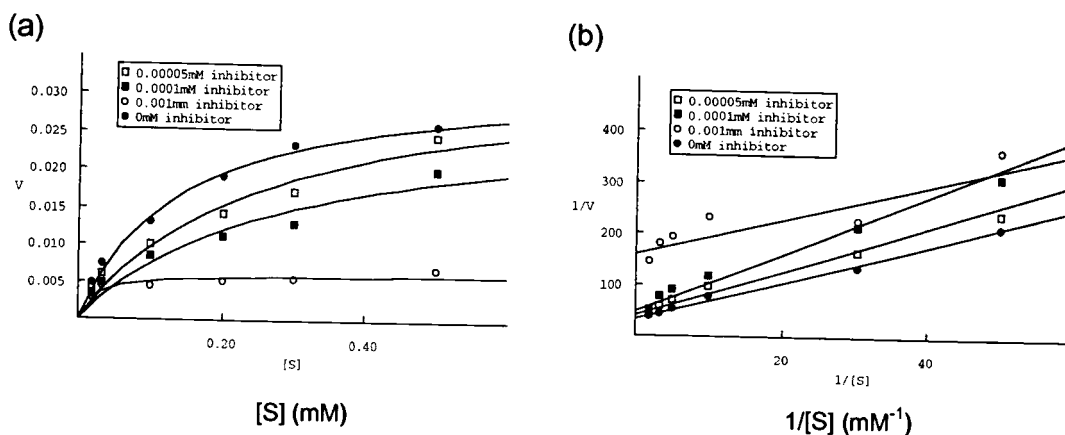


Fig.III.14 Synthesis of hydroxamate analog (**15**) of fosmidomycin.

The synthesis of a hydroxamate analog of fosmidomycin (**15**) was accomplished by introducing the phosphonate group into 4-bromoethylbutyrate. Dibenzyl phosphonate was first deprotonated with NaH and reacted with 4-bromoethylbutyrate to give **30**. Hydrolysis of the ethyl ester to yield **31** was done under mild aqueous condition using 1M NaHCO_3 . Introduction of the *N*-hydroxylamine was first tried by using DCC without an extra coupling reagent. However, as experienced from the fosfoxacin synthesis, the *O*-benzyl hydroxylamine was found to be a weak nucleophile. This required use of a co-amidation reagent. After surveying several coupling reagents, HOBt was successfully used to form the protected hydroxamate (**31**, in Fig.III.14). The final protected product was used for the kinetic study after purification using a cellulose column eluting with water. In the synthesis of fosfoxacin (**11**), the final deprotection step using Pd/H_2 , which was originally planned for the convenience of deprotection, was suspected to cause unexpected impurities. In the synthesis of **15**, however, the same deprotection method, Pd/C and H_2 , was used without any extra impurity problems. Therefore, the problems encountered in the

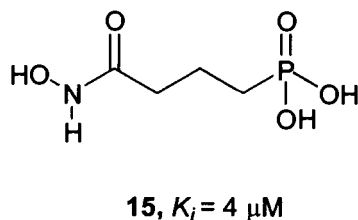
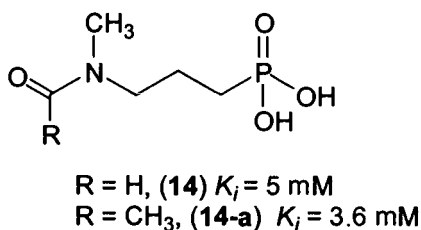
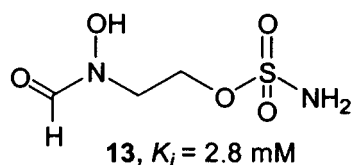
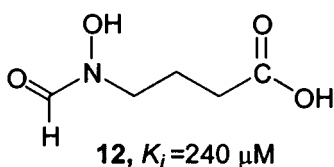
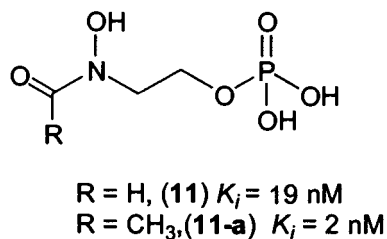
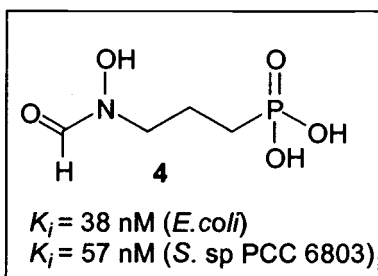
synthesis of fosfoxacin by using Pd/C and H₂ were more serious when the starting material is a phosphate.



(a) Non-linear regression representation of inhibition of DXR by hydroxamate analog (**15**) of fosmidomycin (b) Lineweaver-Burk linear representation of inhibition of DXR by hydroxamate analog (**15**) of fosmidomycin.

Fig.III.15 Inhibition of DXR by hydroxamate analog (**15**) of fosmidomycin.

The K_i value of **15** from Lineweaver-Burk calculation was found to be $4 \mu\text{M}$, which is the second best value next to that of fosfoxacin (**11**)/acetylfosfoxacin (**11-a**). It is, however, 70 times less potent than fosmidomycin (**4**). This result indicates that the *N*-hydroxyl and the carbonyl moiety adjacent to it may be involved in chelation of the divalent metal ion, but that might not be their only role. The fact that changing the position of these two moieties resulted in a significant decrease in inhibition activity demonstrates that these two groups play an additional significant role. As shown in Fig.III.15, the inhibition pattern of this analog also indicated a mixed mechanism. The inhibition constants (K_i) of these new analogs of fosmidomycin are summarized as follows.



Although it has been proposed that fosmidomycin (4) mimics the structure of the proposed intermediate and prevents the intermediate from interacting with DXR, the exact inhibition pattern of these new analogs, including fosmidomycin (4) itself, is still in question. However, the Lineweaver-Burk analyses of these compounds show that all of them follow a mixed (competitive and noncompetitive) inhibition pattern. During the kinetic evaluation experiments for these new analogs, it often occurred that the inhibition efficacy of the analogs was inconsistent. During the assays, some experiments showed the inhibition rate for the first minute or two to be less sharp than the later part of the experiment. This did not occur consistently, *i.e.* the retardation period varied with different concentrations of the same sample.

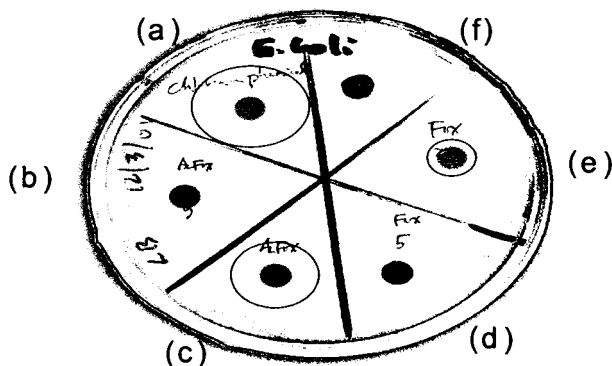
This variable inhibition rate was recently explained by Poulter *et al*, who investigated the steady-state kinetics of fosmidomycin inhibition.²⁹ The

authors showed that the rate of the DXR reaction decreased rapidly during the first two minutes from an initial velocity to a final velocity. It was also reported that the progress curves were linear when DXR was preincubated in a buffer containing fosmidomycin (**4**) and NADPH for 5 min before the reaction was initiated by adding DXP. From these observations, it was suggested that fosmidomycin (**4**) fits a slow tight binding inhibition model.

Fosfoxacin (**11**) and the hydroxamate analog (**15**) were tested to investigate if they also follow the same inhibition pattern as fosmidomycin (**4**) does. The inhibition rate of these two samples, **11** and **15**, was consistent when these were preincubated with DXR before addition of DXP to the assay mixture as Poulter *et al.* reported. These results, however, varied with the concentration of the samples. At lower concentrations, the changes were not significant.

As seen above, fosfoxacin (**11**) and acetylfosfoxacin (**11-a**) showed improved inhibition activity relative to the known inhibitor, fosmidomycin (**4**), against DXR. An unanswered question was how effective these compounds would be *in vivo* antibacterial assays. To address this question, the analogs were tested for their antibacterial activity compared to a commonly used antibiotic, chloramphenicol. Fosfoxacin (**11**) and acetyl fosfoxacin (**11-a**) were tested for their antibacterial activity against *E. coli* through an *in vivo* agar diffusion (Kirby-Bauer disk) test,¹³² and their zones of inhibition were compared with that of chloramphenicol (Fig.III.16). The zones of inhibition for 1 mg of chloramphenicol, 20 μ g of acetylfosfoxacin (**11-a**) and 20 μ g of fosfoxacin (**11**) were, 2.5 cm, 1.8 cm and 0.7 cm respectively. These results demonstrated that fosfoxacin (**11**) and acetyl fosfoxacin (**11-a**) had significant antibacterial activity with only 1/50th of the amount of chloramphenicol. The rest of the analogs were tested under the same conditions. However, none of the analogs tested showed a significant inhibitory effect even with greater amounts (up to 1 mg). In

addition to being tested against *E. coli*, these fosmidomycin analogs were also tested against *Candida albicans*. None of them, however, showed any inhibitory effect, which was expected based on the fact that no yeast is known to utilize the non-mevalonate pathway for isoprenoid biosynthesis.



(a) 20 μ l of 50 μ g/ μ l chloramphenicol solution (1 mg) (b) and (c) 5 and 20 μ g of acetyl fosfoxacin respectively (d) and (e) 5 and 20 μ g of fosfoxacin (f) 20 μ l of H₂O

Fig.III.16 Kirby-Bauer disk test for fosfoxacin (**11**) and acetylfosfoxacin (**11-a**).

The results of the kinetic studies provide the following possible information. First, the phosphate analogs of fosmidomycin (fosfoxacin, **11** and acetylfosfoxacin, **11-a**) are slightly better inhibitors of DXR than fosmidomycin (**4**), which has a phosphonate (K_i value of 19 nM and 2 nM vs 57 nM). However, developing **11** and **11-a** as therapeutically useful antibiotics is not likely because phosphates are quite labile due to ubiquitous phosphatases in cells, while phosphonate compounds are stable to phosphatases. Even though the K_i value of fosfoxacin (**11**) turned out to be about three times lower than that of fosmidomycin (**4**), the K_i value difference between these two compounds does not provide a firm

conclusion about the cause of this difference in their DXR inhibition. These two different K_i values might result from their different capabilities for ionization of a given pH or it might be that the extra oxygen atom in fosfoxacin (**11**) might slightly alter the conformation of the molecule when bound by DXR.

Second, two ionizable groups are important as shown from the far lower inhibition effects of the carboxylate (**12**) and sulfamate (**13**) analog models. Although the carboxylate analog (**12**) has one anionic group, its inhibitory effect was 12,000 fold weaker than that of fosmidomycin (**4**). This observation suggests that both ionizable groups of the phosphonate in fosmidomycin (**4**) contribute to its inhibitory effect, which might be through the formation of hydrogen bonds (or salt bridges) with responsible amino acid residues at the active site of DXR.

Third, the *N*-hydroxyl functionality in fosmidomycin (**4**) plays a crucial role in inhibition probably both by providing a chelation site with a metal ion and by interacting with amino acid residue(s) in the active site of DXR. As seen from a hydroxamate model (**15**), the position of the hydroxyl is important to its inhibition activity. Therefore, it is very likely that there is a key amino acid residue(s) involved in the interaction with the *N*-hydroxyl moiety of fosmidomycin at the active site of DXR in addition to the interaction between the backbone carbonyl and the *N*-hydroxyl.

Fourth, as shown from the examples of FR900098 (**5**), acetyl fosfoxacin (**11-a**), and the *N*-acetyl,*N*-methyl analog (**14-a**), the *N*-acetyl-derivatives in each series showed a slightly greater inhibition activity than their *N*-formyl counterparts. FR900098 (**5**) showed a two-fold lower IC_{50} value than that of fosmidomycin (**4**) against malaria infected mice.³² This runs contradictory to the earlier observation that fosmidomycin (**11**) showed a greater antibacterial effect than FR900098 (**11-a**) against some bacteria strains including *E. coli* (MIC value of 400 vs 12.5 $\mu\text{g/ml}$).¹¹¹ Different

explanations may be suggested to explain this discrepancy. First, it may result from a transport preference between these two compounds across the cell membrane. One of the early studies on fosmidomycin (**4**) reported that it was found to be taken into bacterial cells more efficiently than fosfomycin (**2**).¹⁰⁴ Although the extent of permeability varied with species and fosmidomycin (**4**) and fosfomycin (**2**) do not have a significant difference in their structures, fosmidomycin showed generally better permeability through bacterial cell membrane. Therefore, fosmidomycin (**4**) might have better permeability than FR900098 (**5**) through the cell membrane of bacterial strains tested despite its lower K_i value *in vitro* against DXR. However, the diffusion test result of fosfoxacin (**11**) and acetyl fosfoxacin (**11-a**) in this study showed acetyl fosfoxacin (**11-a**) to be a better inhibitor in the *in vivo* tests against *E. coli*. This might be because the permeability of the fosfoxacin series might have a different preference from the fosmidomycin series. Regardless of what controls their inhibition potency differences *in vivo* and *in vitro*, this example illustrates that the inhibition activity from an *in vitro* experiment cannot be directly translated to that of an *in vivo* experiment.

Lastly, the fosmidomycin analogs showed a mixed inhibition mechanism, which most likely represents the slow, tight-binding inhibition as shown for fosmidomycin (**4**).²⁹ Another significance of the current study is the confirmation that fosfoxacin (**11**), which has been reported as a metabolite of *Pseudomonas fluorescens* PK-52 with antibacterial activity, is a potent inhibitor of DXR along with its acetyl analog (**11-a**). In summary, the optimal inhibitor of DXR based on the study above should have following features: (1) a polar head group with two ionizable groups at biological pH; (2) an α -hydroxy carbonyl unit at the other end to chelate the divalent metal ion with the hydroxyl closer to the polar head group; (3) the

correct length of carbon linkage between the two functionalities above—either three carbons or two carbons and one heteroatom (e.g. oxygen).

The kinetic study results can also be used to envision the architecture of the active site of DXR. As stated earlier, there were two published reports on the X-ray crystal structure of DXR during the latter stage of the inhibitor study.^{96 95} One of the crystal structures, which had better resolution, was acquired using selenomethionyl DXR from *E. coli*, with a final resolution of 2.2 Å.⁹⁶ Although one of them was acquired with NADPH coordinated, neither of them had an inhibitor bound at the active site. Seto *et al.*,⁹⁶ however, reported that there was a sulfate ion seen in their crystal structure, which they suggested might mimic how the phosphonate of fosmidomycin (**4**), or the phosphate of DXP interacts with the amino acid residues at the active site. Although this crystal structure provides significant information about the active site of DXR, there are still many unanswered questions. A key unanswered question is how DXP and fosmidomycin bind to DXR. Based on known biochemical data, attempts were made to place DXP and fosmidomycin at the active site.

First, the nucleotide binding site for various enzymes has been well studied and is known to have a conserved amino acid motif and a similar folding pattern. The conserved NADPH binding motif is present in the *N*-terminal region of *E. coli* DXR, LGKTGSIG. This conserved motif shows a typical $\beta\alpha\beta$ -fold (Rossmann fold)^{133,134} and is proven to be the correct position to which NADPH binds based on the crystal structure.

Second, in a previous mutation study, Seto *et al.*⁶⁸ reported that the mutation of selected amino acid residues led to a significant decrease in DXR activity. These mutation results indicated that Glu²³¹ of DXR from *E. coli* plays an important role in activity, and that His¹⁵³, His²⁰⁹ and His²⁵⁷ are putatively associated with DXP binding.

Third, in the crystal structure of acetohydroxy acid isomeroreductase (AHIR) from spinach, three glutamates, one aspartate, one histidine, one lysine, and one proline participated in an active site network with water molecules, two divalent ions (Mg^{2+}), an inhibitor (IpOHA), and NADPH.⁷⁷ In Seto's crystal structure,⁹⁶ four key residues were distinguished in the catalytic domain, His¹⁵³, His²⁰⁹, Glu²³¹, and His²⁵⁷. In the crystal structure by Jomaa *et al.*, four conserved acidic residues, Asp¹⁵⁰, Glu¹⁵², Glu²³¹, and Glu²³⁴, are "clustered" at the active site.⁹⁵ Similar to the crystal structure of AHIR, DXR also has four acidic residues in its active site; three glutamates and one aspartate. In Seto's crystal structure, the sulfate ion that was trapped in the catalytic pocket appears to be hydrogen bonded to His²⁰⁹. Because this His is located in the loop region with the high B-factor value, which means the position of this loop region is less certain, it is difficult to accurately predict the position of the inhibitor. However, the prediction of the binding pattern of the inhibitor with DXR can be improved based on the known information discussed above, *i.e.* NADPH binding site, active site amino acid array, and the example of IpOHA binding with AHIR at the active site. Additionally, the stereochemical course of the reduction step of DXR is now known.²⁸ Based on these features and the information from the crystal structures, fosmidomycin (**4**) was positioned into the *E. coli* DXR using the ViewerPro[®] program (Fig.III.17).

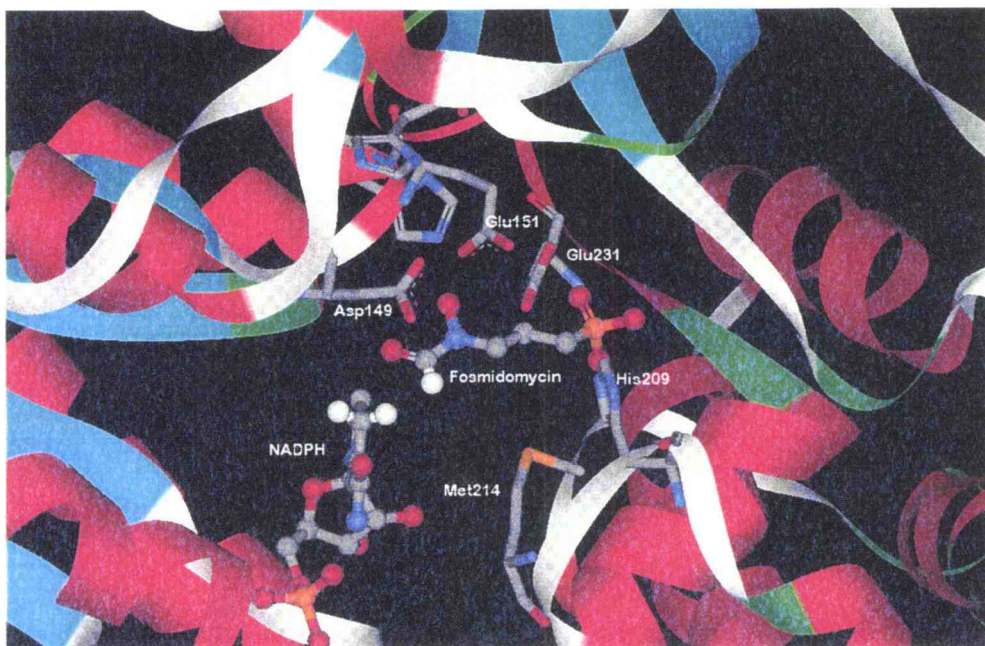


Fig.III.17 NADPH and fosmidomycin (**4**) at the putative active site of DXR based on the crystal structure.⁹⁷ The active site amino acid residues are shown as stick representations. NADPH and fosmidomycin (**4**) are shown as ball and stick. Fosmidomycin was positioned at the active site using the (ViewerPro[®]) program.

Fosmidomycin (**4**) was positioned at the active site with its *N*-hydroxy-*N*-formyl group near the nicotinamide ring of NADPH and its phosphonate near Glu²³¹ and His²⁰⁹ residues that bind the sulfate ion. From the docking picture above, the β 6 helix of the *N*-terminus is set in between NADPH and the inhibitor with several bulky hydrophobic residues, e.g. Leu¹²⁸ and Val¹²⁹, which might be involved in steric discrimination of substrates/inhibitors. The *N*-hydroxyl group of fosmidomycin should be close to Asp150 and His153 so that it can participate in the active site network with these residues, possibly with divalent ion(s), and water molecules. Accurate prediction of the exact fosmidomycin (**4**) binding site at the phosphonate end is difficult because of the uncertainty of the exact location of the loop, which contains

His²⁰⁹ and Met²¹⁴. Either or both of these two amino acids might be closely correlated with Glu²³¹, which is the closest acidic residue to them in the active site. Yajima and Seto *et al* suggested in their crystallography paper⁹⁶ that this loop might work as a “hatch” to close the active site of DXR after the substrate/inhibitor binds to DXR. Therefore, once the substrate/inhibitor enters into the catalytic pocket, it is possible that this loop moves and closes the active site, which will bring these two residues, His²⁰⁹ and Met²¹⁴, closer to the substrate/inhibitor.

In addition to the new analogs discussed above, the syntheses of several more compounds were attempted. The syntheses of these small molecules with various functional groups provided unanticipated challenges. Due to technical hurdles and an emphasis on more readily accessible targets, the syntheses of **33**, **35**, and **36** were not completed. Compounds **34** and **37** were prepared, but stability issues prevented completion of the kinetic analyses. The target compounds are shown in Fig.III.18.

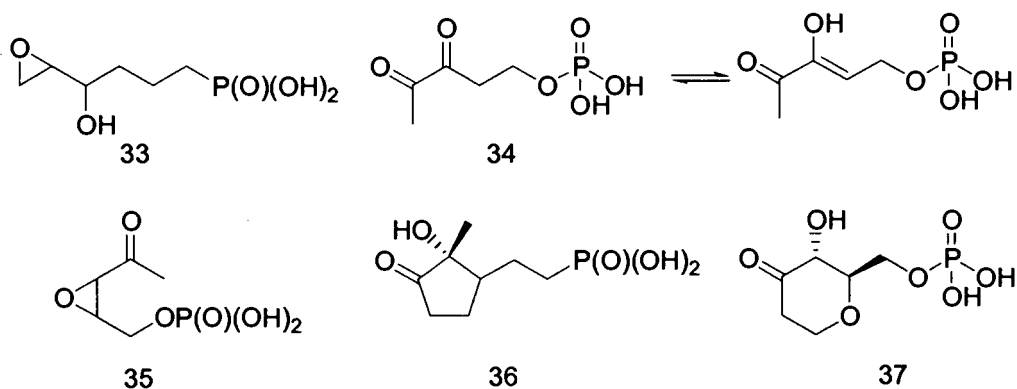


Fig.III.18 Examples of the compounds with incomplete syntheses/kinetic studies.

Compound **34** was designed as a phosphate derivative of laurencione. Laurencione was first reported as a metabolite of a red alga, *Laurencia*

spectabilis.¹³⁵ The chemical synthesis¹³⁶ and biosynthetic route^{137,138} of this compound have been studied, and it has been proposed that laurencione is a precursor of pyridoxol.¹³⁸ Rohmer *et al.* suggested, from the results of labeling studies,¹³⁷ that laurencione is obtained from 1-deoxy-D-xylulose by eliminating water. Because this 1,2-diketo compound will co-exist with its enol form, which has a structure similar to DXP, a phosphate analog of laurencione was designed and the synthesis of it was completed (Fig.III.19).

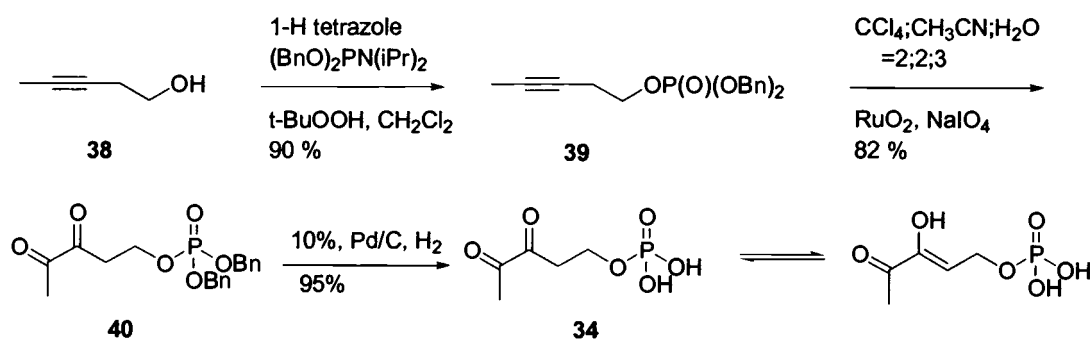
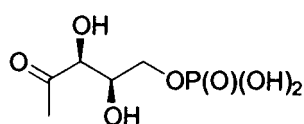


Fig.III.19 Synthesis of laurencione phosphate (34).

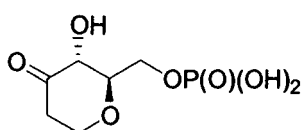
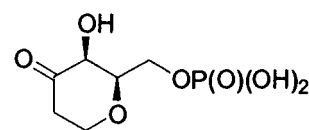
The key step of this synthesis was introducing the 1,2-diketo group in one step by RuO₄ oxidation of the pent-2-yne derivative 39.¹³⁹ However, the deprotected final product was not stable enough to be evaluated for kinetic parameters. The final sample stored in at 4 °C decomposed overnight. It has been reported that laurencione mostly exists in a cyclic form, which is due to the free hydroxyl group at the C5 position.¹³⁵ Once it is protected as a phosphate, it is not expected to undergo the same kind of intramolecular cyclization. From the observation that 34 decomposed so quickly, however, it can be suggested that the phosphate analog of laurencione (34) might undergo some unexpected intermolecular reactions.

The phosphate derivative of glucal (37) was first designed as a cyclic analog of DXP. The advantage expected from the cyclic analog was that

the keto group of this molecule would be present as the *cis*- conformation only. The synthesis of this compound began from the known sugar α -D-glucal, which has the *R*-configuration at the C4 hydroxyl position. The stereochemistry at the C3 position of the natural substrate, DXP, however, is *S*. Therefore, a cyclic analog with the same stereochemistry as DXP was also designed and the synthesis was initiated from α -D-galactal.



DXP

designed phosphate analog
of D-Glucal (**37**)designed phosphate analog
of D-Galactal (**41**)

The starting material, D-glucal (**37**), was insoluble in most organic solvents except acetone. The low yield of the first protecting step was due to the volatility of the protected derivative, **43**. After the reduction, the secondary alcohol was oxidized to a ketone (**45**). Again the volatility of the product caused a low yield. A phosphate was introduced with dibenzyl-diisopropyl phosphoramidite selectively to the primary alcohol to give **47**. The synthesis of the phosphate analog of glucal (**37**) was completed (Fig.III.20) by the deprotection of benzyl phosphate ester, and the final concentration of the product was measured by phosphate analysis. The final product was purified to be tested for its inhibition activity against DXR by cellulose column. Even though the synthesis of **37** gave a fairly pure final product (99 %), the assay could not be completed because DXR appeared to be unstable with this compound. A minor impurity was suspected as the cause of problems, so further purification was performed by using an ion exchange column, a cellulose column, and a charcoal column. The assay was repeated but the DXR activity was still unstable. Because DXR activity is measured by monitoring the consumption of

NADPH, the instability of DXR observed might be due to the instability of NADPH under the assay conditions with **37**. A separate assay with NADPH and **37** without DXR demonstrated that NADPH decomposed more rapidly than the auto-degradation ratio. It was never resolved what was the cause of this increased rate of NADPH consumption.

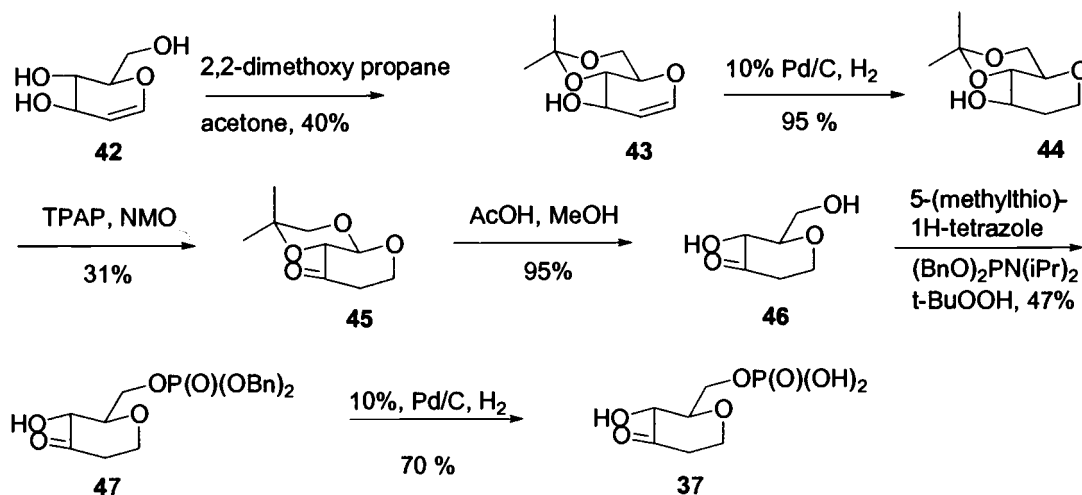


Fig.III.20 Synthesis of the phosphate analog of D-Glucal (**37**).

The synthesis of the phosphate analog of D-galactal (**41**) using a similar synthetic scheme proceeded fairly well until it was found that an intermediate of this synthetic scheme existed as an enol form. During the deprotection of the benzyl groups, the enol double bond was reduced yielding no desired product. If the syntheses/enzyme assays of these compounds had been successful, they could have provided information about the contribution of the conformation of the acetyl group next to the α -hydroxyl.

Exploring the non-mevalonate pathway as a new target for antibiotics has numerous advantages as discussed earlier. However, the development of efficient inhibitors for this pathway is challenging. The

features of optimal inhibitors demand more complicated procedures for the synthesis and the purification. Despite these difficulties, the inhibitors of DXR showed potent antibiotic effects in this study and further suggested future direction for new inhibitors. It is only the early stage of the investigation of the non-mevalonate pathway, but progress that has been accomplished in the past few years provides the fundamental information for future studies on this pathway. The results of the current study thus offer valuable information for the investigation of this pathway for the purpose of developing new antibiotics. In addition, the information from this study will provide a better insight into the DXR active site and will expand our knowledge of the enzymes that catalyze this rather unique isomerization/reduction reaction.

Experimental

General experimental procedures

Ultraviolet (UV) spectra were recorded using a HITACHI U-2000 spectrophotometer. Infrared (IR) spectra were obtained using a Nicolet 510 Fourier transform IR (FTIR) spectrophotometer. Nuclear magnetic resonance (NMR) spectra were reported on Bruker AM 400, AC 300 or DRX 600 instruments, where noted. ^1H and ^{13}C NMR chemical shifts were reported as δ using the residual solvent signal as an internal standard (CHCl_3 at 7.26 ppm for ^1H NMR and 77.00 ppm for the center line of the triplet for ^{13}C NMR samples in CDCl_3). Either *tert*-butanol (31.21 ppm for the CH_3) or MeOH-d_4 (49.15 ppm for the center line of quintet) was added as an internal standard for the samples in D_2O for their ^{13}C NMR. Phosphoric acid (85 %) in water was used as an external standard for ^{31}P NMR spectra (0.00 ppm). Low and high-resolution chemical ionization and fast atom bombardment mass spectra (CIMS and FABMS) were obtained on a Kratos MS50TC spectrometer. Ion Spray mass spectra were obtained on a PerkinElmer SCIEX API3 spectrometer. Silica gel (Merck, grade 60, 220–400 mesh) was used for flash column chromatography.⁹⁷ Merck glass-backed TLC plates (Si gel 60 F₂₅₄) were used for thin-layer chromatography (TLC). The solvents used for most of the synthetic procedures were dried before use as commonly recommended.⁹⁸ The water used in the experiments was double-deionized water (Milli Q Millipore). The cultured bacterial cells were disrupted by sonication with a XL2000 Microson™ (Misonix) ultrasonic cell disruptor. The bacterial culture samples were centrifuged by either Beckman JI-HS or Beckman J2-HS at the temperature as indicated. Commercial grade reagents and the starting materials were purchased from Sigma-Aldrich and used without further purification. Unless

stated otherwise, synthetic reactions were performed in oven-dried glassware under a positive pressure of argon.

Phosphate analysis

Phosphate analyses were done using a modification of a known method.¹²⁸ All of the following solutions were prepared fresh before use. A solution of 1.9 M HClO₄ was prepared by adding 8.4 ml of 70 % HClO₄ to 41.6 ml of water. The molybdate solution was prepared by adding 2.285 g of (NH₄)₆Mo₇O₂₄·4H₂O into a mixture of 48.5 ml H₂O and 1.05 ml conc. H₂SO₄. The aqueous solution of 0.1 mM KH₂PO₄ was prepared by dissolving 13.6 mg of KH₂PO₄ in 10 ml of water then diluting to 100 ml. Toluene and *i*-BuOH were mixed 1:1 (v/v). To each glass tube (2 x 16 cm) were added 0.5 ml of the 1.9 M HClO₄ solution and corresponding amount of KH₂PO₄ solution to make various concentrations (0, 0.1, 0.2, 0.3, 0.4, and 0.5 ml etc. to make 0, 10, 20, 30, 40, and 50 nM etc. of final concentrations) to generate a standard curve. The calculated amounts of the sample solution were added into separate tubes containing 1.9 M HClO₄ solution to make final approximate concentrations within the range of the standard curve. These tubes were placed in a boiling water bath for 30 min before cooling at room temperature for 5 min. Water (3 minus the amount of KH₂PO₄ added) ml, 1 ml of molybdate solution, and 2 ml of *i*-BuOH/toluene were added to each tube. The samples thus prepared were vortexed and the toluene layer was removed before reading at 310 nm. The samples and standards were run in duplicate. The standard curve was generated from six different concentrations of K₂HPO₄. The concentration of phosphate in the sample was determined from the standard curve.

Purification of DXR

A pBAD expression plasmid with the *Synechocystis* sp. PCC6803 *dxr* (pBAD.His-DXR.Bgl, prepared as reported before²⁸) was transformed into *E. coli* Top10 cells and the cells were grown at 30 °C for 3 h before induction with 0.2 % arabinose, followed by an additional 5 h of growth. The cultures were centrifuged, and the collected pellet was frozen at –80 °C. The frozen pellet was thawed at 0 °C for 1 h and re-suspended into the extraction buffer (5 ml of 100 mM Tris·HCl pH 7.5; 5 mM of imidazole; 400 mM NaCl/1 g of wet culture) and incubated with lysozyme (0.75 mg for 2 g of wet weight of cells) at 37 °C for 10 min. The liquid cell culture was sonicated on ice (3 x 10 sec bursts at 7 watts with 30 sec between bursts) and centrifuged for 20 min at 12,000 x g at 4 °C and the supernatant was saved as a cell extract. The cell extract was added to TALON[®] metal affinity resin pre-washed with a wash buffer (50 mM sodium phosphate, 300 mM NaCl in pH 7.0) before gentle agitation for 20 min at room temperature. The supernatant was removed after a centrifugation at 700 x g for 5 min. This procedure was repeated twice before transferring the resin to a disposable plastic column (holding 20 ml) and washing the column twice with 5 bed volumes of wash buffer. The protein sample was eluted by adding 5 bed volumes of stepwise gradient elution buffer (30, 50, 70, 100, 120, and 150 mM imidazole, 50 mM sodium phosphate, and 300 mM NaCl at pH 7.0). The final concentration of the enzyme was determined by Bradford assay,¹⁴⁰ and the activity of DXR was tested following Seto's protocol.⁷⁰ The fractions with the desired protein sample were desalted by dialysis using Slide-A-Lyzer[®] (Pierce) in 100 mM Tris·HCl (pH 7.5, 2 L) overnight at 4 °C.

Enzyme assay

Evaluation of the DXR activity with each new compound was done as described in the literature.⁷⁰ The 500 µl total volume for each assay

consisted of 100 mM Tris-HCl (pH 7.5), 1 mM MnCl₂, 0.2 mM NADPH, DXR in different concentrations, and also varied concentrations of synthetic fosmidomycin analogs. Each assay was initiated by adding DXR and the consumption of NADPH was measured at 340 nm for 4 minutes. Inhibition assays were done with at least four different concentrations of each new analog, and each concentration was tested in triplicate. Inhibition constants were determined using Enzyme Kinetics software v.1.1 (Trinity Software).

*Kirby-Bauer disk test*¹³²

Each fosmidomycin analog was spotted on a 6 mm paper disk (aqueous solution of 20 µl/disk) and the disks were placed on the surface of a Mueller-Hinton agar plate where 50 µl of liquid culture of *E. coli* NCTC90001, grown in LB medium overnight at 37 °C, was streaked over the entire surface of the plate. The plate was incubated overnight at 37 °C. The zone of inhibition was measured at 16 h and 24 h as the diameter of the clear region surrounding the disk on the bacterial lawn.

Synthesis of 2-(N-formyl-N-hydroxyamino)ethylphosphoric acid (Fosfoxacin, 11) and 2-(N-acetyl-N-hydroxyamino)ethylphosphoric acid (N-Acetylfosfoxacin, 11-a)

2-(tert-Butyldimethylsilyloxy)-ethanol (16)

To a solution of ethylene glycol (1 g, 16.1 mmol), triethylamine (TEA, 2.5 ml, 24.1 mmol) and DMAP (20 mg, 0.16 mmol) in CH₂Cl₂ (120 ml) was added TBDMSCl (2.91 g, 19.3 mmol) in 5 portions over 1 h at 0 °C. The resulting heterogeneous reaction mixture was gradually warmed to room temperature. The mixture was stirred for 12 h before dilution with water and CH₂Cl₂. The organic layer was washed successively with solutions of saturated aqueous NaHCO₃, saturated aqueous NH₄Cl, water and brine, dried over MgSO₄, filtered, and concentrated *in vacuo*. The pale yellow oil

was purified by vacuum chromatography¹⁴¹ (SiO₂, EtOAc /hexanes, 1:3) to give a colorless oil (2.9 g, 99 %).

Phosphoric acid, dibenzyl 2-(tert-butyldimethylsilyloxy) ethyl ester (17)

To a solution of **16** (100 mg, 0.6 mmol) in CH₂Cl₂ (30 ml) were added 1-*H*-tetrazole (80 mg, 1.2 mmol) and dibenzyl diisopropyl phosphoramidite (390 μl, 1.2 mmol). The resulting solution was stirred for 4 h at room temperature under Ar at room temperature before *tert*-butyl hydroperoxide (70 % solution, 0.5 ml) was added dropwise at 0 °C. The reaction mixture was warmed to room temperature and stirred for 8h. The mixture was diluted with CH₂Cl₂, and the organic layer was washed with water twice, and the combined aqueous layers were re-extracted with CH₂Cl₂ (5 ml x 3). The combined organic layer was washed with a saturated aqueous solution of sodium bicarbonate, water and brine, dried with MgSO₄, and concentrated *in vacuo*. The concentrate was purified by flash column chromatography (EtOAc/hexanes, 1:3) to afford the desired product (196 mg, 79 %). IR (neat) cm⁻¹ 1251, 1007, 765; ¹H-NMR (300 MHz, CDCl₃) δ (ppm) 7.31-7.37 (m, 10H), 5.05 (d, ³J_{HP} = 8.0 Hz, 2H), 5.04 (d, ³J_{HP} = 7.9 Hz, 2H), 4.04 (dt, ³J_{HP} = 7.1 Hz, J = 5.2 Hz, 2H) 3.76 (dt, J = 5.2 Hz, ⁴J_{HP} = 1.1 Hz, 2H), 0.88 (s, 9H), 0.04 (s, 6H); ¹³C NMR (75 MHz, CDCl₃) δ (ppm) 135.88 (d, ³J_{CP} = 6.9 Hz), 128.53, 128.45, 127.88, 69.18 (d, ²J_{CP} = 5.5 Hz), 68.61 (d, ²J_{CP} = 5.9 Hz), 62.10 (d, ³J_{CP} = 7.9 Hz), 25.81, 18.29, -5.37; ³¹P NMR (121 MHz, CDCl₃) δ (ppm) 0.16 (brs); LRMS (CI) *m/z* 437.19 [M + 1] HRMS (CI) Calcd for C₂₂H₃₄O₅PSi 437.19132, Found 437.19076.

Phosphoric acid, dibenzyl 2-hydroxyethyl ester (18)

Compound **17** (50 mg, 0.1 mmol) was dissolved in methanol before adding Dowex[®] 50WX8-100 (H⁺ form) (1 g) resin. This heterogeneous mixture was stirred for 12 h at room temperature. The resin was filtered off and the

filtrate was concentrated to a pale yellow oil, which was purified by flash chromatography (5 % MeOH/CHCl₃) to provide the product as a colorless oil (32 mg, 87 %). IR (neat) cm⁻¹ 3582, 1230; ¹H-NMR (300 MHz, CDCl₃) δ (ppm) 7.37-7.34 (m, 10H), 5.06 (d, ²J_{HP} = 8.5 Hz, 2H), 5.05 (d, ³J_{HP} = 8.4 Hz, 2H), 4.08 (dt, J = 4.4 Hz, ³J_{HP} = 9.4 Hz, 2H), 3.73 (dt, J = 4.4 Hz, ⁴J_{HP} = 0.9 Hz, 2H), 2.64 (brs, 1H); ¹³C NMR (75 MHz, CDCl₃) δ (ppm) 62.01 (d, ²J_{CP} = 5.3 Hz), 69.59 (d, ²J_{CP} = 5.6 Hz), 69.82 (d, ³J_{CP} = 6.1 Hz), 128.02, 128.62, 128.68, 135.61 (d, ³J_{CP} = 6.5 Hz); ³¹P NMR (121 MHz, CDCl₃) δ (ppm) 1.19; LRMS (FAB) m/z 323.10 [M+1] HRMS (FAB) Calcd for C₁₆H₂₀O₅P 323.10484, Found 323.10496

Phosphoric acid, dibenzyl 2-benzyloxyamino-ethyl ester (19)

To a solution of **18** (67 mg, 0.21 mmol) in CH₂Cl₂ (25 ml) was added 2,6-lutidine (30 μl, 0.25 mmol) under an Ar atmosphere. The solution was cooled to -78 °C before adding trifluoromethane sulfonic anhydride (39 μl, 0.21 mmol) dropwise. After the reaction mixture was stirred at -78 °C for 30 min, O-benzyl hydroxylamine (39 mg, 0.31 mmol) was added dropwise. The solution was stirred for 1 h at -78 °C, warmed to room temperature, and stirred for another 2 h. The reaction mixture was diluted with CH₂Cl₂ and washed with saturated aqueous solutions of NH₄Cl, NaHCO₃, water and brine, dried over MgSO₄, filtered and concentrated to a pale yellow oil *in vacuo*. The resulting residue was purified by flash chromatography (EtOAc/hexanes, 2:1) to yield the product as a colorless oil (74 mg, 83 %): IR (neat) cm⁻¹ 1253, 1011, 732 ; ¹H-NMR (400 MHz, CDCl₃) δ (ppm) 7.31-7.38 (m, 15H), 5.04 (d, ³J_{HP} = 8.3 Hz, 2H), 5.03 (d, ³J_{HP} = 8.3 Hz, 2H), 4.67 (s, 2H), 4.15 (dt, J = 5.1 Hz, ³J_{HP} = 7.2 Hz, 2H), 3.07 (dt, J = 5.1 Hz, ⁴J_{HP} = 1.2 Hz, 2H); ¹³C NMR (100 MHz, CDCl₃) δ (ppm) 137.75, 135.76 (d, ³J_{CP} = 6.2 Hz), 128.56, 128.32, 127.94, 127.82, 128.47, 128.36, 76.04, 69.35 (d, ²J_{CP} = 5.4 Hz), 64.25 (d, ²J_{CP} = 5.8 Hz), 51.68 (d, ³J_{CP} = 7.3 Hz); ³¹P NMR

(121 MHz, CDCl₃) δ (ppm) 0.38;LRMS (FAB): m/z 428.16 [M+1] Calcd for C₂₃H₂₇O₅NP 428.16269, Found 428.16377

Phosphoric acid, dibenzyl 2-(*N*-benzyloxy-*N*-formyl-amino)-ethyl ester (20)

To a room temperature solution of **19** (74 mg, 1.17 mmol) in CH₂Cl₂ (20 ml) was added FMT¹⁴² (50 mg, 0.31 mmol). The resulting solution was stirred for 12 h. The reaction mixture was washed with water, and the aqueous layer was re-extracted with CH₂Cl₂ (5 ml x 2). The combined organic layers were washed with water and brine, dried over MgSO₄, filtered, and concentrated to a yellow film. The crude residue was purified by flash column chromatography (EtOAc/hexanes, 1:2) to afford a colorless film (77 mg, 98 %): IR (neat) cm⁻¹ 1689, 1280, 1018; ¹H-NMR (300 MHz, CDCl₃) δ (ppm) two regioisomers were found as 2:1 ratio: major- 8.18 (br s, 1H), 7.32-7.35 (m, 15H), 5.02 (dd, ³J_{HP} = 9.8 Hz, ²J_{HH} = 1.8 Hz, 4H), 4.13 (m, 2H), 3.77 (m, 2H): minor- 7.87 (br s, 1H), 7.32-7.35 (m, 15H), 5.03 (d, ³J_{HP} = 8.3 Hz, 2H), 5.02 (d, ³J_{HP} = 8.3 Hz, 2H), 4.10 (m, 2H), 3.38 (m, 2H); ¹³C NMR (75 MHz, CDCl₃) δ (ppm) major-163.83, 135.63, 135.58, 134.13, 129.48, 129.11, 128.71, 128.56, 127.98, 78.15, 69.47 (d, ²J_{CP} = 5.8 Hz), 63.14, 49.17: minor-158.79, 135.63, 135.58, 134.13, 129.48, 129.11, 128.71, 128.56, 127.98, 78.15, 69.25 (d, ²J_{CP} = 5.3 Hz), 62.44, 45.25; ³¹P NMR (121 MHz, CDCl₃) δ (ppm) -0.03, 0.26;LRMS (FAB): m/z 456.16 [M+1] HRMS (FAB) Calcd for C₂₄H₂₇O₆NP 456.15760, Found 456.15872

Phosphoric acid, dibenzyl 2-(*N*-acetyl-*N*-benzyloxy-amino)-ethyl ester (20-a)

Compound **19** (74 mg, 1.17 mmol) was dissolved in a 1:1 mixture of Ac₂O and pyridine (25 ml) and stirred for 12 h at room temperature. The solvent was removed *in vacuo* and the residue was purified by flash silica column chromatography (EtOAc/hexanes, 1:1) to give a colorless oil (79 mg, 98 %):

IR (neat) cm^{-1} 1672, 1280, 1018; $^1\text{H-NMR}$ (400 MHz, CDCl_3) δ (ppm) 7.32-7.37 (*m*, 15H), 5.02 (*d*, $^3J_{\text{HP}} = 8.2$ Hz, 2H), 5.01 (*d*, $^3J_{\text{HP}} = 8.1$ Hz, 2H), 4.79 (*s*, 2H), 4.16 (*dt*, $^3J_{\text{HP}} = 7.4$ Hz, $^3J_{\text{HH}} = 5.6$ Hz, 2H), 3.83 (*br s*, 2H), 2.05 (*s*, 3H); $^{13}\text{C NMR}$ (100 MHz, CDCl_3) δ (ppm) 172.93, 135.73, 135.67, 134.30, 129.28, 129.00, 128.73, 128.59, 128.39, 127.98, 76.82, 69.39 (*d*, $^2J_{\text{CP}} = 5.3$ Hz), 63.72 (*d*, $^3J_{\text{CP}} = 5.4$ Hz), 46.44, 20.44; $^{31}\text{P NMR}$ (121 MHz, CDCl_3) δ (ppm) 0.04; LRMS (FAB): *m/z* 470.17 [*M*+1] HRMS Calcd for $\text{C}_{25}\text{H}_{29}\text{O}_6\text{NP}$ 470.17325, Found 470.17204

Phosphoric acid, mono- [2-(*N*-formyl-*N*-hydroxy-amino)-ethyl] ester (11)

A solution of **20** (60 mg, 0.13 mmol) in methanol (10 ml) was stirred with a catalytic amount of 10 % Pd/C under a hydrogen atmosphere (1 atm) at room temperature overnight. The Pd/C was removed by filtration, and the filtrate was concentrated to a pale yellow film. The residue was redissolved in water (2 ml), and the aqueous layer was washed with chloroform (2 ml x 3) before being purified by CF-11 cellulose column chromatography (2.5 x 30 cm) eluting with a continuous gradient of 0 to 1 % (0.1 % TFA/THF) in water. Five ml fractions were collected, and the fractions that were PMA-active were collected and freeze-dried to a colorless film (20 mg, 91 %).

$^1\text{H-NMR}$ (400 MHz, D_2O) δ (ppm) two regio-isomers with 3:7 ratio 8.32 (*bs*, minor) & 7.94 (*bs*, major), 3.93 (*m*, 2H), 3.64 (*m*, 2H) $^{13}\text{C NMR}$ (100 MHz, D_2O) δ (ppm) 160.42, 60.62 (*d*, $^2J_{\text{CP}}=3.0$ Hz), 51.16 (*d*, $^3J_{\text{CP}}=5.0$ Hz) $^{31}\text{P NMR}$ (121 MHz, D_2O) δ (ppm) 3.88; LRMS (FAB): *m/z* 184.0 [*M*-1]; HRMS Calcd for $\text{C}_3\text{H}_7\text{O}_6\text{NP}$ 184.00110, Found 184.00101

Phosphoric acid mono- [2-(*N*-acetyl-*N*-hydroxy-amino)-ethyl]-ester (11-a)

A solution of **20-a** (62 mg, 0.13 mmol) in methanol (10 ml) was stirred with a catalytic amount of 10 % Pd/C under a hydrogen atmosphere (1 atm) at room temperature overnight. The Pd/C was removed by filtration, and the

filtrate was concentrated to a pale yellow film. The residue was redissolved in water, and the aqueous layer was washed with chloroform (5 ml x 3) before applied to a CF-11 cellulose column (2.5 x 30 cm). The desired compound was eluted with a continuous gradient of 0 to 1 % (0.1 % TFA/THF) in water. Five ml fractions were collected, and the PMA-active fractions were collected and freeze-dried to a white solid (24 mg, 93 %).

$^1\text{H-NMR}$ (600 MHz, D_2O) δ (ppm) a mixture of two isomers; 2.17 (s) & 2.16 (s), 3.78-3.83 (*m*, 2H), 4.00-4.02 (*m*, 2H); $^{13}\text{C NMR}$ (100 MHz, D_2O) δ (ppm) 160.95 & 164.92, 60.96 (d, $^2J_{\text{CP}} = 2.0$ Hz), 58.53 & 51.63 (d, $^3J_{\text{CP}} = 6.6$ Hz), 10.84; $^{31}\text{P NMR}$ (121 MHz, D_2O) δ (ppm) 1.53; LRMS (FAB): *m/z* 198.1 [M-1] HRMS Calcd for $\text{C}_4\text{H}_9\text{O}_6\text{NP}$ 198.01675, Found 198.01695

Synthesis of 4-(N-formyl-N-hydroxy-amino)-butyric acid (12, a carboxylate derivative of fosmidomycin)

4-[N-Benzyloxy-N-(toluene-4-sulfonyl)-amino]-butyric acid ethyl ester (21)

Solid sodium (30 mg, 1.23 mmol) was dissolved into fresh dried ethanol (45 ml) then the mixture was warmed to 60 °C. Once the mixture became clear, it was cooled to room temperature before treated with *N*-benzyloxy-toluene-4-sulfonamide (312 mg, 1.13 mmol) in ethanol (5 ml). The reaction mixture was stirred for 2 h at room temperature. To the solution above was added 4-bromobutyric acid ethyl ester (200 mg, 1.02 mmol) dropwise, and the resulting solution was refluxed for 12 h. The reaction was quenched by water and the solvent was removed *in vacuo*. The resulting yellow residue was diluted with EtOAc before the organic layer was washed with saturated aqueous NH_4Cl , water and brine, dried over MgSO_4 , filtered and concentrated to a yellow oil. The residue was purified with flash chromatography (EtOAc/hexanes, 1:9) to give 403 mg of a colorless oil (> 99 %): IR (neat) cm^{-1} 1734, 1364, 1171; $^1\text{H-NMR}$ (400 MHz, CDCl_3) δ

(ppm) 7.74 (d, $J = 8.3$ Hz, 2H), 7.34-7.43 (m, 5H), 7.31 (d, $J = 8.3$ Hz, 2H), 5.10 (s, 2H), 4.12 (q, $J = 7.1$ Hz, 2H), 2.91 (br s, 2H), 2.41 (s, 3H), 2.33 (t, $J = 7.43$ Hz, 2H), 1.81 (p, $J = 7.1$ Hz, 2H), 1.25 (t, $J = 7.1$ Hz, 3H); ^{13}C NMR (100 MHz, CDCl_3) δ (ppm) 172.82, 144.76, 135.18, 130.02, 129.71, 129.56, 129.47, 128.51, 128.71, 79.86, 60.44, 52.61, 31.24, 22.09, 21.59, 14.17; LRMS (CI): m/z 392.1 [M+1] HRMS (CI) Calcd for $\text{C}_{20}\text{H}_{26}\text{O}_5\text{NS}$ 392.15317, Found 392.15365

4-*N*-Hydroxyaminobutyric acid (22)

A solution of **21** (345 mg, 0.89 mmol) in a 1:1 mixture of conc. HCl and acetic acid (50 ml) was refluxed overnight. The solvent was removed *in vacuo* and the residue was dissolved in water (10 ml). The aqueous layer was washed with chloroform and then concentrated to a brown residue. The crude product was purified with Dowex 50X8-100 resin, eluting with 2N NH_4OH . The fractions were pooled and freeze-dried to a pale yellow film (85 mg, 81 %). ; ^1H -NMR (400 MHz, MeOH-d_4) δ (ppm) 2.99 (t, $J = 7.5$ Hz, 2H), 2.27 (t, $J = 7.4$ Hz, 2H), 1.88 (p, $J = 7.5$ Hz, 2H); ^{13}C NMR (100 MHz, MeOH-d_4) δ (ppm) 182.64, 40.42, 35.51, 24.73; LRMS (CI): m/z 120 [M+1] HRMS Calcd for $\text{C}_4\text{H}_{10}\text{O}_3\text{N}$ 120.06607, Found 120.06608

4-(*N*-Formyl-*N*-hydroxyamino)-butyric acid (12)

Compound **22**, 15 mg, 0.12 mmol) was stirred in 500 μl of acetyl formic anhydride¹⁴³ at room temperature for 12 h. The reaction mixture was concentrated to a yellow brown oil and purified with Varian Bond Elute[®] C_{18} column eluting with gradient from 0 to 100 % MeOH in H_2O . The fractions which were FeCl_3 -active by TLC were pooled and freeze-dried to a pale yellow solid (13 mg, 72 %). IR (neat) cm^{-1} ; ^1H -NMR (400 MHz, MeOH-d_4) δ (ppm) 1:1 mixture of two isomers: 7.92 & 8.25 (2s, 1H), 3.53 & 3.58 (2t, $J = 6.6$ Hz, 2H), 2.20-2.24 (m, 2H), 1.88-1.95 (m, 2H); ^{13}C NMR (100 MHz,

MeOH-d₄) δ (ppm) 180.65, 164.19 & 159.79, 35.12 & 34.62, 24.71, 23.84; LRMS (CI): m/z 147 [M⁺] HRMS Calcd for C₅H₉O₄N 147.05318, Found 147.05450

4-(*N*-acetyl-*N*-hydroxyamino)-butyric acid (**12-a**)

4-*N*-hydroxyaminobutyric acid (**22**, 28 mg, 0.23 mMol) was stirred in a 1:1 mixture of acetic anhydride and pyridine (5 ml) for 12 h at room temperature. The solvent was removed *in vacuo*, and the yellow residue was purified with Varian Bond Elute[®] C₁₈ column eluting with gradient of methanol in H₂O (0 to 100 %). The collected fractions (5 to 15 % MeOH) were concentrated and further purified by AG1-x10 (100-200 mesh, Cl⁻ form) eluting with 2N-NH₄OH. The fractions that were active (FeCl₃ TLC stain) were pooled and lyophilized to form a white solid (26 mg, 70 %). ¹H-NMR (400 MHz, D₂O) δ (ppm) 3.09 (t, J = 7.2 Hz, 2H), 2.29 (t, J = 7.2 Hz, 2H), 1.85 (s, 3H), 1.68 (p, J = 7.2 Hz, 2H); ¹³C NMR (100 MHz, MeOH-d₄) δ (ppm) 179.13, 172.68, 47.36, 33.51, 22.85, 19.18; LRMS (CI): m/z 162.1 [M+1]

*Synthesis of sulfamic acid 2-(*N*-formyl-*N*-hydroxy-amino)-ethyl ester (**13**, a sulfamic acid derivative of fosmidomycin)*

Sulfamic acid 2-(*tert*-butyldimethylsilyloxy)-ethyl ester (**23**)

Sulfamoyl chloride was prepared as described.¹²⁹ The impure needle shaped crystals were identified as the desired product from the IR spectrum [IR (neat, cm⁻¹) 3625, 3381, 3278, 1546, 1384, 1185, 1064, 924] which matched the reported values.¹⁴⁴

To a solution of 2-(*tert*-butyldimethylsilyloxy)ethanol (90 mg, 0.51 mmol) in DMA (7 ml) was added triethylamine (86 μ l, 0.61 mmol). The solution was cooled in an ice bath before adding sulfamoyl chloride (118 mg, 1.0 mmol) under a N₂ atmosphere, then stirred for 2 h at 0 °C. The reaction mixture

was warmed to room temperature and stirred for 3 h. The reaction mixture was diluted EtOAc and the resulting organic layer was washed successively with saturated aqueous solutions of NaHCO₃ and NH₄Cl, water and brine. The combined organic layer was dried over MgSO₄, filtered, concentrated, and the residual TEA was removed *in vacuo* to afford a pale yellow oil (60 mg). IR (neat) cm⁻¹ 2954, 2932, 1712, 1560, 1366, 1184, 936; ¹H-NMR (300 MHz, CDCl₃) δ (ppm) 5.43 (bs), 4.25 (t, *J* = 4.8 Hz, 2H), 3.89 (t, *J* = 4.8 Hz, 2H), 0.88 (s, 9H), 0.08 (s, 6H); ¹³C NMR (75 MHz, CDCl₃) δ (ppm) 72.05, 61.48, 25.76, 18.26, -5.44; LRMS (CI): *m/z* 256.1 [M+1]

Sulfamic acid 2-hydroxyethyl ester (24)

Compound **23** (ca 60 mg of crude product from the previous step) in methanol (10 ml) was treated with 0.5 g (wet weight) of AG 50W X8-100 (H⁺ form) and stirred for 5 h at room temperature. The resin was removed by filtration and the filtrate was concentrated to a yellow oil. The crude oil was purified on a Varian Bond Elute[®] C18 column eluting with a gradient of methanol in H₂O (0 to 100 %). The product eluted around 5 % methanol in H₂O and was concentrated to a pale yellow oil (35 mg, 50 % for two steps). IR (neat) cm⁻¹ 3343, 2974, 2926, 2889, 1449, 1380, 1180, 1088, 1049, 881; ¹H-NMR (300 MHz, MeOH-d₄) δ (ppm) 4.11 (t, *J* = 4.8 Hz, 2H), 3.73 (t, *J* = 4.8 Hz, 2H); ¹³C NMR (75 MHz, MeOH-d₄) δ (ppm) 72.33, 61.20; LRMS (CI): *m/z* 142 [M+1] HRMS Calcd for C₂H₈O₄NS 142.01740, Found 142.01770

Sulfamic acid 2-(*N*-benzyloxyamino)-ethyl ester (25)

To a solution of **24** (28 mg, 0.2 mmol) in dry CH₂Cl₂ (10 ml) was added 2,6-lutidine (31.9 mg, 0.3 mmol). The solution was cooled to -78 °C before adding trifluoromethane sulfonic anhydride (40 μl, 0.24 mmol) dropwise. After the reaction mixture was stirred at -78 °C for 30 min, *O*-benzyl

hydroxylamine (49 mg, 0.4 mmol) was added dropwise. The solution was stirred for 1 h at $-78\text{ }^{\circ}\text{C}$, warmed to room temperature, and stirred for another 2 h. The reaction mixture was diluted with CH_2Cl_2 and washed with saturated aqueous NaHCO_3 , dried over MgSO_4 , filtered, and concentrated. The resulting yellow oil was purified by flash column chromatography (EtOAc/hexanes, 3:2) to yield a pale yellow oil (39 mg, 80 %). IR (neat) cm^{-1} 3343, 2974, 2926, 2889, 1449, 1380, 1180, 1088, 1049, 881, 785; $^1\text{H-NMR}$ (300 MHz, MeOH-d_4) δ (ppm) 7.39-7.31 (m, 5H), 4.72 (s, 2H), 4.28 (t, $J = 5.3\text{ Hz}$, 2H), 3.19 (t, $J = 5.3\text{ Hz}$, 2H); $^{13}\text{C NMR}$ (75 MHz, MeOH-d_4) δ (ppm) 129.47, 129.33, 128.83, 77.00, 67.52, 51.50

Sulfamic acid 2-(N-formyl-N-hydroxy-amino)-ethyl ester (13)

To a solution of **25** (35 mg, 0.14 mmol) in CH_2Cl_2 (10 ml) was added FMT (45 mg, 0.28 mmol) at room temperature, and the resulting solution was stirred for 12 h. The reaction mixture was concentrated *in vacuo* and purified by flash column chromatography (EtOAc/hexanes, 2:1) to give a pale yellow oil (35 mg, 90 %). The residue (32 mg, 0.12 mmol) was dissolved in methanol (10 ml) and a catalytic amount of 10 % Pd/C was added to the solution. The heterogeneous mixture was stirred for 12 h under a slight positive pressure of H_2 gas (1 atm) at room temperature. The reaction mixture was filtered and concentrated to a pale yellow oil before purification on a Varian Bond Elute[®] C18 column eluting with a stepwise gradient (0 to 70 %) methanol in H_2O . The desired product was eluted with 15 % methanol/ H_2O and the fractions were pooled and lyophilized to give a yellow syrup (11 mg, 50 %). $^1\text{H-NMR}$ (400 MHz, MeOH-d_4) δ (ppm) 1:2 ratio of 8.38 & 7.98 (s), 4.33 (t, $J = 5.5\text{ Hz}$, 2H), 3.92 (t, $J = 5.5\text{ Hz}$, 2H); $^{13}\text{C NMR}$ (100 MHz, MeOH-d_4) δ (ppm) 164.9 & 160.0, 65.95, 51.05; LRMS (CI): m/z 185 [M+1] HRMS Calcd for $\text{C}_3\text{H}_8\text{O}_5\text{N}_2\text{S}$ 184.01539, Found 184.01571

Synthesis of (3-N-Acetyl N-methylamino-propyl)-phosphonic acid (14-a, a N-Methyl derivative of fosmidomycin)

N- (3-Bromopropyl)-4, N-dimethylbenzenesulfonamide (27)

To a heterogeneous mixture of NaH (120 mg, 2.75 mmol) in dry THF (100 ml) was transferred a room temperature solution of *N*-tosyl-*N*-methyl amine (500 mg, 2.72 mmol) in THF (20 ml) via a cannula at 0°C. One hour later, 1,3-dibromopropane (500 mg, 2.5 mmol) was added dropwise at 0°C. The reaction mixture was stirred for 12 h at room temperature, then refluxed for a final 3 h before quenching with water. The solvent was removed *in vacuo* and the crude product was dissolved in EtOAc (30 ml). The organic fraction was washed with saturated aqueous NH₄Cl, water and brine, dried over MgSO₄, filtered and concentrated to a pale yellow oil. The residue was purified by flash chromatography (EtOAc/hexanes, 1:9) to get a colorless oil (250 mg, 34 %, 65 % based on recovered starting material). IR (neat) cm⁻¹ 1366, 1170; ¹H-NMR (400 MHz, CDCl₃) δ (ppm) 7.68 (d, *J* = 8.4 Hz, 2H), 7.33 (d, *J* = 8.4 Hz, 2H), 3.47 (t, *J* = 6.5 Hz, 2H), 3.13 (t, *J* = 6.7 Hz, 2H), 2.11 (p, *J* = 6.6 Hz, 2H), 2.75 (s, 3H), 2.43 (s, 3H); ¹³C NMR (100 MHz, CDCl₃) δ (ppm) 143.50, 134.23, 129.74, 127.45, 48.80, 35.63, 31.28, 30.14, 21.51; LRMS (CI): *m/z* 306 [M+1] HRMS Calcd for C₁₁H₁₇O₂N⁷⁹BrS 306.10634, Found 306.10655

{3-[Methyl- (toluene-4-sulfonyl)-amino]-propyl}phosphonic acid diethyl ester (28)

To a heterogeneous mixture of NaH (42 mg, 1.01 mmol) in dry THF (50 ml) was added diethyl phosphite (126 μl, 0.98 mmol) dropwise at 0°C and stirred for 2 h. A solution of **27** (250 mg, 0.82 mM, in 5 ml of THF) was added to the mixture at 0 °C via a syringe. The mixture was warmed to room temperature and stirred for 12 h. The solvent was removed *in vacuo* and the residue was dissolved in EtOAc (10 0ml). The organic layer was

washed with a solution of saturated aqueous NH_4Cl , water and brine, dried over MgSO_4 , filtered and concentrated, before being purified by flash chromatography (3 % $\text{MeOH}/\text{CH}_2\text{Cl}_2$) to yield 210 mg of a colorless oil (70 %). IR (neat) cm^{-1} 1162, 1245, 1350; $^1\text{H-NMR}$ (300 MHz, CDCl_3) δ (ppm) 7.65 (d, $J = 8.4$ Hz, 2H), 7.31 (d, $J = 8.4$ Hz, 2H), 4.03-4.20 (m, 4H), 3.04 (t, $J = 6.3$ Hz, 2H), 2.71 (s, 3H), 2.43 (s, 3H), 1.78-1.86 (m, 4H), 1.37 (t, $J = 6.8$ Hz, 3H); $^{13}\text{C NMR}$ (75 MHz, CDCl_3) δ (ppm) 143.25, 134.12, 129.53, 127.16, 61.42 (d, $^2J_{\text{CP}} = 6.4$ Hz), 50.12 (d, $^3J_{\text{CP}} = 18.7$ Hz), 34.52, 22.40 (d, $J_{\text{CP}} = 142.8$ Hz), 21.28, 20.65 (d, $^2J_{\text{CP}} = 3.9$ Hz), 16.25 (d, $^3J_{\text{CP}} = 5.8$ Hz); $^{31}\text{P NMR}$ (121 MHz, CDCl_3) δ (ppm) 32.55; LRMS (FAB): m/z 364.1 [M+1] HRMS Calcd for $\text{C}_{15}\text{H}_{27}\text{O}_5\text{NPS}$ 364.13476, Found 364.13451

(3-*N*-Methylamino-propyl)-phosphonic acid (29)

Compound **28** (250 mg, 0.68 mmol) was dissolved in a 1:1 mixture of acetic acid and conc. HCl (total 30 ml) and refluxed overnight. The solvent was removed under reduced pressure and the yellow residue was purified by cation exchange chromatography using Dowex 50X8-100 and eluting with 1 N NH_4OH . The fractions that were PMA-active by TLC were pooled and freeze-dried to a white solid (72 mg, 70 %). $^1\text{H-NMR}$ (300 MHz, MeOH-d_4) δ (ppm) 2.98 (t, $J = 6.1$ Hz, 2H), 2.59 (s, 3H), 1.86-1.97 (m, 2H), 1.58-1.68 (m, 2H); $^{13}\text{C NMR}$ (75 MHz, MeOH-d_4) δ (ppm) 50.59 (d, $^3J_{\text{CP}} = 16.12$ Hz), 33.37, 26.08 (d, $J_{\text{CP}} = 132.5$ Hz), 21.16 (d, $^2J_{\text{CP}} = 3.2$ Hz); $^{31}\text{P NMR}$ (121 MHz, MeOH-d_4) δ (ppm) 22.19; LRMS (FAB): m/z 154 [M+1] HRMS Calcd for $\text{C}_4\text{H}_{13}\text{O}_3\text{NP}$ 154.06331, Found 154.06315

[3-(*N*-Acetyl-*N*-methyl-amino)-propyl]-phosphonic acid (14-a)

Compound **29** (30 mg, 0.19 mmol) was dissolved in a 1:1 mixture of acetic anhydride/pyridine (6 ml) and stirred at room temperature for 5 h. The solvent was removed *in vacuo*, and the residue was purified on a Varian

Bond Elute[®] C₁₈ disposable column eluting with a stepwise gradient MeOH (0 to 100 %) in water. The product eluted at 15 % MeOH along with minor impurities. The fractions were pooled, concentrated and basified with NaHCO₃, before being applied onto an AG1-X10 (100-200 mesh, Cl⁻ form) ion exchange column. The desired product eluted with 1N NH₄OH, but a yellow containment was also present. The concentrated residue was purified further by C₁₈ silica chromatography eluting with water to give 5 mg of a white solid after lyophilization (13 %). ¹H-NMR (400 MHz, D₂O) δ (ppm) 1:1 mixture of isomers 3.23-3.33 (m, 2H), 2.77 & 2.92 (2s, 3H), 1.96 & 1.99 (2s, 3H), 1.61-1.71 (m, 2H), 1.36-1.47 (m, 2H); ¹³C NMR (100 MHz, D₂O) δ (ppm) 1:1 mixture of isomers 174.49 & 174.37, 51.95 (d, ³J_{CP} = 18.9 Hz) & 48.72 (d, ³J_{CP} = 19.7 Hz), 36.58 & 33.69, 25.44 (d, J_{CP} = 134.2 Hz) & 25.14 (d, J_{CP} = 134.5 Hz), 22.22 (d, ²J_{CP} = 3.0 Hz) & 21.39 (d, ²J_{CP} = 3.8 Hz), 21.29 & 20.66; ³¹P NMR (121 MHz, D₂O) δ (ppm) 25.87 & 26.29; LRMS (ion spray): m/z 196.0 [M+1], 218.0 [M+Na]

Synthesis of (3-Hydroxamic-propyl)-phosphonic acid (15, a Hydroxamate Derivative of fosmidomycin)

4-(Bisbenzyloxyphosphonyl)-butyric acid ethyl ester (30)

To a 0 °C suspension of NaH (60 % in mineral oil, 250 mg, 5.6 mmol) in dry THF (150 ml) was added dibenzyl phosphite (1.25 ml, 5.6 mmol) and the resulting mixture was stirred for 1 hr at 0 °C. 4-Bromobutyric acid ethyl ester (1 g, 5.1 mmol) was added dropwise at 0 °C, and the resulting clear solution was warmed to room temperature before being refluxed overnight. The reaction was quenched by saturated aqueous NH₄Cl. The organic layer was diluted with EtOAc (100 ml) and washed with saturated aqueous NaHCO₃, water and brine. The organic layer was dried over MgSO₄, filtered, and concentrated. The crude product was purified by flash chromatography (EtOAc/hexanes, 1:1) to give 600 mg of a colorless oil (55

%, 89 % based on recovered starting material). IR (neat) cm^{-1} 1735, 1216, 787; $^1\text{H-NMR}$ (300 MHz, CDCl_3) δ (ppm) 7.35-7.26 (m, 10H), 5.08-4.92 (m, 4H), 4.09 (q, $J = 7.1$ Hz, 2H), 2.35 (t, $J = 7.1$ Hz, 2H), 1.93-1.75 (m, 4H), 1.22 (t, $J = 7.1$ Hz, 3H); $^{13}\text{C NMR}$ (75 MHz, CDCl_3) δ (ppm) 172.5, 136.2, 128.48, 127.82, 67.03 (d, $^2J_{\text{CP}} = 6.3$ Hz), 60.30, 34.27 (d, $^3J_{\text{CP}} = 16.3$ Hz), 25.17 (d, $J_{\text{CP}} = 141.2$ Hz), 17.91 (d, $^2J_{\text{CP}} = 4.5$ Hz), 14.10; $^{31}\text{P NMR}$ (121 MHz, CDCl_3) δ (ppm) 33.39; LRMS (CI) m/z 377.1 [M+1] HRMS Calcd for $\text{C}_{20}\text{H}_{26}\text{O}_5\text{P}$ 377.15179, Found 377.15102

4-(Bisbenzyloxyphosphonyl)-butyric acid (31)

Compound **30** (600 mg, 1.7 mmol) was dissolved in a 1:1 mixture of water and methanol (total 30 ml). Solid NaHCO_3 was added to the solution to a final concentration of 1M before the resulting mixture was refluxed overnight. The solvent was removed *in vacuo*, and the resulting residue was redissolved in water. The solution was acidified with 1N HCl before being extracted with EtOAc (5 ml x 3). The combined organic fractions were dried over MgSO_4 , filtered and concentrated to a yellow oil. The residue was purified by flash chromatography (5 % MeOH/ CHCl_3) to yield a colorless oil (373 mg, 68 %). IR (neat) cm^{-1} 3389, 1724, 1212; $^1\text{H-NMR}$ (300 MHz, CDCl_3) δ (ppm) 10.48 (br s, 1H), 7.39-7.27 (m, 10H), 5.04 (d, $^3J_{\text{HP}} = 8.9$ Hz, 2H), 4.99 (d, $^3J_{\text{HP}} = 7.8$ Hz, 2H), 2.39 (t, $J = 6.7$ Hz, 2H), 1.98-1.80 (m, 4H); $^{13}\text{C NMR}$ (75 MHz, CDCl_3) δ (ppm) 176.44, 136.07 (d, $^3J_{\text{CP}} = 5.9$ Hz), 128.52, 128.38, 127.91, 67.37 (d, $^2J_{\text{CP}} = 6.4$ Hz), 33.96 (d, $^3J_{\text{CP}} = 16.4$ Hz), 24.97 (d, $J_{\text{CP}} = 141.1$ Hz), 17.66 (d, $^2J_{\text{CP}} = 4.4$ Hz); $^{31}\text{P NMR}$ (121 MHz, CDCl_3) δ (ppm) 33.88; LRMS (CI): m/z 349.1 [M+1] HRMS Calcd for $\text{C}_{18}\text{H}_{22}\text{O}_5\text{P}$ 349.12049, Found 349.12022

(3-Benzyloxycarbamoylpropyl)-phosphonic acid dibenzyl ester (32)

To a solution of **31** (85 mg, 0.24 mmol) in dry THF (20 ml) were added DCC (50 mg, 0.29 mmol) and HOBt (36 mg, 0.29 mmol) and the mixture was stirred for 3 h at room temperature. Then *O*-benzyl hydroxylamine (38 mg, 0.3 mmol) was added, and the resulting solution was stirred overnight at room temperature. The solvent was removed *in vacuo* and the residue was dissolved in EtOAc (30 ml). The organic layer was washed with saturated aqueous NaHCO₃, water and brine, dried over MgSO₄, filtered, and concentrated. The residue was purified by flash chromatography (EtOAc/hexanes, 3:1) to afford a colorless oil (72 mg, 65 %). IR (neat) cm⁻¹ 1688, 1219; ¹H-NMR (300 MHz, CDCl₃) δ (ppm) 7.35-7.33 (m, 15H), 5.04-4.87 (m, 6H), 2.14 (bs, 2H), 1.98-1.73 (m, 4H); ¹³C NMR (75 MHz, CDCl₃) δ (ppm) 169.78, 136.75 (d, ³J_{CP} = 4.7 Hz), 135.39, 129.09, 128.62, 127.95, 78.05, 67.29 (d, ²J_{CP} = 6.3 Hz), 32.36 (d, ³J_{CP} = 9.8 Hz), 24.28 (d, J_{CP} = 143.9 Hz), 18.45 (d, ²J_{CP} = 2.8 Hz); ³¹P NMR (121 MHz, CDCl₃) δ (ppm) 33.56; LRMS (CI): *m/z* 453.17 [M+1] HRMS Calcd for C₂₅H₂₈O₅NP 435.17051, Found 453.17198

(3-Hydroxycarbamoylpropyl)-phosphonic acid (15)

The solution of **32** (65 mg, 0.14 mmol) in methanol (20 ml) was stirred with a catalytic amount of 10 % Pd/C under a positive pressure of hydrogen (1 atm) at room temperature for 12 h. The Pd/C was removed by filtration, and the filtrate was concentrated, dissolved in water (10 ml), and washed with CHCl₃ (5 ml x 2). The aqueous layer was concentrated and purified with a Varian Bond Elute[®] C18 column eluting with water. The FeCl₃-active fractions were pooled and concentrated. A final purification step utilized a CF-11 cellulose column, eluting with water. The fractions that were PMA-active by TLC stain were collected and lyophilized to a white solid (23 mg, 89 %). ¹H-NMR (400 MHz, D₂O) δ (ppm) 2.18 (t, J = 7.2 Hz, 2H), 1.79-1.69

(m, 2H), 1.66-1.58 (m, 2H); ^{13}C NMR (100 MHz, D_2O) δ (ppm) 172.97, 33.56 (d, $^3J_{\text{CP}} = 17.6$ Hz), 26.63 (d, $J_{\text{CP}} = 134.2$ Hz), 19.64 (d, $^2J_{\text{CP}} = 3.9$ Hz); ^{31}P NMR (121 MHz, CDCl_3) δ (ppm) 29.70; LRMS (ion spray): m/z 183.0 [M+]

Synthesis of phosphoric acid mono-(3,4-dioxopentyl)ester (34, Laurencione phosphate)

Phosphoric acid dibenzyl ester pent-3-ynyl ester (39)

To a solution of pent-3-yn-1ol (**38**, 500 mg, 5.94 mmol) in dry CH_2Cl_2 (50 ml) were added 1-H tetrazole (620 mg, 8.9 mmol) and diisopropyldibenzyl phosphoramidite (3.01 ml, 8.9 mmol) at room temperature. The resulting solution was stirred for 5 h at room temperature under Ar and cooled to 0 °C before adding *tert*-butyl hydroperoxide (70 % solution, 0.5 ml) dropwise. The reaction mixture was then stirred for 8 h at room temperature. The mixture was diluted with CH_2Cl_2 (50 ml), the organic layers were washed with water, and the combined aqueous layers were re-extracted with CH_2Cl_2 (10 ml x 3). The combined organic layer was washed with a saturated aqueous sodium bicarbonate, water and brine, dried with MgSO_4 , and concentrated *in vacuo*. The concentrate was purified by flash column chromatography (EtOAc/hexanes, 2:5) to afford the desired product (1.8 g, 90 %). ^1H -NMR (300 MHz, CDCl_3) δ (ppm) 7.36-7.31 (m, 10 H), 5.04 (dd, $^3J_{\text{HP}} = 8.2$ Hz, $^2J_{\text{HH}} = 1.4$ Hz, 4H), 4.07-3.99 (m, 2H), 2.47-2.42 (m, 2H), 1.72 (t, $J = 2.5$ Hz, 3H); ^{13}C NMR (75 MHz, CDCl_3) δ (ppm) 135.67 (d, $^3J_{\text{CP}} = 6.9$ Hz), 128.35, 128.28, 127.65, 77.60, 73.96, 69.14 (d, $^2J_{\text{CP}} = 5.4$ Hz), 65.82 (d, $^2J_{\text{CP}} = 2.8$ Hz), 20.69 (d, $^3J_{\text{CP}} = 7.4$ Hz), 3.30; ^{31}P NMR (121 MHz, CDCl_3) δ (ppm) -0.19

Phosphoric acid dibenzyl ester 3,4-dioxo-pentyl ester (40)

To a heterogeneous mixture of **39** (100 mg, 0.29 mmol) in 7 ml of a mixture of $\text{CCl}_4/\text{CH}_3\text{CN}/\text{H}_2\text{O}$ (2:2:3) was added $\text{Ru(IV)O}_2\cdot\text{H}_2\text{O}$ (0.84 mg, 0.006 mmol) and NaIO_4 (255 mg, 1.29 mmol). The resulting mixture was stirred vigorously for 1 h at room temperature. The solvent was removed *in vacuo* before the resultant residue was dissolved in CH_2Cl_2 (20 ml). The organic layer was washed with water (3 x 3 ml) and the combined aqueous layers were re-extracted with CH_2Cl_2 (3 x 5 ml). The combined organic layers were dried over MgSO_4 , stirred with charcoal, and filtered through Florisil[®] and Celite[®] before concentration to a yellow-green residue. The resulting residue was purified by flash chromatography (EtOAc/hexanes, 2:5) to give a pale yellow oil (130 mg, 82 %). $^1\text{H-NMR}$ (300 MHz, CDCl_3) δ (ppm) 7.35-7.32 (m, 10 H), 5.03 (dd, $^3J_{\text{HP}} = 8.2$ Hz, $^2J_{\text{HH}} = 2.0$ Hz, 4H), 4.28 (dt, $^3J_{\text{HP}} = 7.7$ Hz, $J = 6.1$ Hz, 2H), 3.03 (dt, $J = 6.1$ Hz, $^4J_{\text{HP}} = 0.87$ Hz, 2H), 2.31 (s, 3H); $^{13}\text{C NMR}$ (100 MHz, CDCl_3) δ (ppm) 196.50, 195.49, 135.68 (d, $^3J_{\text{CP}} = 6.4$ Hz), 128.59, 127.99, 62.39 (d, $^2J_{\text{CP}} = 4.4$ Hz), 61.96 (d, $^3J_{\text{CP}} = 5.4$ Hz), 36.49 (d, $^3J_{\text{CP}} = 7.1$ Hz), 23.38; $^{31}\text{P NMR}$ (121 MHz, CDCl_3) δ (ppm) -0.06; LRMS (FAB) m/z 377.1.2 [M+1] 333.1 [M- CH_3CO] HRMS Calcd for $\text{C}_{19}\text{H}_{22}\text{O}_6\text{P}$ 377.11540 Found 377.11519

Phosphoric acid mono-(3,4-dioxo-pentyl)ester (**34**, Laurencione phosphate)

To a solution of **40** (50 mg, 0.13 mmol) in methanol (7 ml) was added a catalytic amount of 10 % Pd/C. The mixture was stirred under a positive pressure of H_2 gas (1 atm) at room temperature for 5 h. The heterogeneous reaction mixture was filtered and concentrated to a colorless film. This residue was dissolved in water (10 ml) and the aqueous solution was washed with EtOAc (4 x 3 ml). The aqueous layer was concentrated and the residue was purified with a Varian Bond Elute[®] C_{18} column eluting with a stepwise gradient of 0 to 30 % MeOH in H_2O . The desired product eluted with 5 % MeOH and was concentrated to a colorless film (25 mg, 95

%). $^1\text{H-NMR}$ (300 MHz, D_2O) δ (ppm) 4.14-4.08 (m, 2H), 3.69-3.63 (m, 2H), 2.69-2.65 (m, 2H), 2.17 (s, 3H); $^{13}\text{C NMR}$ (75 MHz, MeOH-d_4) δ (ppm) 175.76, 62.22, 36.49 (d, $^3J_{\text{CP}} = 7.1$ Hz), 25.63; $^{31}\text{P NMR}$ (121 MHz, CDCl_3) δ (ppm) 0.61; LRMS (FAB) m/z 197.2 [M+1] HRMS Calcd for $\text{C}_5\text{H}_{10}\text{O}_6\text{P}$ 197.02150 Found 197.02141

Synthesis of Phosphoric acid mono-(3-hydroxy-4-oxo-tetrahydro-pyran-2-ylmethyl) ester (37)

4,6-O-Isopropylidene-D-glucal (43)

To a solution of D-glucal (**42**, 180 mg, 1.2 mmol) in dry acetone (5 ml) was added a catalytic amount of TsOH and 2,2-dimethoxy propane (141 mg, 1.35 mmol) at room temperature. The solvent was removed after 1 h. The residue was dissolved into EtOAc (20 ml) and the organic solution was washed with a saturated aqueous sodiumbicarbonate before dried over MgSO_4 , filtered, and concentrated. The removal of the solvent and concentration of the resulting residue was performed with a caution because of possible loss due to the volatility of the desired product (*in vacuo* at low temperature, 15 °C). The resulting residue was purified by flash chromatography (EtOAc/hexanes, 2:5) to give a colorless film (90 mg, 40 %). $^1\text{H-NMR}$ (300 MHz, CDCl_3) δ (ppm) 6.3 (dd, $J = 6.1$ Hz, $J = 1.7$ Hz, 1H), 4.7 (dd, $J = 6.1$ Hz, $J = 1.9$ Hz, 1H), 4.35-4.33 (m, 1H), 3.96-3.92 (m, 1H), 3.85-3.71 (m, 3H), 1.53 (s, 3H), 1.43 (s, 3H); $^{13}\text{C NMR}$ (75 MHz, CDCl_3) δ (ppm) 144.24, 104.02, 100.04, 73.70, 69.48, 67.33, 61.78, 29.19, 19.27; LRMS (CI) m/z 186.1 [M+1]

1,5-Anhydro-2-deoxy-4,6-O-isopropylidene arabino-hexitol (44)

To a solution of **43** (24 mg, 0.13 mmol) in methanol (5 ml) was added a catalytic amount of 10 % Pd/C. The heterogeneous mixture was stirred at room temperature under a positive pressure of H_2 (1 atm) for 2 h. The

reaction mixture was filtered and concentrated to a colorless oil (22 mg, 95 %). $^1\text{H-NMR}$ (300 MHz, CDCl_3) δ (ppm) 3.95 (ddd, $J = 11.8, 5.3, 1.3$ Hz, 1H), 3.86 (dd, $J = 10.7, 5.4$ Hz, 1H), 3.76-3.66 (m, 2H), 3.56-3.42 (m, 2H), 3.19-3.11 (m, 1H), 2.02-1.95 (m, 1H), 1.83-1.68 (m, 1H), 1.55 (s, 3H), 1.41 (s, 3H); $^{13}\text{C NMR}$ (75 MHz, CDCl_3) δ (ppm) 99.98, 76.66, 72.28, 70.07, 66.45, 62.44, 33.57, 29.37, 19.42; LRMS (CI) m/z 187.1 [M+]

1,5-Anhydro-2-deoxy-4,6-O-isopropylidene D-erythro-3-hexulose (45)

To a solution of **44** (20 mg, 0.1 mmol) in dry CH_2Cl_2 (5 ml) were added NMO (14 mg, 0.12 mmol), molecular sieves (4Å), and a catalytic amount of TPAP. The heterogeneous reaction mixture was stirred for 12 h at room temperature. The mixture was filtered through Celite and charcoal and concentrated to a yellow-green oil. The residue was filtered again through Florisil and silica gel bed (5x5 cm). The residue was purified by flash chromatography (EtOAc/hexanes, 1:3) to give a colorless oil (7 mg, 31 %). $^1\text{H-NMR}$ (300 MHz, CDCl_3) δ (ppm) 4.36 (dd, $J = 10.1, 1.5$ Hz, 1H), 4.27 (ddd, $J = 11.3, 7.7, 1.0$ Hz, 1H), 3.99 (dd, $J = 10.8, 5.4$ Hz, 1H), 3.91-3.79 (m, 2H), 3.42 (dt, $J = 10.1, 5.4$ Hz, 1H), 2.85-2.72 (m, 1H), 2.48 (ddd, $J = 14.4, 2.9, 1.0$ Hz, 1H), 1.51 (s, 3H), 1.49 (s, 3H); $^{13}\text{C NMR}$ (75 MHz, CDCl_3) δ (ppm) 201.20, 100.60, 77.45, 75.33, 68.31, 62.78, 42.17, 29.06, 19.00; LRMS (CI) m/z 185.1 [M+]

3-Hydroxy-2-hydroxymethyl-tetrahydro-pyran-4-one (46)

The solution of **45** (20 mg, 0.11 mmol) in 10 % acetic acid in methanol (5 ml) was stirred for 12 h at room temperature. The solvent was removed *in vacuo* to provide the product as a colorless oil (15 mg, 95 %). $^1\text{H-NMR}$ (300 MHz, CDCl_3) δ (ppm) 4.34 (ddd, $J = 11.4, 7.6, 1.2$ Hz, 1H), 4.18 (d, $J = 10.1$ Hz, 1H), 3.99-3.83 (m, 2H), 3.73-3.64 (m, 1H), 3.39-3.30 (m, 1H), 2.86-2.74 (m, 1H), 2.55 (ddd, $J = 12.0, 2.5, 1.1$ Hz, 1H); $^{13}\text{C NMR}$ (75 MHz,

CDCl_3) δ (ppm) 207.35, 83.83, 73.92, 67.35, 62.76, 40.72; LRMS (CI) m/z 146.1 [M+]

Phosphoric acid dibenzyl ester 3-hydroxy-4-oxo-tetrahydro-pyran-2-ylmethyl ester (47)

To a solution of **46** (24 mg, 0.16 mmol) in dry CH_2Cl_2 (7 ml) were added 5-(methylthio)-1-H-tetrazole (25 mg, 0.21 mmol) and dibenzyl diisopropyl phosphoramidite (74 mg, 0.21 mmol). The resulting solution was stirred for 4 h at room temperature under Ar at room temperature before *tert*-butyl hydroperoxide (70 % solution, 0.3 ml, 0.2 mmol) was added dropwise at 0 °C. The reaction mixture was warmed to room temperature and stirred for 8 h. The mixture was diluted with CH_2Cl_2 (20 ml), and the organic solution was washed with water, and the aqueous layer was re-extracted with CH_2Cl_2 . The combined organic layers were washed with a saturated aqueous sodium bicarbonate, water and brine, dried with MgSO_4 , and concentrated *in vacuo*. The concentrate was purified by flash column chromatography (EtOAc/hexanes, 3:1) to give a colorless oil (30 mg, 47 %). $^1\text{H-NMR}$ (300 MHz, CDCl_3) δ (ppm) 7.37-7.34 (m, 10H), 5.08 (dd, $J = 7.9$, 2.0 Hz, 4H), 4.39-4.24 (m, 2H), 4.07-4.04 (m, 1H), 3.62 (dt, $J = 6.0$, 2.7 Hz, 2H), 3.41-3.35 (m, 1H), 2.78-2.66 (m, 1H), 2.54-2.49 (m, 1H); $^{13}\text{C NMR}$ (100 MHz, CDCl_3) δ (ppm) 206.90, 136.21, 128.96, 128.92, 128.36, 128.31, 82.62 (d, $J = 6.8$ Hz), 73.70, 69.73 (d, $J = 5.2$ Hz), 67.40 (d, $J = 5.3$ Hz), 41.08; $^{31}\text{P NMR}$ (121 MHz, CDCl_3) δ (ppm) 0.38; LRMS (FAB) m/z 407.2 [M+1]

Phosphoric acid mono-(3-hydroxy-4-tetrahydro-pyran-2-ylmethyl) ester (37)

To a solution of **47** (20 mg, 0.05 mmol) in methanol (5 ml) was added a catalytic amount of 10 % Pd/C. The heterogeneous reaction mixture was stirred at room temperature for 5 h under a positive pressure of H_2 (1 atm).

The mixture was filtered and concentrated to a colorless oil. The residue was purified by Varian Bond Elute[®] C₁₈ column eluting with a stepwise gradient methanol (0 to 60 %) in water to afford a colorless film (7 mg, 70 %). ¹H-NMR (300 MHz, D₂O) δ (ppm) 4.29-4.13 (m, 1H), 3.99-3.42 (m, 5H), 2.39-2.34 (m, 2H); ³¹P NMR (121 MHz, CDCl₃) δ (ppm) 2.29; LRMS (FAB) *m/z* 225.0 [M-1] HRMS Calcd for C₆H₁₀O₇P 225.01642 Found 225.01734

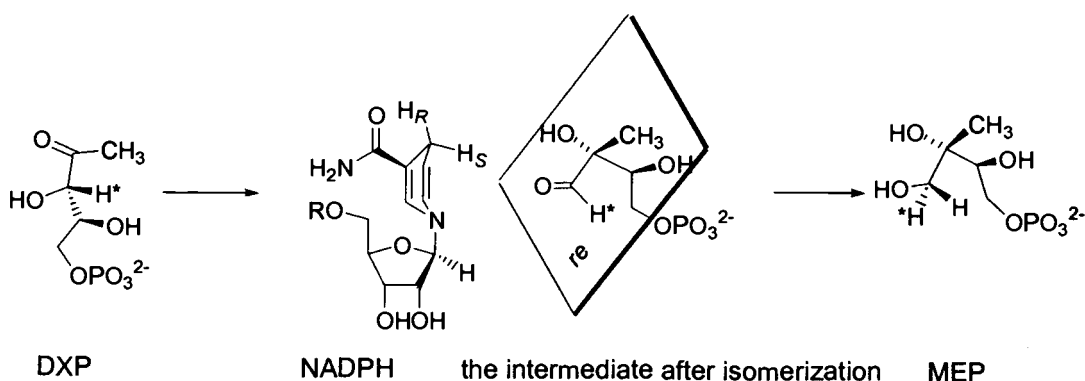
CHAPTER IV

CONCLUSIONS

In this dissertation, 1-deoxy-D-xylulose-5-phosphate isomeroreductase (DXR), a key enzyme in the non-mevalonate pathway to isoprenoid biosynthesis, was investigated in terms of the stereochemistry of its reduction step and the structural requirements for fosmidomycin type inhibitors. Because the non-mevalonate pathway is used only by certain types of organisms, e.g. eubacteria, plants, some algae, and malaria protozoa, investigation of the non-mevalonate pathway has drawn particular interest as a new target for alternate antibiotics, herbicides, and antimalarial agents. Investigation of DXR is significant in that DXR can be a very specific target to efficiently block this pathway. In addition, DXR and an investigation of its active site are of interest in that DXR is one of only two known examples of isomeroreductases. A deeper understanding of these enzymes will expand our knowledge on the tremendous variety of enzyme catalyzed reaction mechanisms.

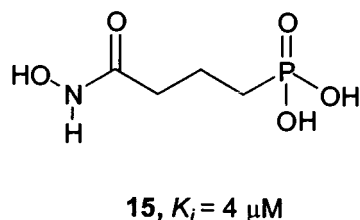
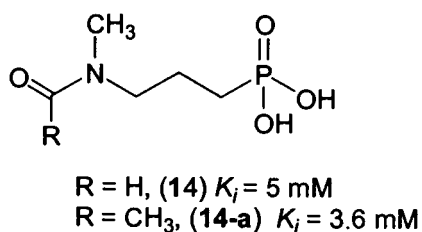
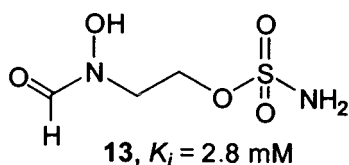
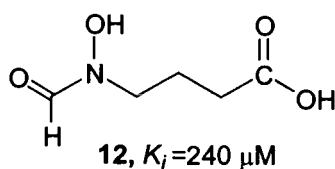
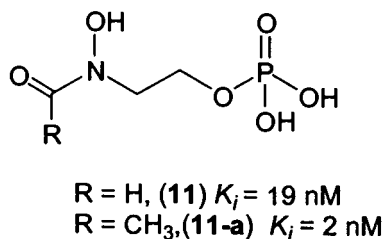
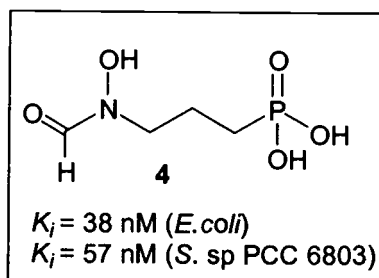
In order to better understand the non-mevalonate pathway, the key enzyme DXR, has been the focus of this study. In Chapter II, the stereochemical course of the reduction step by DXR was investigated using NMR techniques, synthetic DXP, synthetic derivatives of MEP, recombinant DXR, and stereospecifically labeled NADPH. The two hydrogens at the C1 position of MEP have different origins, one from DXP and the other from NADPH, therefore, identifying the origin of these two hydrogens will define the stereochemical route of the reduction step of this DXR mediated reaction. In order to spectroscopically distinguish the diastereotopic hydrogens at C1 of MEP, a rotationally restricted derivative of 2-C-methylerythritol was necessary. The bisacetonide derivative of ME was

synthesized and used as a standard compound in which the diastereotopic hydrogens were fully assigned. A series of experiments revealed that: (1) the *pro-S* hydrogen at the C1 position of MEP originates from the hydrogen at C3 of DXP; (2) the hydride from NADPH is transferred to the *re* face the putative aldehyde intermediate; and that (3) DXR is a class B dehydrogenase in which the *pro-S* hydride of NADPH is transferred to the substrate.

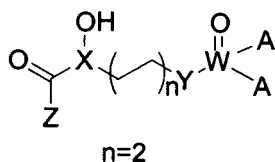


Fosmidomycin, a natural product which is known to inhibit DXR, is believed to be a mimic of the putative intermediate of the isomerization/reduction step by DXR. Fosmidomycin efficiently inhibits bacterial and plant DXRs, which has brought significant attention to DXR inhibitors and also encouraged further investigation on this type of molecule.

In chapter III, therefore, inhibitors of DXR were designed and synthesized based on the structure of fosmidomycin to further understand the structural features necessary for its potent inhibition. Although the syntheses and the purification of these highly polar, charged compounds were not as straightforward as they first appeared, several mechanistic probes were synthesized and tested for their inhibition efficacy against DXR.



These data provide the first quantitative evaluation of a series of compounds based on the structure of fosmidomycin. Fosfoxacin, a phosphate analog of fosmidomycin showed a better inhibition activity than fosmidomycin against DXR. These data also demonstrated that the ionizable acid groups, the *N*-hydroxyl group, and the acyl function adjacent to the *N*-hydroxyl group play important roles in fosmidomycin's inhibition activity. Based on these results, effective inhibitors of DXR should possess the following features:



- W = Heteroatom, P
- A = Negatively charged or ionizable groups
- X = N
- Y = C or O
- Z = H or CH₃

The ideal structure of the inhibitor from this study also provides information about what type of amino acids at the DXR active site might interact with the inhibitor (substrate). Specifically: (1) the significant difference in the K_i values between fosfoxacin/fosmidomycin and the carboxylate derivative of fosmidomycin suggests that the two oxyanions might be required for optimal binding; (2) the *N*-acyl, *N*-hydroxyl group of fosmidomycin has been proven to be necessary, presumably to interact with a divalent metal ion, from the greater K_i values for the *N*-methyl and hydroxamate derivatives of fosmidomycin; and (3) the *N*-acyl, *N*-hydroxyl group of fosmidomycin may interact with one or more basic amino acid residues based on differential inhibition observed for the hydroxamate derivative of fosmidomycin. From these results, it appears as though the active site of DXR has a restricted space in which the substrate binds and a very low tolerance for large structural changes.

The results from the studies in chapters II and III of this dissertation offer a better description of the DXR step in the pathway regarding the stereochemical course of the reduction and the quantitative evaluation of inhibition by fosmidomycin analogs. Both results should allow researchers to design more effective inhibitors of DXR. The information from the analog study, along with results from the study on the stereochemical course of the reduction step, provides valuable insight into spatial restriction at the active site of DXR. The results of the analog study can also be used as complementary data to the crystallography studies, which have failed to obtain the crystal structure with an inhibitor bound to DXR. Furthermore, this information should encourage further studies on DXR toward developing better alternate antibiotics, herbicides and antimalarial agents.

BIBLIOGRAPHY

- (1) Spurgeon, S. L.; Porter, J. W. In *Biosynthesis of Isoprenoid Compounds*; Porter, J. W., Ed.; John Wiley and Sons: New York, 1981; Vol. 1, pp 3-40.
- (2) Rohmer, M. *Comprehensive Natural Product Chemistry*; Elsevier: New York, 1999; Vol. 2.
- (3) Cane, D. E. *Comprehensive Natural Product Chemistry*; Elsevier: New York, 1999; Vol. 2.
- (4) Trzaskos, J. M. *Regulation of Isoprenoid metabolism: Biosynthesis and utilization of Isoprenoids: Overview of research directions*; American Chemical Society: Washington DC, 1992; Vol. 497.
- (5) Alexander, R. W. *Trends Biochem. Sci.* **2001**, *26*, 152.
- (6) Bochar, D. A.; Friesen, J. A.; Stauffacher, C. V.; Rodwell, V. W. *Biosynthesis of Mevalonic acid from Acetyl-CoA*; Elsevier: New York, 1999; Vol. 2.
- (7) Rohmer, M.; Sutter, B.; Sahm, H. *J. Chem. Soc. Chem. Commun.* **1989**, 1471-1472.
- (8) Flesch, G.; Rohmer, M. *Eur. J. Biochem.* **1988**, *175*, 405-411.
- (9) Pandian, S.; Saengchjan, S.; Raman, T. S. *Biochem. J.* **1981**, *196*, 675-681.
- (10) Anastasis, P.; Freer, I.; Oveton, K. H.; Picken, D.; Rycroft, D. S.; Singh, S. B. *J. Chem. Soc. Perkin Trans I* **1987**, 2427-2436.
- (11) Zhou, D.; White, R. *Biochem. J.* **1991**, *273*, 627-634.
- (12) Cane, D. E.; Rossi, T.; Tillman, A. M.; Pachlatko, J. P. *J. Am. Chem. Soc.* **1981**, *103*, 1838-1843.
- (13) Schwarz, M.; Arigoni, D. *Comprehensive Natural Product Chemistry*; 1st ed.; Elsevier: New York, 1999; Vol. 2.
- (14) Rohmer, M.; Knani, M. h.; Simonin, P.; Sutter, B.; Sahm, H. *Biochem. J.* **1993**, *295*, 517-524.

- (15) Broers, S. T. J.; Ph. D. Dissertation, Eidgenössische Technische Hochschule: Zürich, 1994.
- (16) Rohmer, M.; Seemann, M.; Horbach, S.; Bringer-Meyer, S.; Sahm, H. *J. Am. Chem. Soc.* **1996**, *118*, 2564-2566.
- (17) Yokota, A.; Sasajima, K.-i. *Agric. Biol. Chem.* **1984**, *48*, 149-158.
- (18) Yokota, A.; Sasajima, K.-i. *Agric. Biol. Chem.* **1986**, *50*, 2517-2524.
- (19) Lange, B. M.; Wildung, M. R.; McCaskill, D.; Croteau, R. *Proc. Natl. Acad. Sci. USA* **1998**, *95*, 2100-2104.
- (20) Sprenger, G. A.; Schorken, U.; Wiegert, T.; Grolle, S.; de Graaf, A. A.; Taylor, S. V.; Begley, T. P.; Bringer-Meyer, S.; Sahm, H. *Proc. Natl. Acad. Sci. USA* **1997**, *94*, 12857-12862.
- (21) Lois, L. M.; Campos, N.; Putra, S. R.; Danielsen, K.; Rohmer, M.; Boronat, A. *Proc. Natl. Acad. Sci. USA* **1998**, *95*, 2105-2110.
- (22) Ostrovsky, D.; Shashkov, A.; Sviridov, A. *Biochem. J.* **1993**, *259*, 901-902.
- (23) Ostrovsky, D.; Diomina, G.; Lysak, E.; Matveeva, E.; Ogrel, O.; Trutko, S. *Arch. Microbiol.* **1998**, *171*, 69-72.
- (24) Rohmer, M. *Nat. Prod. Rep.* **1999**, *16*, 565-574.
- (25) Duvoid, T.; Cali, P.; Bravo, J.-M.; Rohmer, M. *Tetrahedron Lett.* **1997**, *38*, 6181-6184.
- (26) Takahashi, S.; Kuzuyama, T.; Watanabe, H.; Seto, H. *Proc. Natl. Acad. Sci. USA* **1998**, *95*, 9879-9884.
- (27) Kuzuyama, T.; Takahashi, S.; Watanabe, H.; Seto, H. *Tetrahedron Lett.* **1998**, *39*, 4509-4512.
- (28) Proteau, P. J.; Woo, Y.-H.; Williamson, R. T.; Phaosiri, C. *Org. Lett.* **1999**, *1*, 921-923.
- (29) Koppisch, A. T.; Fox, D. T.; Blagg, B. S. J.; Poulter, C. D. *Biochemistry* **2002**, *41*, 236-243.
- (30) Lichtenthaler, H. K. *Annu. Rev. Plant Physiol. Plant Mol. Biol.* **1999**, *50*, 47-65.

- (31) Rohdich, F.; Kis, K.; Bacher, A.; Eisenreich, W. *Curr. Opin. Chem. Biol.* **2001**, *5*, 535-540.
- (32) Jomaa, H.; Wiesner, J.; Sanderbrand, S.; Altincicek, B.; Weidemeyer, C.; Hintz, M.; Eberl, M.; Zeidler, J.; Lichtenthaler, H. K.; Soldati, D.; Beck, E. *Science* **1999**, *285*, 1573-1576.
- (33) Schwender, J.; Müller, C.; Zeidler, J.; Hartmut, Z.; Lichtenthaler, H. K. *FEBS Lett* **1999**, *455*, 140-144.
- (34) S, G.; S, B.-M.; H., S. *FEMS Microbiol. Lett.* **2000**, *191*, 131-137.
- (35) Rohdich, F.; Wungsintaweeikul, J.; Fellermeier, M.; Sagner, S.; Herz, S.; Kis, K.; Eisenreich, W.; Bacher, A.; Zenk, M. H. *Proc. Natl. Acad. Sci. USA* **1999**, *96*, 11758-11763.
- (36) Rohdich, F.; Wungsintaweeikul, J.; Eisenreich, W.; Richter, G.; Schuhr, C. A.; Hecht, S.; Zenk, M. H.; Bacher, A. *Proc. Natl. Acad. Sci. USA* **2000**, *97*, 6451-6456.
- (37) Kuzuyama, T.; Takagi, M.; Kaneda, K.; Dairi, T.; Seto, H. *Tetrahedron Lett.* **2000**, *41*, 703-706.
- (38) Lüttgen, H.; Rohdich, F.; Herz, S.; Wungsintaweeikul, J.; Hecht, S.; Schuhr, C. A.; Fellermeier, M.; Sagner, S.; Zenk, M. H.; Bacher, A.; Eisenreich, W. *Proc. Natl. Acad. Sci. USA* **2000**, *97*, 1062-1067.
- (39) Kuzuyama, T.; Takagi, M.; Kaneda, K.; Watanabe, H.; Dairi, T.; Seto, H. *Tetrahedron Lett.* **2000**, *41*, 2925-2928.
- (40) Herz, S.; Wungsintaweeikul, J.; Schuhr, C. A.; Hecht, S.; Lüttgen, H.; Sagner, S.; Fellermeier, M.; Eisenreich, W.; Zenk, M. H.; Bacher, A.; Rohdich, F. *Proc. Natl. Acad. Sci. USA* **2000**, *97*, 2486-2490.
- (41) Hecht, S.; Eisenreich, W.; Adam, P.; Amslinger, S.; Kis, K.; Bacher, A.; Arigoni, D.; Rohdich, F. *Proc. Natl. Acad. Sci. USA* **2001**, *98*, 14837-14842.
- (42) Rohdich, F.; Hecht, S.; Gärtner, K.; Adam, P.; Krieger, C.; Amslinger, S.; Arigoni, D.; Bacher, A.; Eisenreich, W. *Proc. Natl. Acad. Sci. USA* **2002**, *99*, 1158-1163.
- (43) Richard, S. B.; Bowman, M. E.; Kwiatkowski, W.; Kang, I.; Chow, C.; Lillo, A. M.; Cane, D. E.; Noel, J. P. *Nat Struct. Biol.* **2001**, *8*, 641-648.

- (44) Takagi, M.; Kuzuyama, T.; Kaneda, K.; Watanabe, H.; Dairi, T.; Seto, H. *Tetrahedron Lett.* **2000**, *41*, 3395-3398.
- (45) Richard, S. B.; Ferrer, J.-L.; Bowman, M. E.; Lillo, A. M.; Tetzlaff, C. N.; Cane, D. E.; Noel, J. P. *J. Biol. Chem.* **2002**, *277*, 8667-8672.
- (46) Campos, N.; Rodríguez-Concepción, M.; Seemann, M.; Rohmer, M.; Boronat, A. *FEBS Lett.* **2001**, *488*, 170-173.
- (47) Hintz, M.; Reichenberg, A.; Altincicek, B.; Bahr, U.; Gschwind, R. M.; Kollas, A.-K.; Beck, E.; Wiesner, J.; Eberl, M.; Jomaa, H. *FEBS Lett.* **2001**, *509*, 317-322.
- (48) Belmant, C.; Espinosa, E.; Poupot, R.; Peyrat, M.-A.; Guiraud, M.; Poquet, Y.; Bonneville, M.; Fournié, J.-J. *J. Biol. Chem.* **1999**, *274*, 32079-32084.
- (49) Cunningham, F. X.; Lafond, T. P.; Gantt, E. *J. Bact.* **2000**, *182*, 5841-5848.
- (50) Altincicek, B.; Hintz, M.; Sanderbrand, S.; Wiesner, J.; Beck, E.; Jomaa, H. *FEMS Microbiol. Lett.* **2000**, *190*.
- (51) Adam, P.; Hecht, S.; Eisenreich, W.; Kaiser, J.; Gräwert, T.; Arigoni, D.; Bacher, A.; Rohdich, F. *Proc. Natl. Acad. Sci. USA* **2002**, *99*, 12108-12113.
- (52) Ershov, y.; Gantt, R. R.; Cunningham, F. X.; Gantt, E. *FEBS Lett.* **2000**, *473*, 337-340.
- (53) Giner, J.-L.; Jaun, B.; Arigoni, D. *J. Chem. Soc. Chem. Commun.* **1998**, *17*, 1857-1858.
- (54) Kaneda, K.; Kuzuyama, T.; Takagi, M.; Hayakawa, Y.; Seto, H. *Proc. Natl. Acad. Sci. USA* **2001**, *Vol. 98*, 932-937.
- (55) Durbecq, V.; Sainz, G.; Oudjama, Y.; Clantin, B.; Bompard-Gilles, C.; Tricot, C.; Caillet, J.; Stalon, V.; Droogmans, L.; Villeret, V. *EMBO J.* **2001**, *20*, 1530-1537.
- (56) Leyes, A. E.; Baker, J. A.; Poulter, C. D. *Org. Lett.* **1999**, *1*, 1071-1073.
- (57) Leyes, A. E.; Baker, J. A.; Hahn, F. M.; Poulter, C. D. *J. Chem. Soc. Chem. Commun.* **1999**, *8*, 717-718.

- (58) Charon, L.; Hoeffler, J.-F.; Pale-Grosdemange, C.; Lois, L. M.; Campos, N.; Boronat, A.; Rohmer, M. *Biochem. J.* **2000**, *346*, 737-742.
- (59) Rodríguez-Concepción, M.; Campos, N.; Lois, L. M.; Maldonado, C.; Hoeffler, J.-F.; Grosdemange-Billiard, C.; Rohmer, M.; Boronat, A. *FEBS Lett.* **2000**, *473*, 328-332.
- (60) Disch, A.; Schwender, J.; Muller, C.; Lichtenthaler, H. K.; Rohmer, M. *Biochem. J.* **1998**, *333*, 381-388.
- (61) Rohdich, F.; Kis, K.; Bacher, A.; Eisenreich, W. *Curr. Opin. Chem. Biol.* **2001**, *5*, 535-540.
- (62) Eisenreich, W.; Rohdich, F.; Bacher, A. *Trends Plant Sci.* **2001**, *6*, 78-84.
- (63) Seto, H.; Watanabe, H.; Furihata, K. *Tetrahedron Lett.* **1996**, *37*, 7979-7982.
- (64) Lange, B. M.; Rujan, T.; Martin, W.; Croteau, R. *Proc. Natl. Acad. Sci. USA* **2000**, *97*, 13171-13177.
- (65) Dumas, R.; Biou, V.; Halgand, F.; Douce, R.; Duggleby, R. G. *Acc. Chem. Res.* **2001**, *34*, 399-408.
- (66) Dumas, r.; Cornillon-Bertrand, C.; Guigue-Talet, P.; Genix, P.; Douce, R.; Job, D. *Biochem. J.* **1994**, *301*, 813-820.
- (67) Chundururu, S.; Mrachko, G. T.; Calvo, K. C. *Biochemistry* **1989**, *28*, 486-493.
- (68) Dumas, R.; Butikofer, M.-C.; Job, D.; Douce, R. *Biochemistry* **1995**, *34*, 6026-6036.
- (69) Kuzuyama, T.; Takahashi, S.; Takagi, M.; Seto, H. *J. Biol. Chem.* **2000**, *275*, 19928-19932.
- (70) Tanner, M. E. *Acc. Chem. Res.* **2002**, *35*, 237-246.
- (71) Kuzuyama, T.; Shimizu, T.; Takahashi, S.; Seto, H. *Tetrahedron Lett.* **1998**, *39*, 7913-7916.

- (72) Zeidler, J.; Schwender, J.; Muller, C.; Wiesner, J.; Weidemeyer, C.; Beck, E.; Jomaa, H.; Lichtenthaler, H. K. *Z. Naturforsch.* **1998**, 980-986.
- (73) Fellermeier, M.; Kis, K.; Sagner, S.; Maier, U.; Bacher, A.; Zenk, M. H. *Tetrahedron Lett.* **1999**, 40, 2743-2746.
- (74) Reichenberg, A.; Wiesner, J.; Weidemeyer, C.; Dreiseidler, E.; Sanderbrand, S.; Altincicek, B.; Beck, E.; Schlitzer, M.; Jomaa, H. *Bioorganic Med. Chem. Lett.* **2001**, 11, 833-835.
- (75) Wiesner, J.; Henschker, D.; Hutchinson, D. B.; Beck, E.; Jomaa, H. *Antimicrobial Agents and Chemotherapy* **2002**, 46, 2889-2894.
- (76) Silverman, R. B. *The organic chemistry of enzyme catalyzed reactions*; Academic Press: San Diego, 2000.
- (77) Arfin, S. M.; Ratzkin, B.; Umbarger, H. E. *Biochem. Biophys. Res. Commun.* **1969**, 37, 902-908.
- (78) Biou, V.; Dumas, R.; Cohen-Addad, C.; Douce, R.; Job, D.; Pebay-Peyroula, E. *EMBO J.* **1997**, 16, 3405-3415.
- (79) *Pyridine Nucleotide Coenzymes : Chemical, Biochemical, and Medical Aspects, Part A*; Wiley: New York, 1987; Vol. 2.
- (80) Yun, M.; Park, C.-G.; Kim, J.-Y.; Park, H.-W. *Biochemistry* **2000**, 39, 10702-10710.
- (81) Branden, C.-I.; Eklund, H. *Dehydrogenases Requiring Nicotinamide Coenzymes*; Birkhauser: Basel, 1980; Vol. 36.
- (82) Anthonsen, T.; Hagen, S.; Sallam, M. A. *Phytochemistry* **1980**, 19, 2375-2377.
- (83) Anthonsen, T.; Hagen, S.; Sallam, M., A. E. *Phytochemistry* **1980**, 19, 2375-2377.
- (84) Hoeffler, J.-F.; Grosdemange-Billiard, C.; Rohmer, M. *Tetrahedron Lett.* **2000**, 41, 4885-4889.
- (85) Giner, J.-L. *Tetrahedron Lett.* **1998**, 39, 2479-2482.
- (86) Jacobsen, E. N.; Marko, I.; France, M. B.; Svendsen, J. S.; Sharpless, K. B. *J. Am. Chem. Soc.* **1989**, 111, 737-739.

- (87) Sharpless, K. B.; Amberg, W.; Bennani, Y. L.; Crispino, G. A.; Hartung, J.; Jeong, K.-S.; Kwong, H.-L.; Morikawa, K.; Wang, Z.-M.; Xu, D.; Zhang, X.-L. *J. Org. Chem* **1992**, *57*, 2768-2771.
- (88) Mostad, S. B.; Helming, H. L.; Groom, C.; Glasfeld, A. *Biochem. Biophys. Res. commun.* **1997**, *233*, 681-686.
- (89) Jeong, S.-S.; Gready, J. E. *Anal. Biochem.* **1994**, *221*, 273-277.
- (90) Charon, L.; Hoeffler, J.-F.; Pale-Grosdemange, C.; Rohmer, M. *Tetrahedron Lett.* **1999**, *40*, 8369-8373.
- (91) Nambiar, K. P.; Stauffer, D. M.; Kolodziej, P. A.; Benner, S. A. *J. Am. Chem. Soc.* **1983**, *105*, 5886-5890.
- (92) Dave, K. G.; Dunlap, R. B.; Jain, M. K.; Cordes, E. H.; Wenkert, E. *J. Biol. Chem.* **1968**, *243*, 1073-1074.
- (93) Hecht, S.; Kis, K.; Eisenreich, W.; Amslinger, S.; Wungsintaweeikul, J.; Herz, S.; Rohdich, F.; Bacher, A. *J. Org. Chem.* **2001**, *66*, 3948-3952.
- (94) Garavito, R. M.; Rossmann, M. G.; Argos, P.; Eventoff, W. *Biochemistry* **1977**, *16*, 5065-5071.
- (95) You, K.-S.; Lyle J. Arnold, J.; Allison, w. S.; Kaplan, N. O. *TIBS* **1978**, *3*, 265-268.
- (96) Reuter, K.; Sanderbrand, S.; Jomaa, H.; Wiesner, J.; Steinbrecher, I.; Beck, E.; Hintz, M.; Klebe, G.; Stubbs, M. T. *J. Biol. Chem.* **2002**, *277*, 5378-5384.
- (97) Yajima, S.; Nonaka, T.; Kuzuyama, T.; Seto, H.; Ohsawa, K. *J. Biochem.* **2002**, *131*, 313-317.
- (98) Arigoni, D.; Giner, J.-L.; Sagner, S.; Wungsintaweeikul, J.; Zenk, M. H.; Kis, K.; Bacher, A.; Eisenreich, W. *Chem. Commun.* **1999**, *12*, 1127-1128.
- (99) Radykewicz, T.; Rohdich, F.; Wungsintaweeikul, J.; Herz, S.; Kis, K.; Eisenreich, W.; Bacher, A.; Zenk, M. H.; Arigoni, D. *FEBS Lett* **2000**, *465*, 157-160.
- (100) Still, W. C.; Kahn, M.; Mitra, A. *J. Org. Chem.* **1978**, *43*, 2923-2925.

- (101) Perrin, D. D.; Armarego, W. L. F. *Purification of Laboratory Chemicals*; 3rd ed.; Pergamon Press: New York, 1988.
- (102) Shikhiev, I. A.; Karaev, S. F.; Alieva, S. Z.; Yur'eva, G. A. *Zh. Org. Khim.* **1975**, *11*, 2134-2137.
- (103) Seto, H.; Kuzuyama, T. *Nat. Prod. Rep.* **1999**, *16*, 589-596.
- (104) Horiguchi, M.; Kandatsu, M. *Nature* **1959**, *184*, 901-902.
- (105) Alhadeff, J. A.; Bruggen, J. T. V.; Daves, G. D. J. *Biochim. Biophys. Acta.* **1972**, *286*, 103-106.
- (106) Cook, A. M.; Daughton, C. G.; Alexander, M. *J. Bacteriol.* **1978**, *133*, 85-90.
- (107) Kojo, h.; Shigi, Y.; Nishida, M. *J. Antibiot.* **1980**, *33*, 44-48.
- (108) Chopra, I. *J. Appl. Bacteriol.* **1988**, *65*, 149S-166S.
- (109) Okuhara, M.; Kuroda, Y.; Goto, T.; KOkamoto, M.; Terano, H.; Kohsaka, M.; Aoki, H.; Imanaka, H. *J. Antibiot.* **1980**, *33*, 13-17.
- (110) Iguchi, E.; Okuhara, M.; Aoki, H.; Imanaka, H. *J. Antibiot.* **1980**, *33*, 18-23.
- (111) Okuhara, M.; Kuroda, Y.; Okamoto, M.; Terano, H.; Kohsaka, M.; Imanaka, H. *J. Antibiot.* **1980**, *33*, 24-28.
- (112) Hashimoto, M.; Hemmi, K.; Takeno, H.; Kamiya, T. *Tetrahedron Lett.* **1980**, *21*, 99-102.
- (113) Hemmi, K.; Takeno, H.; Hashimoto, M.; Kamiya, T. *Chem. Pharm. Bull.* **1981**, *29*, 646-650.
- (114) Hemmi, K.; Takeno, H.; Hashimoto, M.; Kamiya, T. *Chem. Pharm. Bull.* **1982**, *30*, 111-118.
- (115) Kamiya, T.; Hemmi, K.; Takeno, H.; Hashimoto, M. *Tetrahedron Lett.* **1980**, *21*, 95-98.
- (116) Mine, Y.; Kamimura, T.; Shigeo, N.; Nishida, M. *J. Antibiot.* **1980**, *33*, 36-43.

- (117) Kuemmerle, H.-P.; Murakawa, T.; Sakamoto, H.; Sato, N.; Konishi, T.; Santis, F. D. *Int. J. Clin. Pharmacol.* **1985**, *23*, 521-528.
- (118) Kuemmerle, H.-P.; Murakawa, T.; Soneoka, K.; Konishi, T. *Int. J. Clin. Pharmacol.* **1985**, *23*, 515-520.
- (119) Shigi, Y. *J. Antimicrob. Chemoth.* **1989**, *24*, 131-245.
- (120) Mueller, C.; Schwender, J.; Zeider, J.; Lichtenthaler, H. K. *Biochem Soc. Trans* **2000**, *28*, 792-793.
- (121) Sparks, D. L.; Martin, T. A.; Gross, D. R.; Hunsaker, J. C. R. *Microsc. Res. Tech.* **2000**, *50*, 287-290.
- (122) Arigoni, D.; Giner, J.-L.; Sagner, S.; Wungsintaweekul, J.; Zenk, M. H.; Kis, K.; Bacher, A.; Eisenreich, W. *J. Chem. Soc. Chem. Commun.* **1999**, *12*, 1127-1128.
- (123) Hagand, F.; Vives, F.; Dumas, R.; Biou, V.; Andersen, J.; Andrieu, J.-P.; Cantegril, R.; Gagnon, J.; Douce, R.; Forest, E.; Job, D. *Biochemistry* **1998**, *37*, 4773-4781.
- (124) Katayama, N.; Tsubotani, S.; Nozaki, Y.; Harada, S.; Ono, H. *J. Antibiot.* **1990**, *53*, 238-246.
- (125) Takahashi, E.; Kimura, T.; Nakamura, K.; Arahira, M.; Iida, M. *J. Antibiot.* **1995**, *48*, 1124-1129.
- (126) Smrcka, A. V.; Jensen, R. G. *Plant Physiol.* **1988**, *86*, 615-618.
- (127) Takahashi, E.; Kimura, T.; Nakamura, K.; Arahira, M.; Iida, M. *J. Antibiot.* **1995**, *48*, 1124-1129.
- (128) Alpert, A. J. *J. Chromatogr.* **1990**, *499*, 177-196.
- (129) Blagg, B. S. J.; Poulter, C. D. *J. Org. Chem.* **1999**, *64*, 1508-1511.
- (130) Davisson, V. J.; Woodside, A. B.; Poulter, D. C. *Methods Enzymol.* **1985**, *110*, 130-144.
- (131) Martin, J. B.; Doty, D. M. *Anal. Chemistry* **1949**, *21*, 965-967.
- (132) Peterson, E. M.; Brownell, J.; Vince, R. *J. Med. Chem* **1992**, *35*, 3991-4000.

- (133) Howarth, N. M.; Purohit, A.; Reed, M. J.; Potter, B. V. L. *J. Med. Chem.* **1994**, *37*, 219-221.
- (134) Okada, M.; Iwashita, S.; Koizumi, N. *Tetrahedron Lett.* **2000**, *41*, 7047-7051.
- (135) R. N, J.; DC, E. *Arch. Pathol. Lab. Med.* **1985**, *109*, 595-601.
- (136) Branden, C.; Tooze, J. *Introduction to Protein Structure*; 2nd ed.; Garland Publishing, Inc.: New York, 1999.
- (137) Wierenga, R. K.; Terpstra, P.; Hol, W. G. *J. Mol. Biol* **1986**, *187*, 101-107.
- (138) Bernart, M. W.; Gerwick, W. H.; Corcoran, E. E.; Lee, A. Y.; Clardy, J. *Phytochemistry* **1992**, *31*, 1273-1276.
- (139) Alterman, W.; Kimpe, N. D.; Kalinin, V. *J. Nat. Prod.* **1997**, *60*, 385-386.
- (140) Putra, S. R.; Charon, L.; Danielsen, K.; Pale-Grosdemange, C.; Lois, L.-M.; Campos, N.; Boronat, A.; Rohmer, M. *Tetrahedron Lett.* **1998**, *39*, 6185-6188.
- (141) Wolf, e.; Kennedy, I. A.; Himmeldirk, K.; Spenser, I. D. *Can. J. Chem.* **1997**, *75*, 942-948.
- (142) Aelterman, W.; kimpe, N. D.; Kalinin, V. *J. Nat. Prod.* **1997**, *60*, 385-386.
- (143) NJ., K. *Methods Mol. Biol.* **1994**, *32*, 9-15.
- (144) O'Neil, I. A. *Synlett.* **1991**, 661-662.
- (145) Yazawa, H.; Goto, S. *Tetrahedron Lett.* **1985**, *26*, 3703-3706.
- (146) Strazzolini, P.; Giumanini, A. G.; Cauci, S. *Tetrahedron* **1990**, *46*, 1081-1118.
- (147) Tozer, M. J.; Buck, I. M.; Cooke, T.; Kalindjian, S. B.; McDonald, I. M.; Pether, M. J.; Steel, K. I. M. *Bioorganic Med. Chem. Lett.* **1999**, *9*, 3103-3108.